

General Disclaimer

One or more of the Following Statements may affect this Document

- This document has been reproduced from the best copy furnished by the organizational source. It is being released in the interest of making available as much information as possible.
- This document may contain data, which exceeds the sheet parameters. It was furnished in this condition by the organizational source and is the best copy available.
- This document may contain tone-on-tone or color graphs, charts and/or pictures, which have been reproduced in black and white.
- This document is paginated as submitted by the original source.
- Portions of this document are not fully legible due to the historical nature of some of the material. However, it is the best reproduction available from the original submission.

NASA CR- 144777

A CALIBRATION OF DETECTORS AND GRATINGS
BETWEEN 100 AND 600 Å

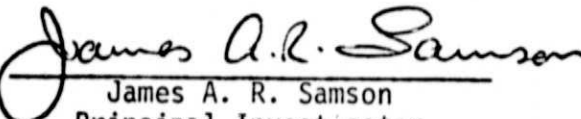
(NASA-CR-144777) A CALIBRATION OF DETECTORS
AND GRATINGS BETWEEN 100 AND 600 ÅNGSTROMS
Final Report, Nov. 1972 - Dec. 1975
(Nebraska Univ.) 87 F HC \$5.00 CSCI 14E

N76-27537

Unclas
63/35 44734

FINAL REPORT
(Nov. 1972-Dec. 1975)
Contract NAS5-23125

Prepared for:
National Aeronautics and Space Administration
Goddard Space Flight Center
Greenbelt, MD

Prepared by:

James A. R. Samson
Principal Investigator
Behlen Laboratory of Physics
University of Nebraska-Lincoln
Lincoln, NE 68588



December 1975

INDEX

<u>SECTION</u>	<u>PAGE</u>
I. Introduction	1
II. Calibration of Magnetic Electron Multipliers	2
III. Measurement of Grating Efficiency	21
IV. Polarization Produced by Gratings	24
V. Photoelectric Yield Studies of Various Cathodes	36
1. LiF, NaF, MgF_2 , RbF_2 , SrF_2 , CaF, CsI, KI.	36
Humidity Tests	45
2. Pt	62
3. BeCu	62
4. Be, BeO	68
5. W	79
VI. Appendix	81

I. INTRODUCTION

This is a final report of a continuous study of calibration and efficiency measurements of magnetic electron multipliers, diffraction gratings, and photocathodes over the wavelength range 100 to 600 Å. For some of the measurements it was found necessary to use the Synchrotron radiation from the Wisconsin storage ring, in Madison, Wisconsin. The remaining measurements were performed in the Vacuum UV Laboratory of the Physics Department, University of Nebraska.

The report is divided into four sections. Each section describes a particular class of measurement and thus the sections are not in chronological order. The classifications are, calibration of magnetic electron multipliers, measurement of grating efficiencies, measurement of the polarization produced by diffraction gratings, and measurements of the photoelectric yields of various photocathodes. Further discussion of the material reported here can be found in the monthly reports 1 through 37.

II. CALIBRATION OF MAGNETIC ELECTRON MULTIPLIERS

1. Introduction

Three Bendix magnetic electron multipliers (MEM's), type 3T2 with cathodes of tungsten and lithium fluoride were studied. Measurements of the surface sensitivity of the cathodes were performed as well as absolute efficiency measurements. The MEM's are labelled,

MEM #131 (tungsten)
#PN758 (LiF)
#P0028 (LiF) .

The sensitivity of the surface area was probed by different photon beam sizes. Because of the small size of the synchrotron beams (4mm high) same measurements in the Laboratory were also performed with the same dimensions. Other measurements used larger dimensions. Although a variety of sizes were used the final data were taken with photon beam cross sections of 19 x 1.5 mm and 4 x 1.5 mm.

2. Cathode area sensitivity

The mapping of the cathode sensitivity was done by allowing the photon beam to sweep out a path along the center of the cathode. The multiplier was moved relative to the photon beam. Two measurements were made at right angles to each other. To clarify the discussion that follows Figs. 1 and 2 will be referred to in order that the location of the photon beam on the cathode is uniquely defined. The position of the flight monochromator slit is marked in Fig. 1 by the "60% distance" from the multiplying section.

Measurements were made with both 584 Å and 304 Å radiation. The

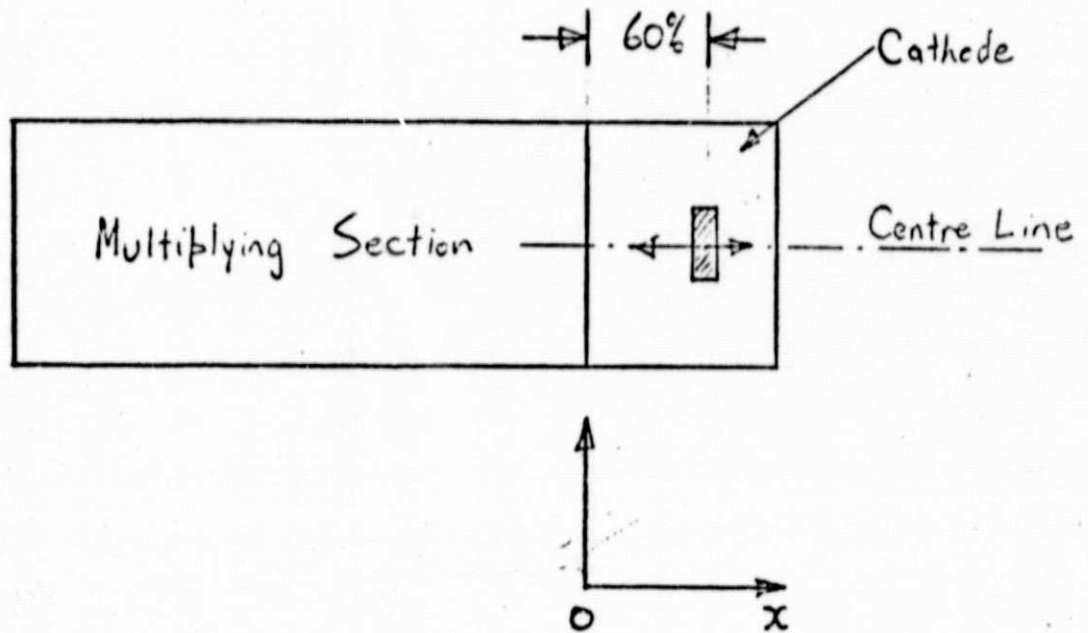


Fig. 1 MEM showing position of cathode illumination by the shaded box. Movement is along the center line. The co-ordinate axis system refers to position along the center line.

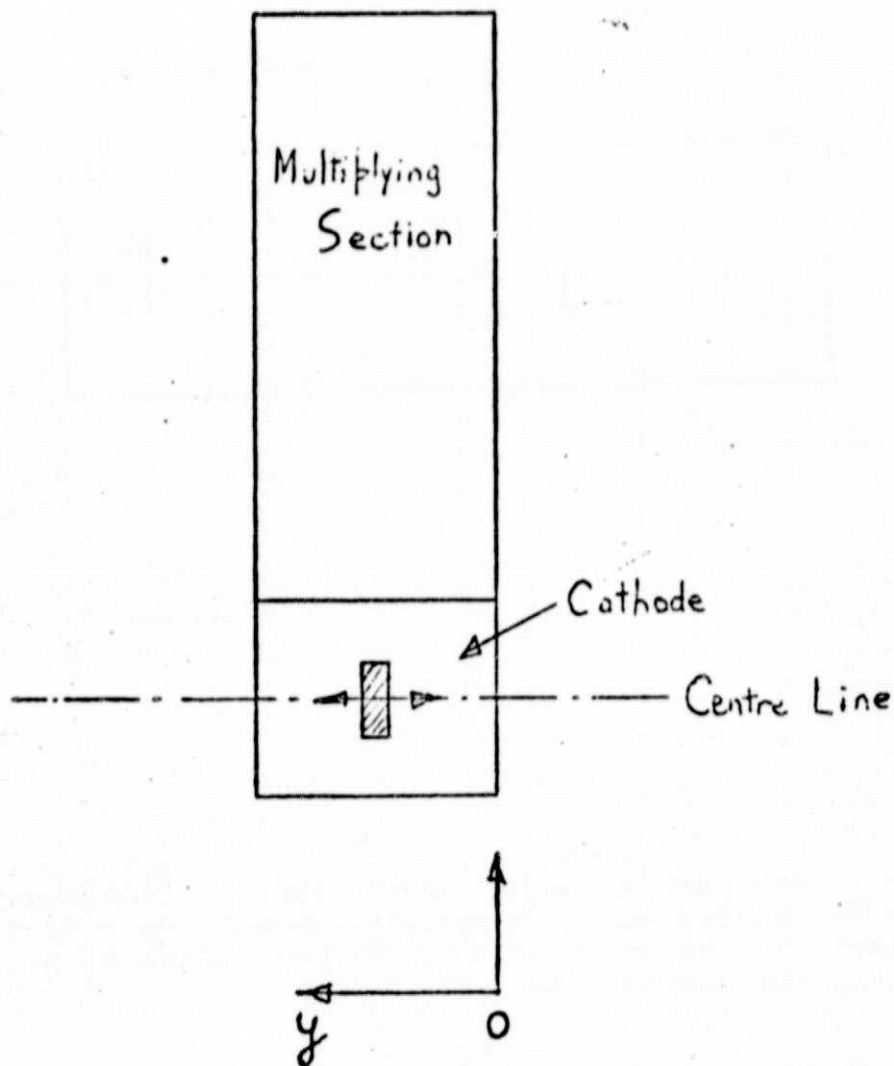


Fig. 2 MEM showing position of cathode illumination by the shaded box. Movement is along the center line. The co-ordinate axis system refers to position along the center line.

cathode area sensitivity was always the same regardless of the wavelength.

Numerous measurements were made with different multiplier voltages, discriminator settings, and attenuation settings. Although the absolute signals changed the relative sensitivity of the cathode surface remained unaltered (see monthly report #4).

Final measurements were thus performed at 584 \AA and with the electrical settings used at GSFC, namely,

multiplier voltage = 1500 V
discriminator level = 10 V
attenuation = 1 .

The following three Figures, Figs. 3, 4, and 5 refer to the MEM's #131, #PN758, and #P0028. The scanning orientation is side on as in Fig. 1. In Figs. 3a, 4a, and 5a the photon beam cross section is $4 \times 1.5 \text{ mm}$. In Figs. 3b, 4b, and 5b the cross section is $19 \times 1.5 \text{ mm}$. The zero position is that located nearest to the multiplying section.

Figures 6, 7, and 8 show the results of turning each multiplier end on (Fig. 2 orientation) and scanning across the cathode, again along a center line. The photon beam cross section was $4 \times 1.5 \text{ mm}$.

The efficiency of the MEM is extremely sensitive to the position illuminated on the cathode. Figures 9 and 10 repeat the measurements on the tungsten (#131) cathode viewed end on as in Fig. 2, however, with the illuminated area moved up 2mm beyond the center line towards the multiplying section (Fig. 9) and moved 2mm below the center line (Fig. 10). To emphasize the variation in sensitivity of the cathode Fig. 11 reproduces results published by Macar et al., Applied Optics 9, 581 (1970). These results apply to an MEM 38. Other results are shown in Fig. 12 by Heroux, Appl. Optics 7, 2561 (1968) and in Fig. 13 by Timothy et al., Appl. Optics 6, 1323 (1967).

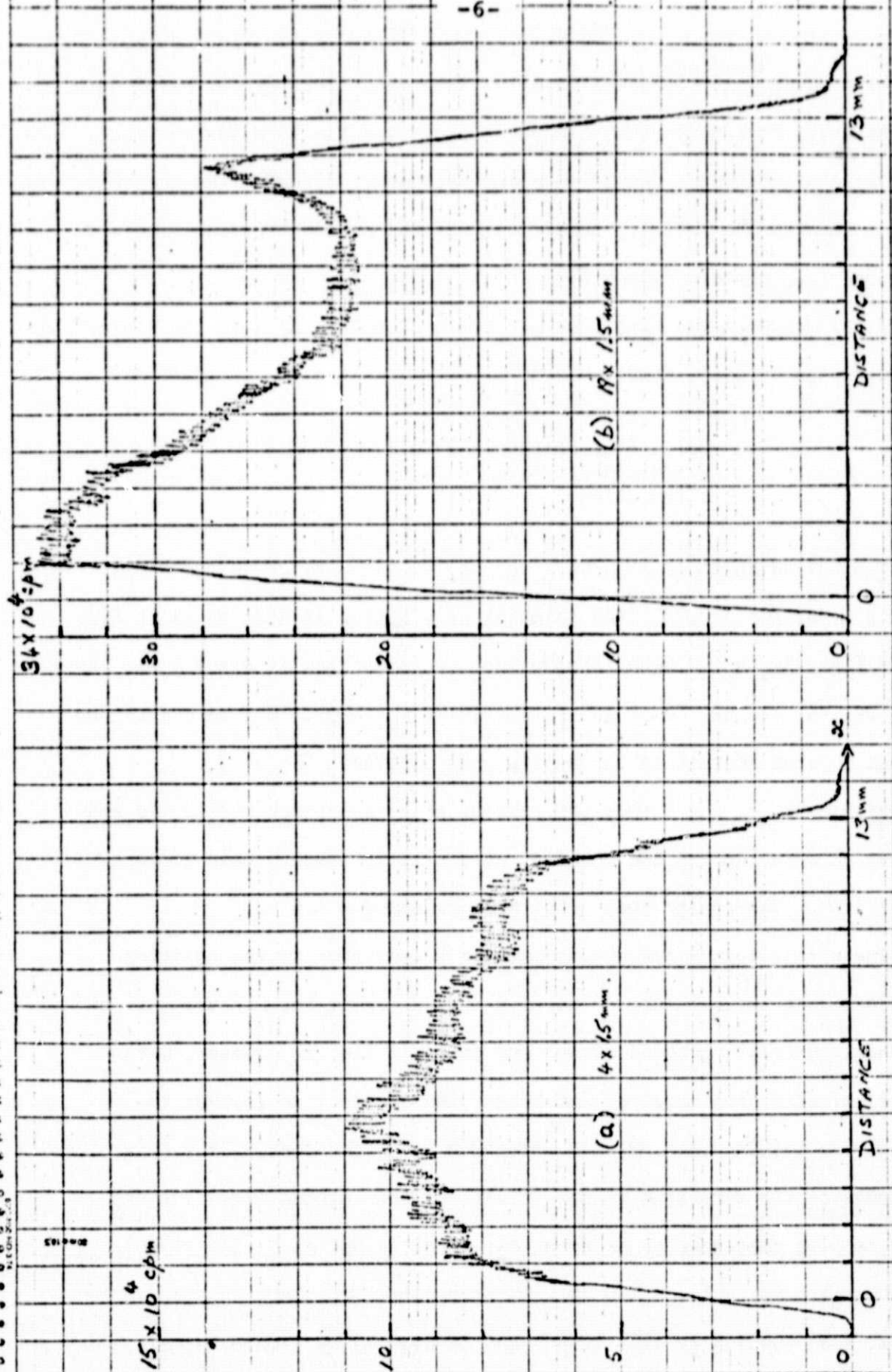


FIG. 3a,b. MEM#131 (N). CATHODE SENSITIVITY SIDE ON (SEE FIG. 1).

15 x 10⁴ cpm

10

5

0

DISTANCE

(a) 4 x 1.5 mm

14 mm

30 x 10⁴ cpm

30

10

0

0

DISTANCE

(b) 19 x 1.5 mm

14 mm

FIG. 4a,b. MEM #PN758 (LIP). CATHODE SENSITIVITY SIDE ON. (SEE FIG. 1).

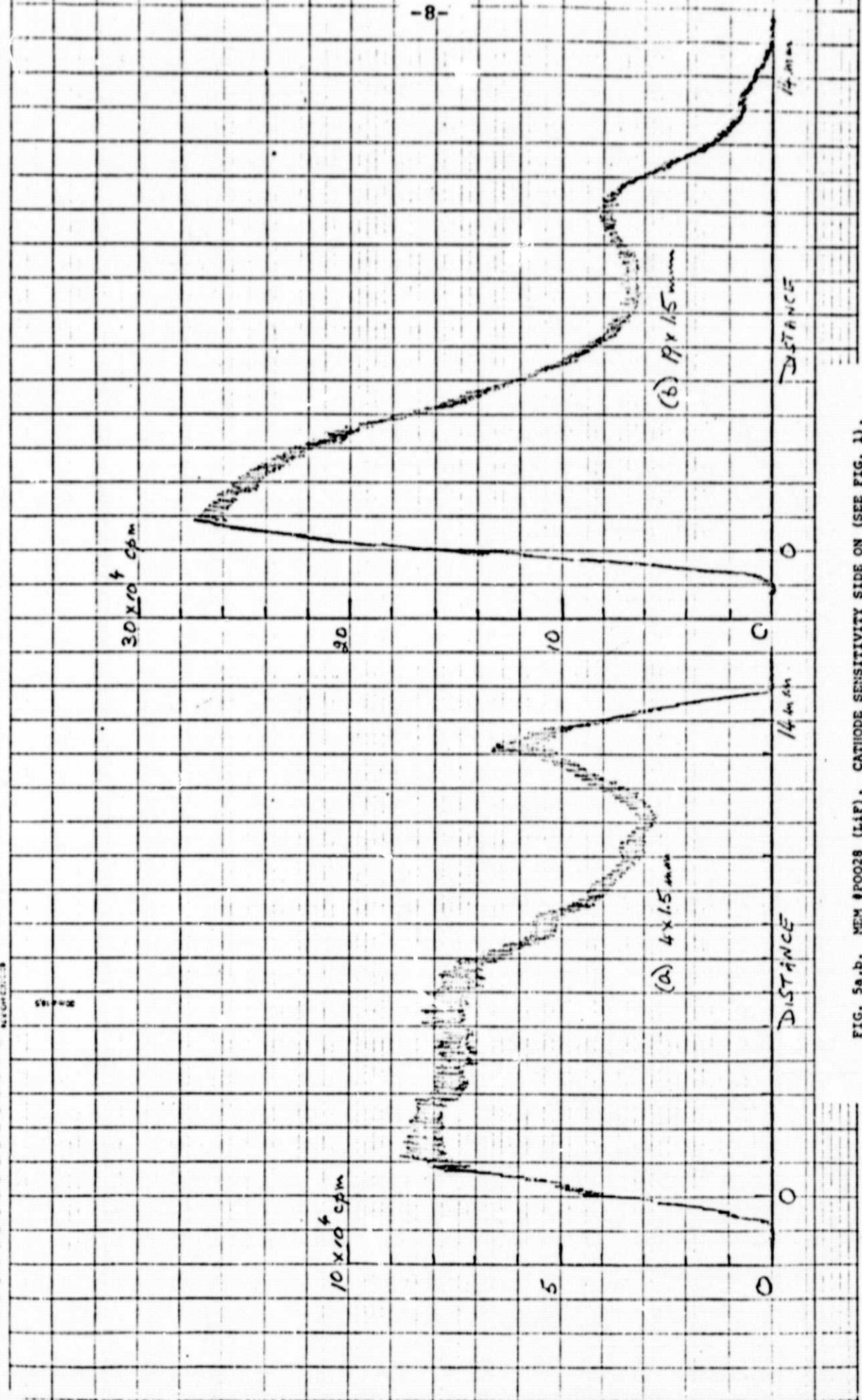


FIG. 5a,b. MEM #0028 (LiF). CATHODE SENSITIVITY SIDE ON (SEE FIG. 1).

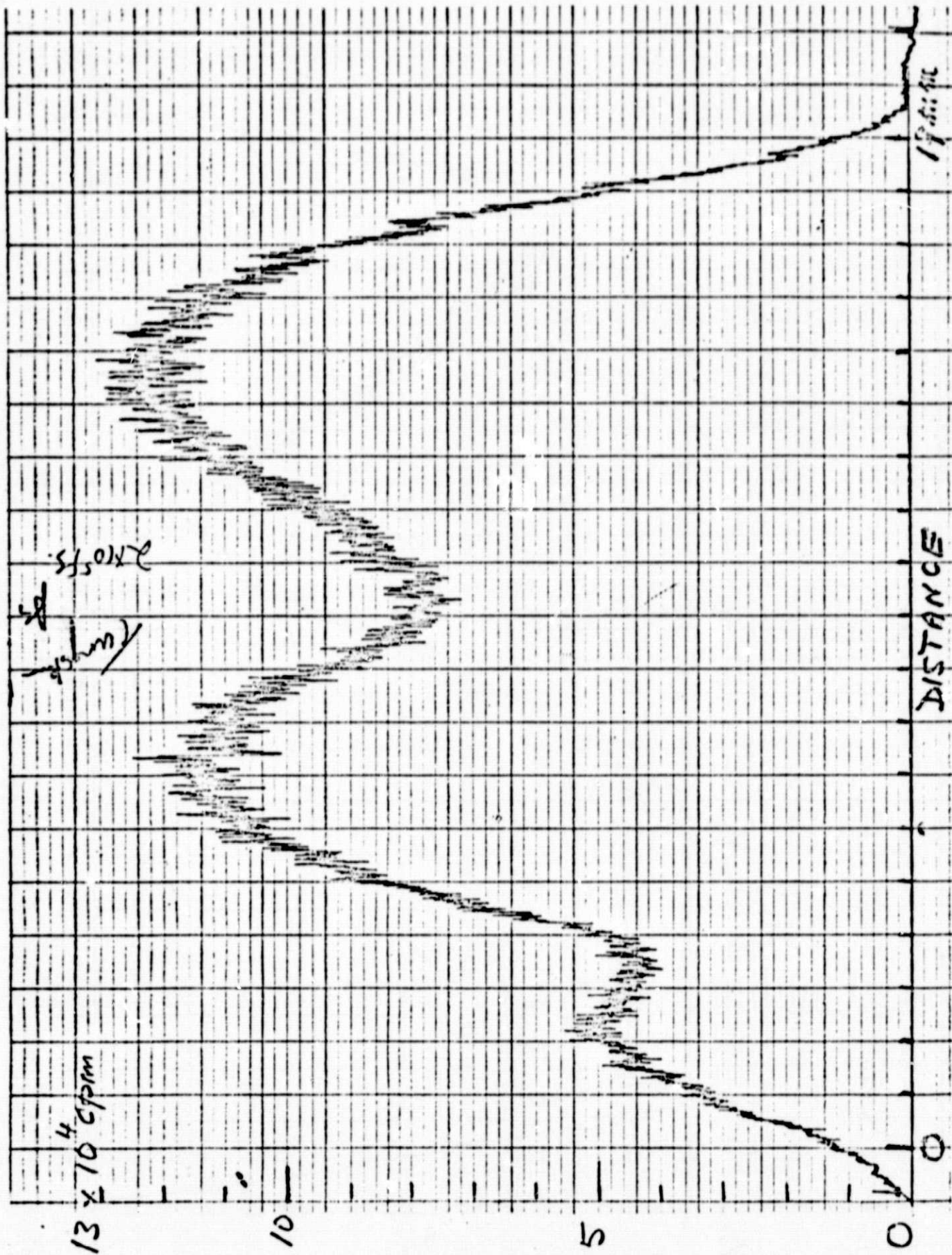


Fig 6. MEM #131. Cathode sensitivity end on (see Fig. 2).

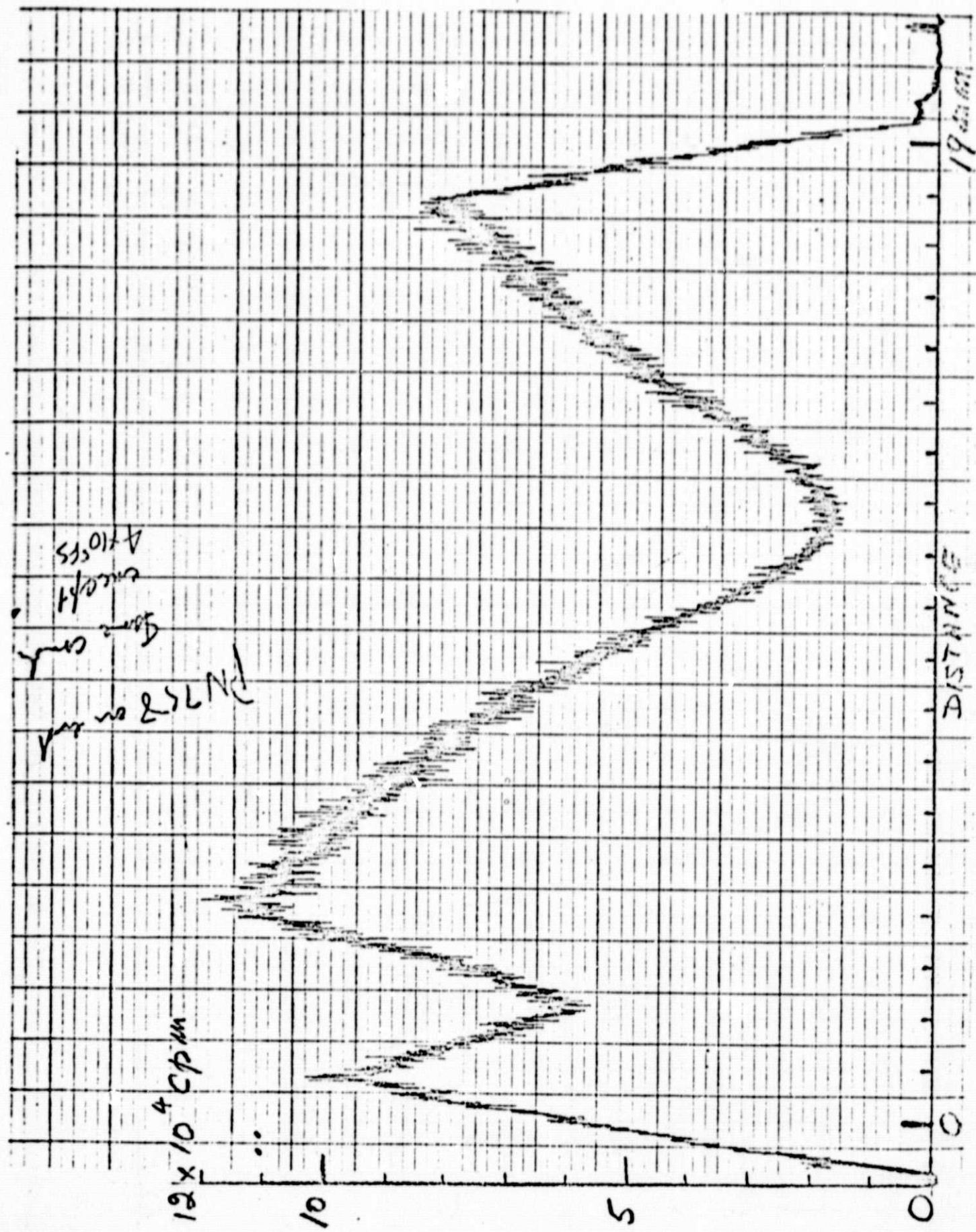
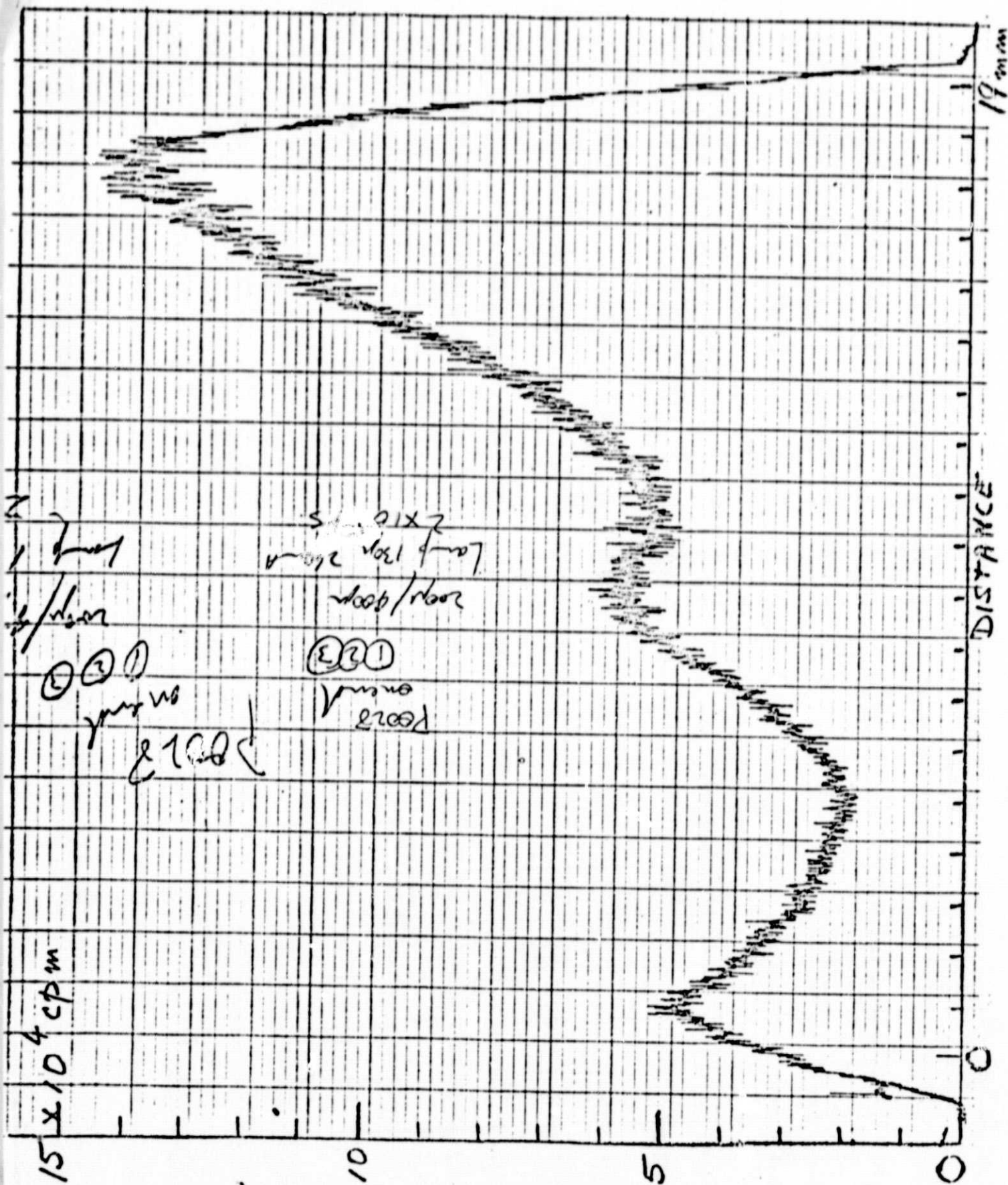


Fig. 7. MEM #PN758. Cathode sensitivity end on (see Fig.2).



Tungsten MEM End on. Mark \approx 2mm above center.

1.3×10^4 cpm

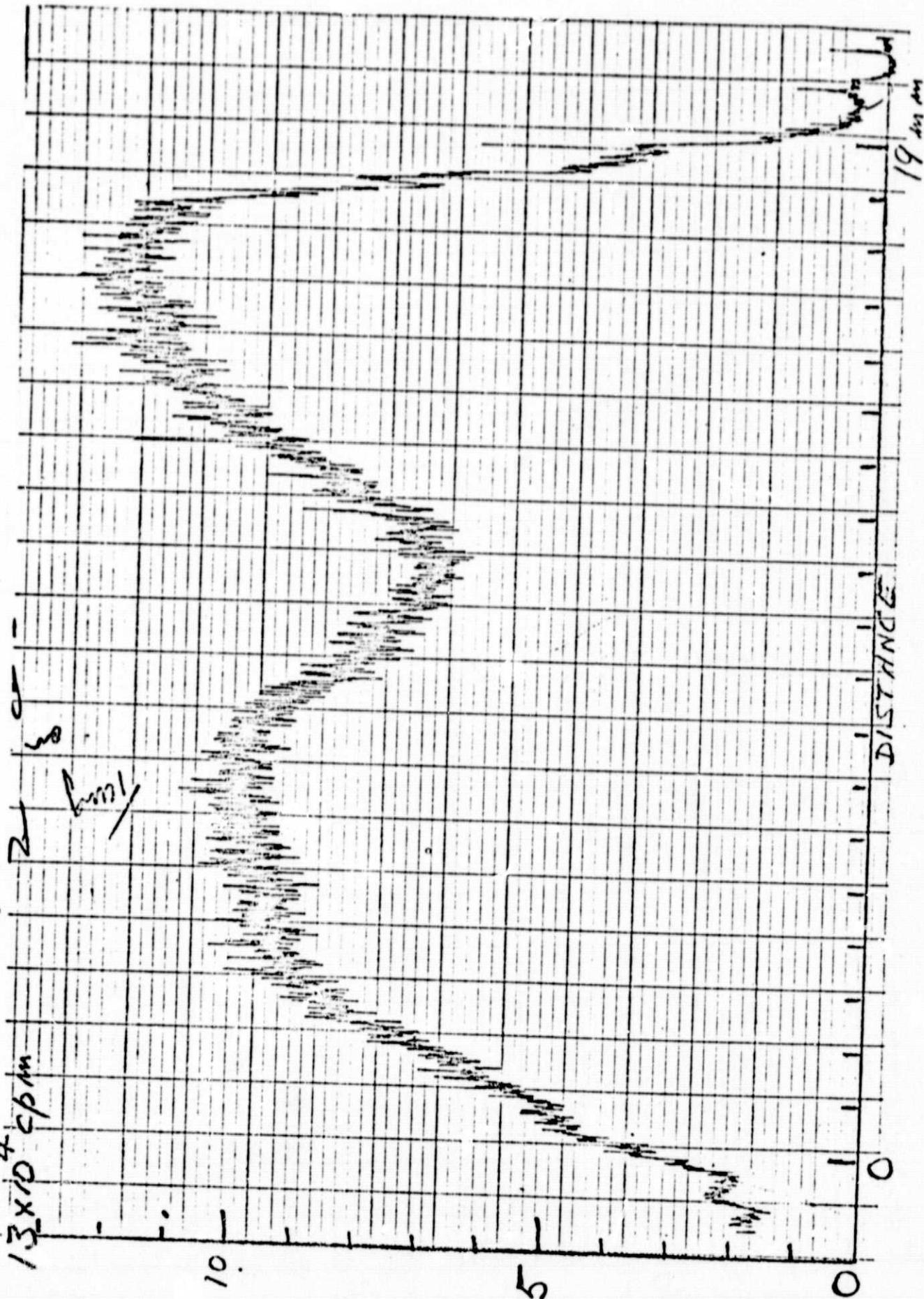


Fig. 9. MEM #131. Cathode sensitivity end on. Scan 2mm above center line on side of multiplying section.

Tungsten MEM End on Mark \approx 2mm below center.

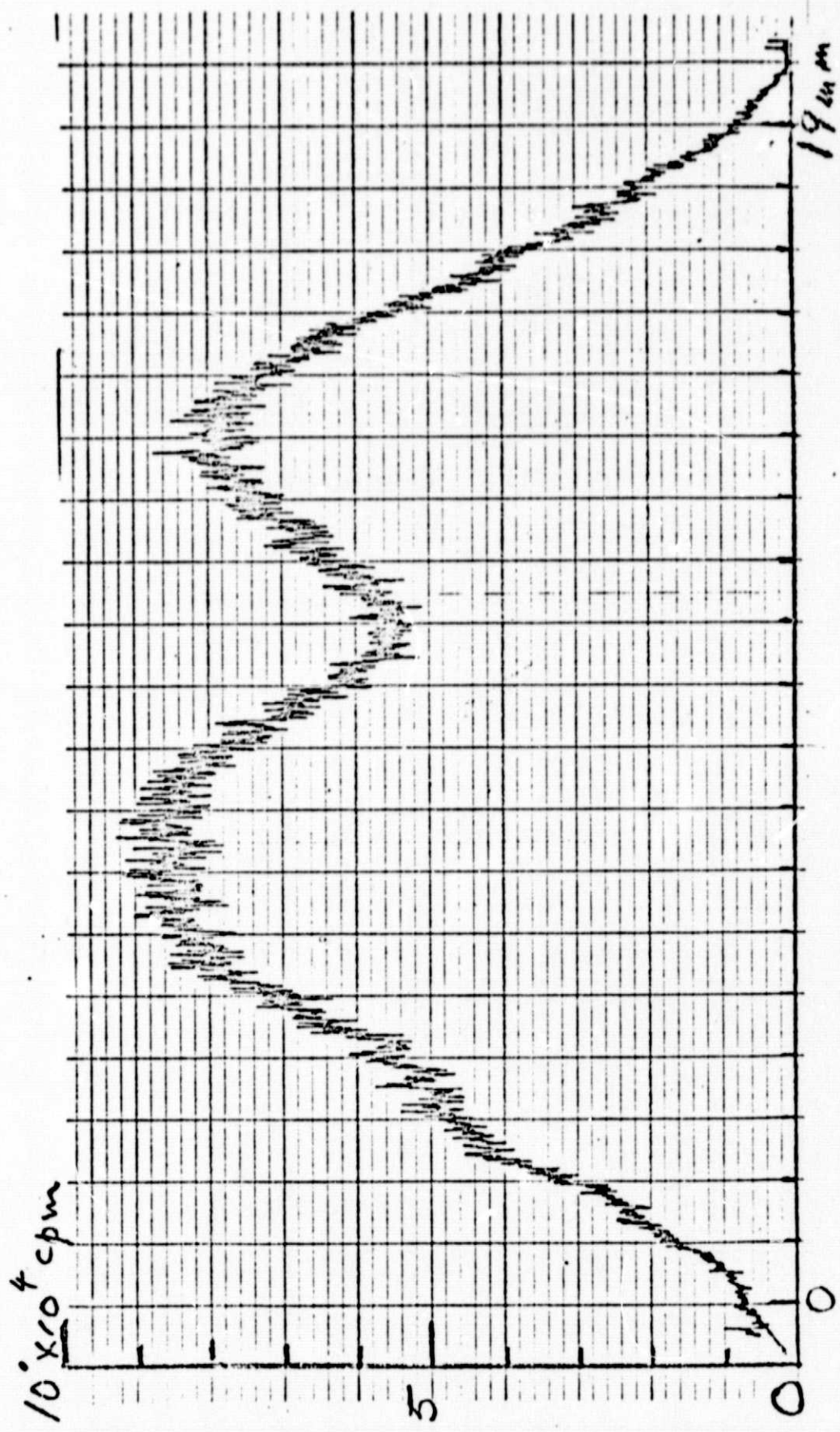


Fig. 10. MEM #131. Cathode sensitivity end on. Scan 2mm below center line on opposite side of multiplying section.

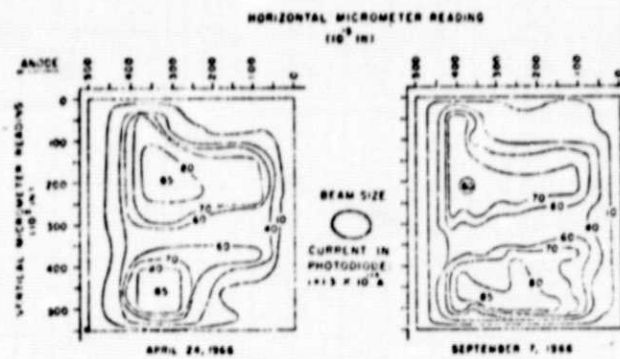


Fig. 11. Cathode map, MEM 38.

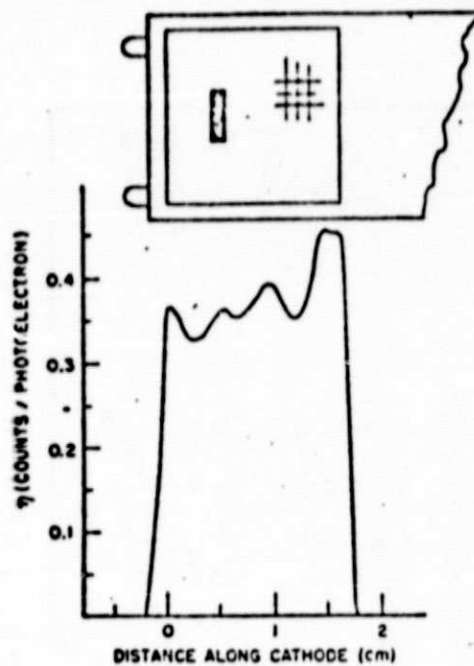


Fig. 12 Variation of the photoelectron counting efficiency η with position of illumination on the photocathode. The area of the cathode illuminated is indicated by the solid rectangle above the curve.

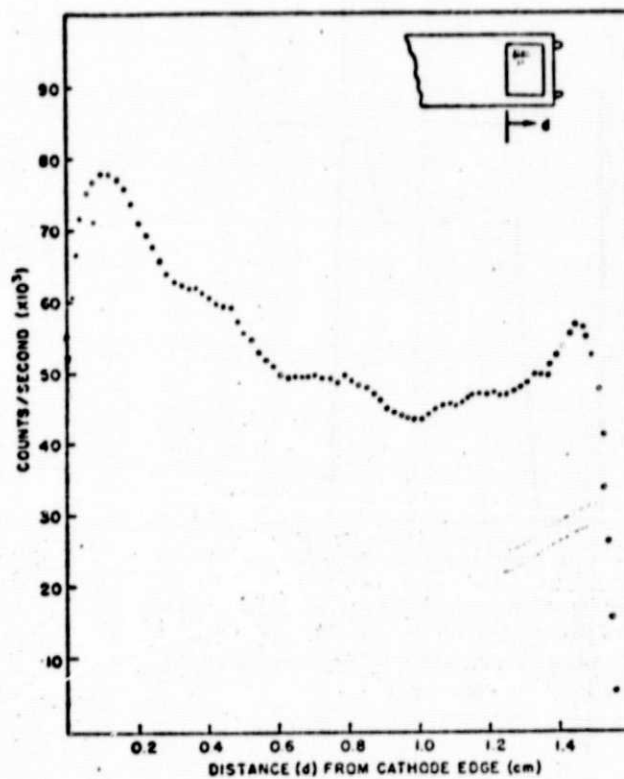


Fig. 13 Variation of magnetic electron multiplier response with position on the photocathode. Negative mode. DSIE potential -2000 V. Case at FSOE potential.

3. Absolute multiplier efficiency

The response of each magnetic electron multiplier was measured with respect to a known intensity of the incident radiation. That is, the efficiency of a multiplier is defined as,

$$\text{Efficiency} = \frac{\text{number of counts/sec}}{\text{number of incident photons/sec}} \quad (1)$$

The efficiency will vary, of course, with the voltage placed on the MEM's, on the particular settings of the discriminator and other electronics and on the position of the cathode illuminated by the incident radiation. However, the shape of the curve, or relative efficiency, as a function of wavelength does not depend upon the area exposed to the radiation.

The procedure adopted was to compare the signal from the MEM's with the response from a calibrated aluminum photo-cathode. The photo-cathode was in turn calibrated against the rare gas ion chambers.

The light source used was the synchrotron radiation from the storage ring at the University of Wisconsin. This source provided a continuum of radiation from the visible to the x-ray region. However, a short wavelength limit was imposed at about 170 \AA because it was necessary to use an aluminum thin film filter to minimize scattered radiation. The aluminum filter cuts off at 170 \AA . In addition, aluminum filters were used as attenuators to reduce the signal from the MEM's below the saturation level of 10^5 cps. These filters were removed to obtain a measurable signal from the aluminum photo-cathode.

The results obtained with the synchrotron were actually relative efficiencies vs wavelength. The results were put on an absolute basis by normalizing to the absolute efficiencies of the multipliers at 584 \AA and 304 \AA as obtained in the Laboratory. The high voltage was 1500 V,

the discriminator setting was 10 V, and the attenuation setting was 1. The area illuminated was 1.5 mm x 4 mm and positioned at 60% of the cathode length from the multiplying section as shown in Fig. 1. The results of the efficiencies of the three MEM's are shown in Fig. 14 from 650 to 170 Å.

The shape of the curves follows that of the published photoelectric efficiency of each photo-cathode. The absolute magnitude of the major peak in the LiF curves is lower than that of tungsten at the same wavelength (540 Å.) This varies from the behaviour of a fresh thin coating of LiF on a photo-cathode. However, these are old coatings and exposed to normal laboratory conditions of humidity. The unknown thickness of the coatings may affect the absolute yield of the cathode. Certainly, the LiF MEM #0028 is considerably less efficient than the PN 758 multiplier.

An interesting feature occurs with the LiF cathodes at 204 Å. A very high efficiency occurs, but over an extremely short wavelength range (less than 2 Å). This is undoubtedly caused by ejection of electrons from the Li K-shell. The narrowness of this structure illustrates the advantage of a continuum source of radiation to make these yield measurements.

The yields continue to rise towards shorter wavelengths but they must start decreasing again before 120 Å according to results published by Lukirskii et al. (see Techniques of VUV Spectroscopy by Samson, page 233.)

The data in Fig. 14 refer to a photon beam of cross section 4 x 1.5 mm. In order that the data may be used for a beam of 19 x 1.5 mm cross sections the following procedure was adopted.

From the definition of efficiency, Eq. (1), we have to determine the increased counts produced by using a larger aperture. The increase in the number of incident photons/sec is simply related to the ratio of the apertures.

REPRODUCIBILITY OF THE
ORIGINAL PAGE IS POOR

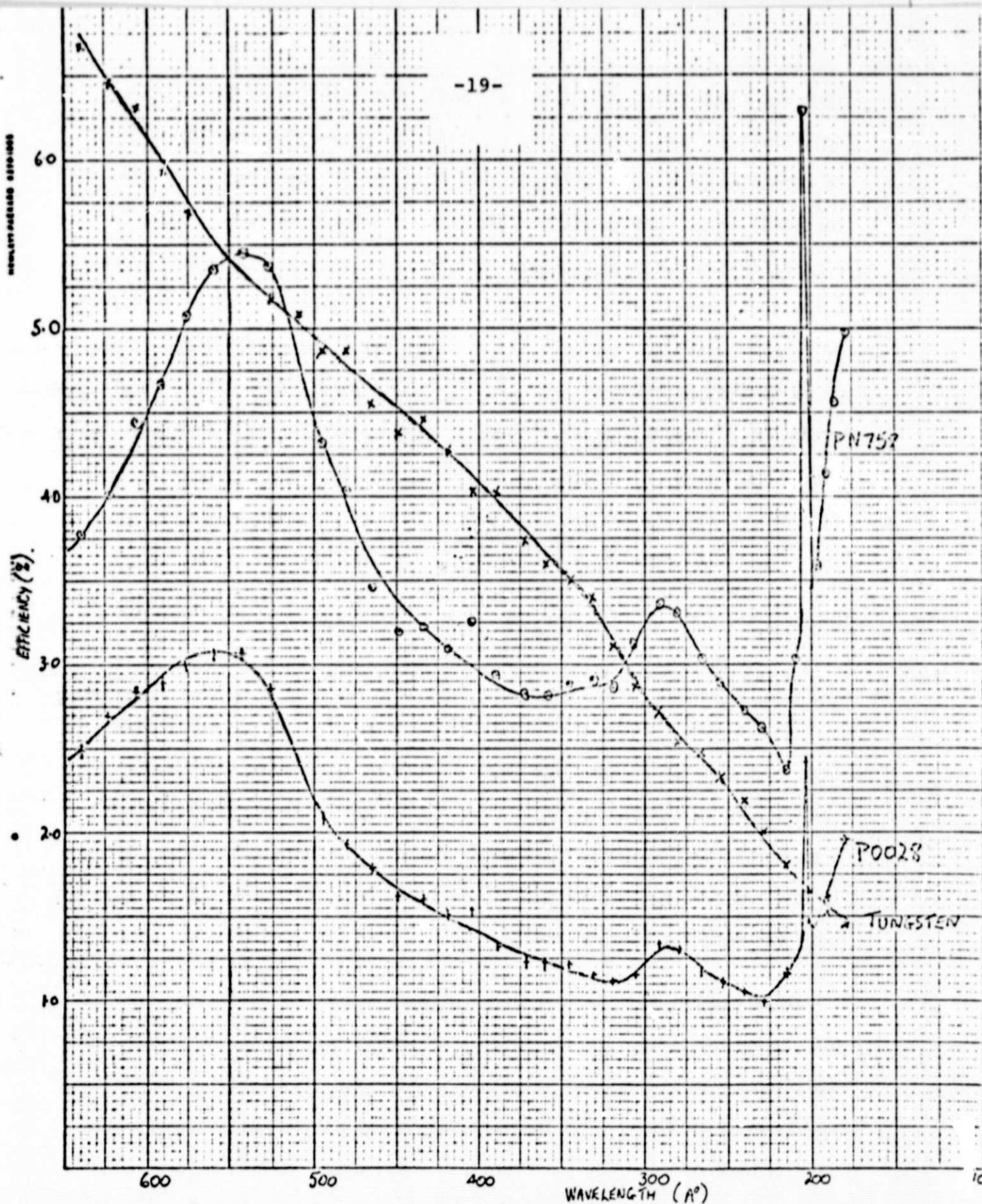


Fig. 14. Absolute efficiency of the Magnetic Electron Multipliers #131 (tungsten), #PN758 (Li F), and #P0028 (Li F) as a function of wavelength.

That is, the denominator of Eq. (1) must be multiplied by 19/4. If the sensitivity of the cathodes was constant in the y-direction then the No. of counts would also be multiplied by this ratio. However, as we have seen the sensitivity varies with position on the cathode surface. Thus, in Fig. 6 for the tungsten photo-cathode we can determine the number of counts using the entire length of cathode (19 x 4 mm) relative to a central strip of length equal to 4 x 4 mm. Using a planimeter the ratio of counts for 19 mm to 4 mm is equal to 4/1. Similar measurements using Fig. 7 and 8 give ratios of 7.1/1 and 5.6/1 for the LiF cathodes #PN758 and # P0028, respectively. This means that the efficiency of the multipliers can be obtained from Fig. 14 for a photon beam of 19 mm in length by multiplying the results in the Figure by the following factors.

MEM #131	Multiply by 0.84
#PN758	Multiply by 1.50
#P0028	Multiply by 1.18

For a more precise correction the data of Figs. 6, 7, and 8 should have been made along the "60% line" of Fig. 1. However, the tungsten data of Fig. 10 is almost exactly on the "60% line". Comparing the central 4 mm sensitivity with the full cathode length yields a ratio of 3.93/1 in this case. That is, the correction factor is 0.83 in excellent agreement with our more approximate result.

One problem with an extended continuum source of radiation, such as synchrotron radiation, is the problem of identifying second or higher order radiation. In the present work this problem was minimized by the use of an aluminum filter (about 1000 Å thick). The filter has a transmission band between 170 and 800 Å. Thus, no second order radiation appears between 170 and 340 Å. At 340 Å the second order of the aluminum edge is observed and accounts for about 9% of the signal. Thus, the data at longer wavelengths was further improved by normalizing the results to data at the 584 Å He I line.

III. MEASUREMENT OF GRATING EFFICIENCY

The efficiency of a replical L & L grating, serial No. 1203-1-5, was measured in the 1st and 2nd orders in the wavelength range 150 to 555 Å. This was a 1 M grating with 1152 lines/mm. Measurements were made at an angle of incidence of 82.5°.

The efficiency of the grating was defined as the intensity of radiation of a given wavelength entering a given order divided by the intensity of radiation of the same wavelength incident on the grating.

A grazing incidence spectrometer was constructed to house the test grating. A photo-diode detector was designed to travel along the Rowland Circle to measure the intensity of the diffracted orders. A rotatable second photo-diode was placed so that it could intercept the incident monochromatic radiation and give a measure of its intensity. The sensitivity of the two photo-diodes were measured relative to one another. The first photo-diode detector was made from aluminum 7 cm in height. This assured that the entire astigmatic image was collected.

The efficiency of the grating was measured over the full ruled area. However, to simulate the actual illumination conditions of the grating when in flight the central 56% horizontal portion of the grating was masked. The loss in signal caused by this masking precluded measurements of the weaker emission lines in our light source. However, sufficient data were obtained over the spectral range to show that the overall curve followed, in shape, that taken for the entire grating surface. In general, the masked grating was about 10% more efficient than the unmasked grating.

The efficiency data for the masked and unmasked grating are tabulated in Table I and displayed in Fig. 15.

The incident monochromatic radiation was baffled so that the light just filled the test grating. A rotatable photodiode was located between the last baffle and the grating.

In order to baffle the central 56% horizontal portion of the grating the central portion of the last baffle (nearest the grating) was blocked off by a piece of tape. The grating illumination was observed in white light and the size and position of the tape adjusted until the desired illumination was obtained.

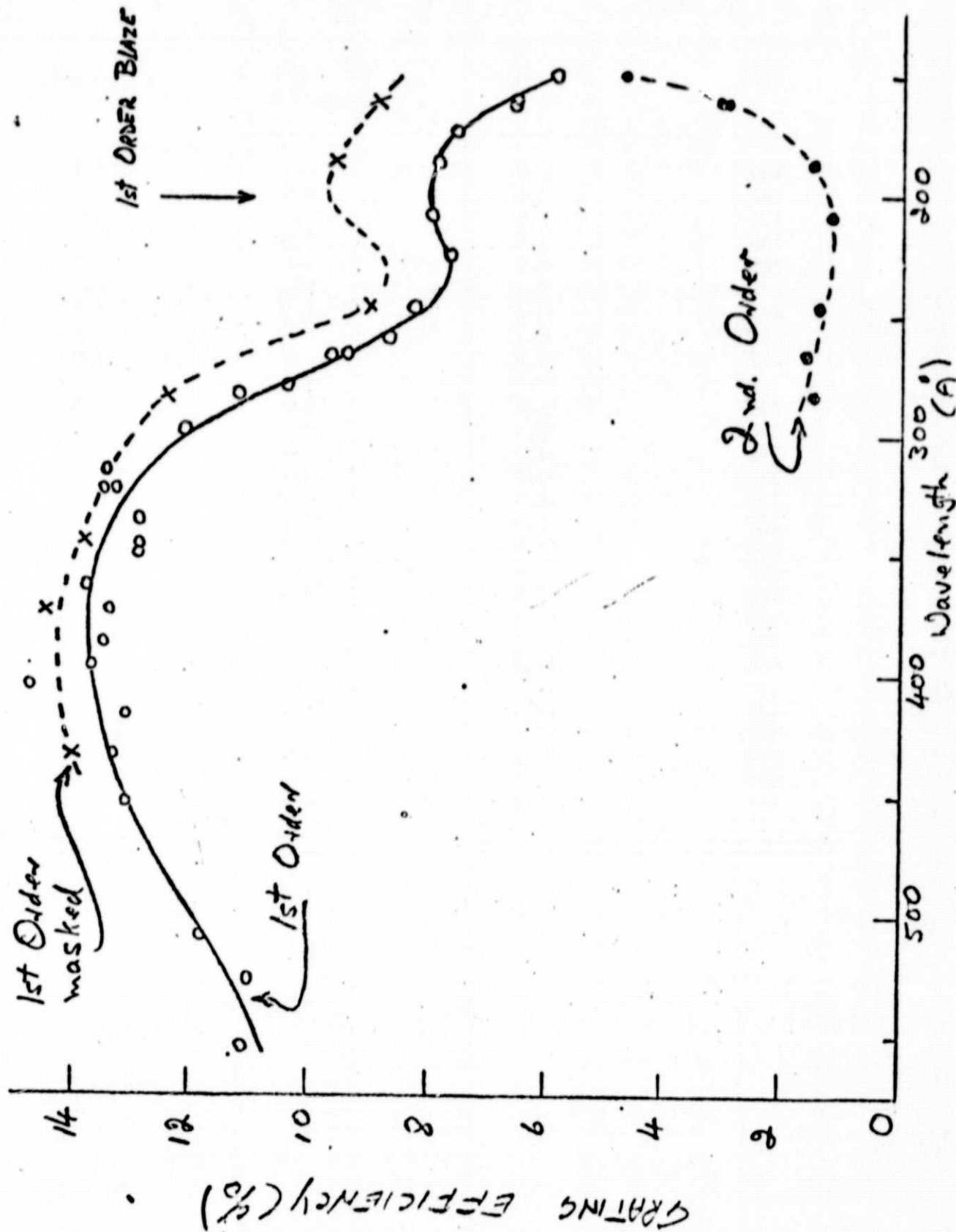


Fig. 15. Grating efficiency.

TABLE I. Efficiency Measurements for B & L Grating #1203-1-5.

$\lambda(\text{\AA})$	1 st Order %	1 st Order (masked) %	2 nd Order %
150	5.9	---	4.7
162	6.6	8.9	3.1
173	7.6	---	---
186	7.9	9.6	1.5
209	8.0	---	1.2
225	7.7	---	---
247	8.3	9.0	1.4
260	8.7	---	---
267	9.5	---	1.6
280	10.4	---	---
284	11.2	12.4	1.5
298	12.1	---	---
315	13.5	---	---
323	13.4	---	---
335	12.9	---	---
345	12.9	13.8	---
350	12.9	---	---
363	13.8	---	---
375	13.4	14.5	---
387	13.5	---	---
396	13.7	---	---
405	14.8	---	---
416	13.1	---	---
434	13.3	14.0	---
452	13.1	---	---
510	11.8	---	---
526	11.0	---	---
555	11.1	---	---

REPRODUCIBILITY OF THE
ORIGINAL PAGE IS POOR

IV. POLARIZATION PRODUCED BY GRATINGS

The degree of polarization of the NASA/GSFC grating was measured in the first order from 200 to 584 Å, in zero order at 584 Å, and in second order for the HeII 304 Å line. The measurements were made at an angle of incidence of 82.5°. The results are shown in Fig 16.

There is an interesting trend in the data. Starting with a rather high degree of polarization at 584 Å (about 31%) the polarizing effect of the grating decreases to a minimum around 300 Å (304 Å has a degree of polarization = 3%) then starts to rise again at shorter wavelengths. Unfortunately the signals were too weak to measure polarization effects at shorter wavelengths. However, the polarizing effect could be studied for zero order 584 Å. This was possible by using a helium dc glow discharge at high pressure. Thus, the only significant radiation present at wavelengths shorter than 1200 Å was the 584 Å line. A low degree of polarization was obtained (9.5%).

The degree of polarization seems to be strongly dependent on the order, thus, the 584 Å first order line is about 3 times greater than the zero order line. This trend holds also for the 304 Å line. In second order (8.5%) the degree of polarization is again about 3 times larger than the 1st order. No general statement can be made at this time, but there is a suggestion that the degree of polarization is a function of the diffraction angle β in addition to the normal effect of reflection from a metal surface. More evidence of this will be discussed below.

Although 1st order 584 and 2nd order 304 Å have about the same angle of diffraction their optical constants (n and k) and reflectance are quite different and so it is not surprising that they do not have equal degrees

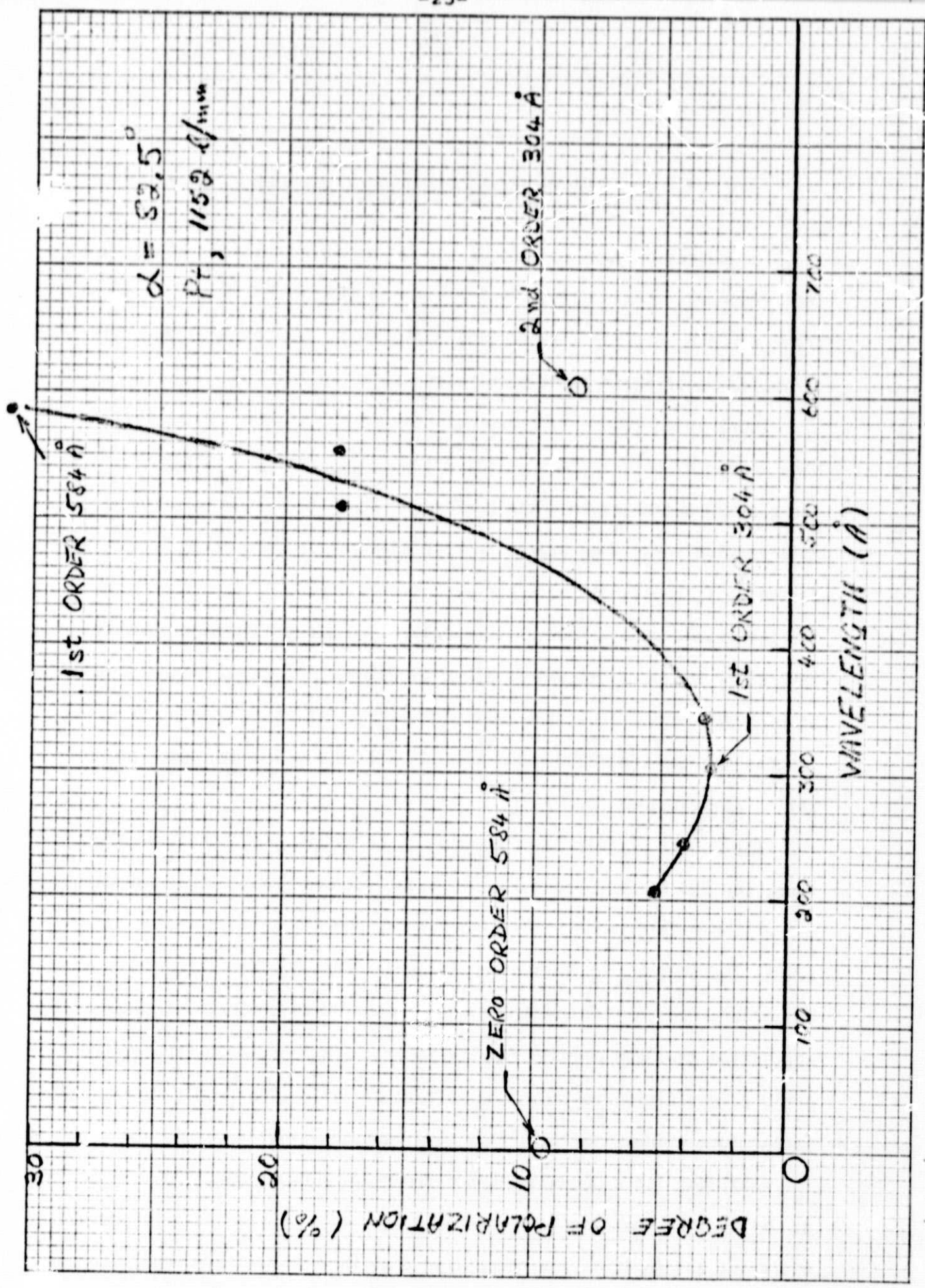


Fig. 16. GSFC grating

of polarization.

In Fig. 17 the degree of polarization of the GSFC grating is shown for an angle of incidence of 80° . At this angle of incidence the test apparatus could not utilize lines of wavelength longer than 440 \AA (or $2 \times 220 \text{ \AA}$). Thus, measurements were made from 200 to 435 \AA in the first order, with a single measurement of the second order 209 \AA line and the zero order of 584 \AA .

The degree of polarization for the zero order 584 \AA line was 14.5%, for the first order 304 \AA line it was 6.8%, and for the 1st and 2nd order line at 209 \AA the degree of polarization was 0.7% and 10.4%, respectively.

The trend for the degree of polarization to increase as the wavelength increases is similar to the results measured at 82.5° . The large value of P for zero order 584 \AA suggests that P may reach about 45% in first order, assuming that the relation of a factor of three increase that was observed at 82.5° still holds for 80° angle of incidence.

The degree of polarization of the NASA/GSFC McPherson grazing incidence monochromator was measured between 200 and 800 \AA . The grating was a 600 line/mm aluminum replica. The angle of incidence depended on the mode of operation. With the light source stationary and the detector moved to scan the spectrum $\alpha = 82^\circ$. On the other hand, with the light source moving and the detector fixed ($\beta = 82^\circ$) the angle of incidence varied with wavelength from $\alpha = 82^\circ$ to 70° . The actual values are given in Table II. Although the angles of incidence vary in the two modes of operation there is a symmetry between α and β . For example, in the fixed light source mode $\alpha = 82^\circ$ and $\beta = 70^\circ$ at 800 \AA and the inside spectrum is used. When the light source moves we have $\alpha = 70^\circ$ and $\beta = 82^\circ$ at 800 \AA and the outside spectrum is used. Thus, in both cases the blazed wavelength is constant.

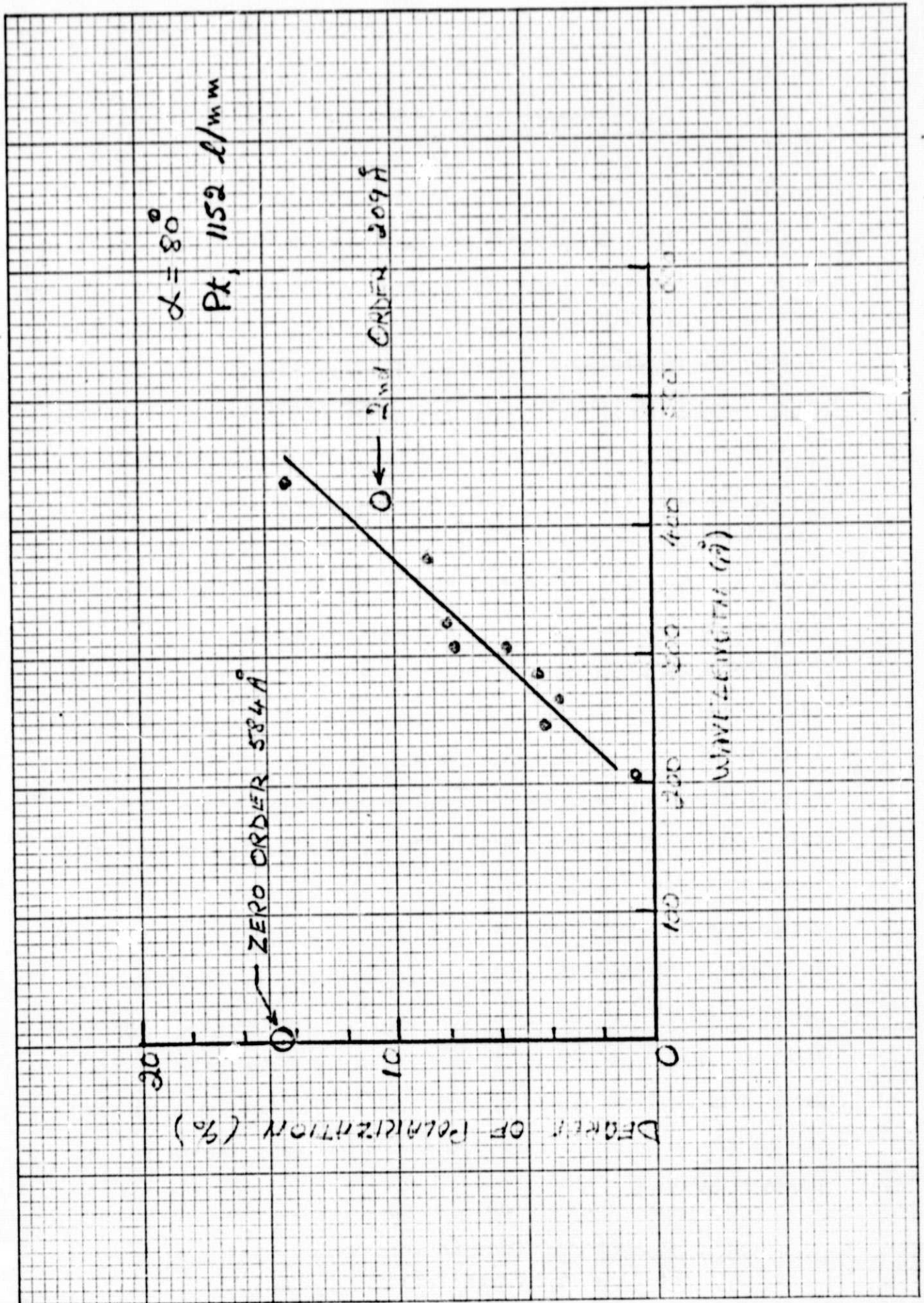


Fig. 17. GSFC grating.

TABLE II. Variation in angle of incidence with
the McPherson Grazing Incidence Monochromator
with a moving light source ($\beta = 82^\circ$)

$\lambda(\text{\AA})$	α°
0	82
100	79.8
200	78.0
300	76.5
400	75.1
500	73.8
600	72.6
700	71.5
800	70.4

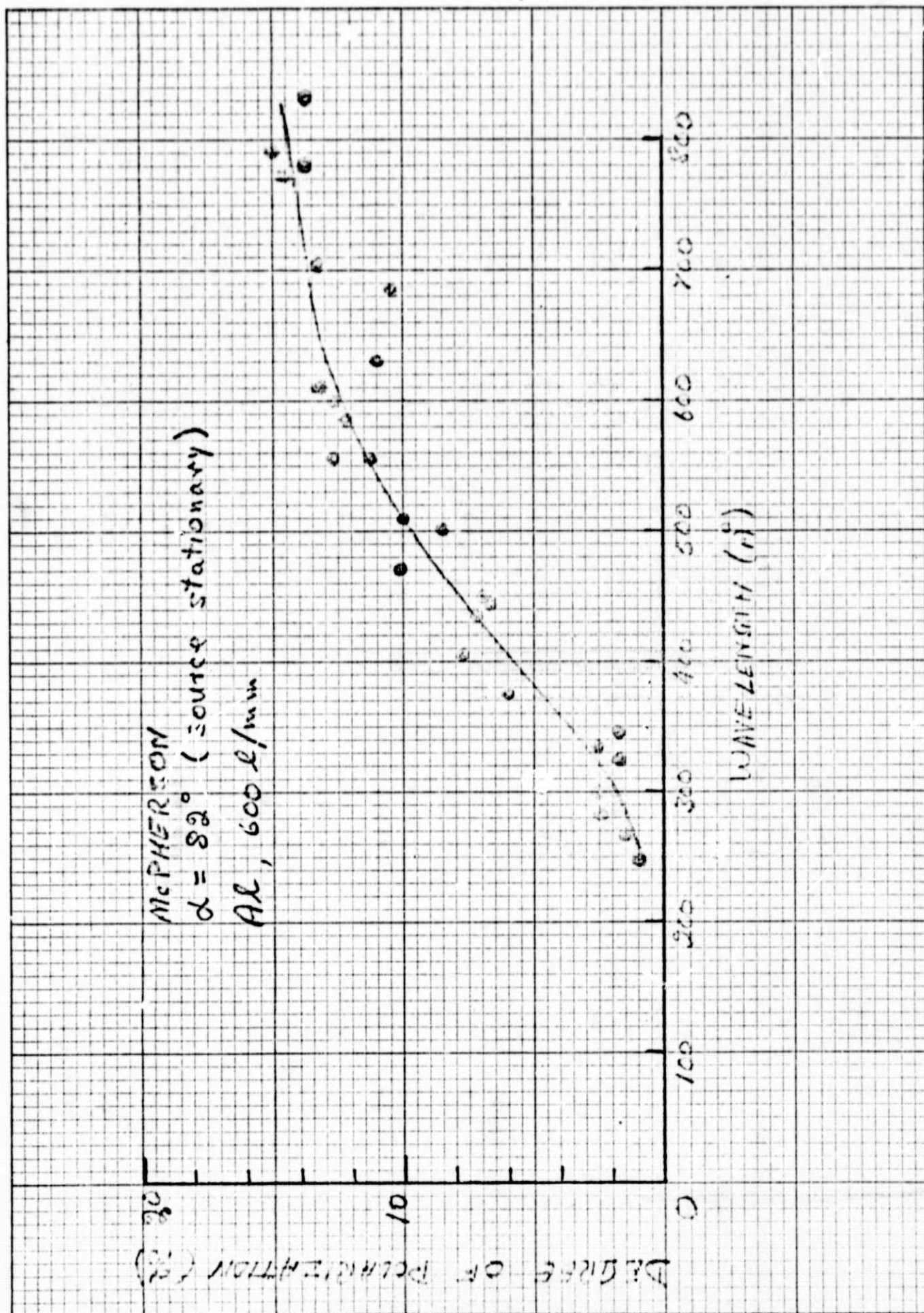
The symmetry between α and β and the constancy of the blazed wavelength appears to be significant because the degree of polarization of the instrument is independent of the mode of operation. The results of our measurements are shown in Figs. 18 and 19.

The degree of polarization of our Vodar Grazing Incidence Monochromator was measured between 185 Å and 560 Å. The grating was a 600 line/mm platinized replica. The angle of incidence was fixed at 84°. The results are shown in Fig. 20.

The results with the Vodar instrument follow the same trend that we have observed with all other instruments and with a variety of coatings (Al or Pt, new or old).

The results to date on grazing incidence polarization effects between 180 and 800 Å have shown a consistent trend with wavelength. Namely, a decrease in polarization with a decrease in wavelength. A study of the optical constants n and k of various materials shows that almost all materials have decreasing values of k as the wavelength decreases below 800 Å. A calculation of the degree of polarization for $\alpha = 82^\circ$ with a fixed n and varying k shows that the degree of polarization decreases as k decreases (See Fig. 21). For most materials n is either decreasing or is constant between 200 and 800 Å (ref: H. J. Hagemann, W. Gudat, and C. Kunz, DESY report SR-74/7, May 1974). Certainly this is approximately true for Au and Al_2O_3 as shown in Table III. Thus, we feel that the general statement can be made that the degree of polarization produced at grazing angles of incidence will decrease with wavelength, at least down to 200 Å.

A search of the literature reveals that only two measurements have been made previously on the degree of polarization produced by a grazing incidence monochromator as a function of wavelength. Both of these reports



K-E 10 X 10 TO THE INCH 46 0700
7 X 10 INCHES
KEUFFEL & ESSER CO.

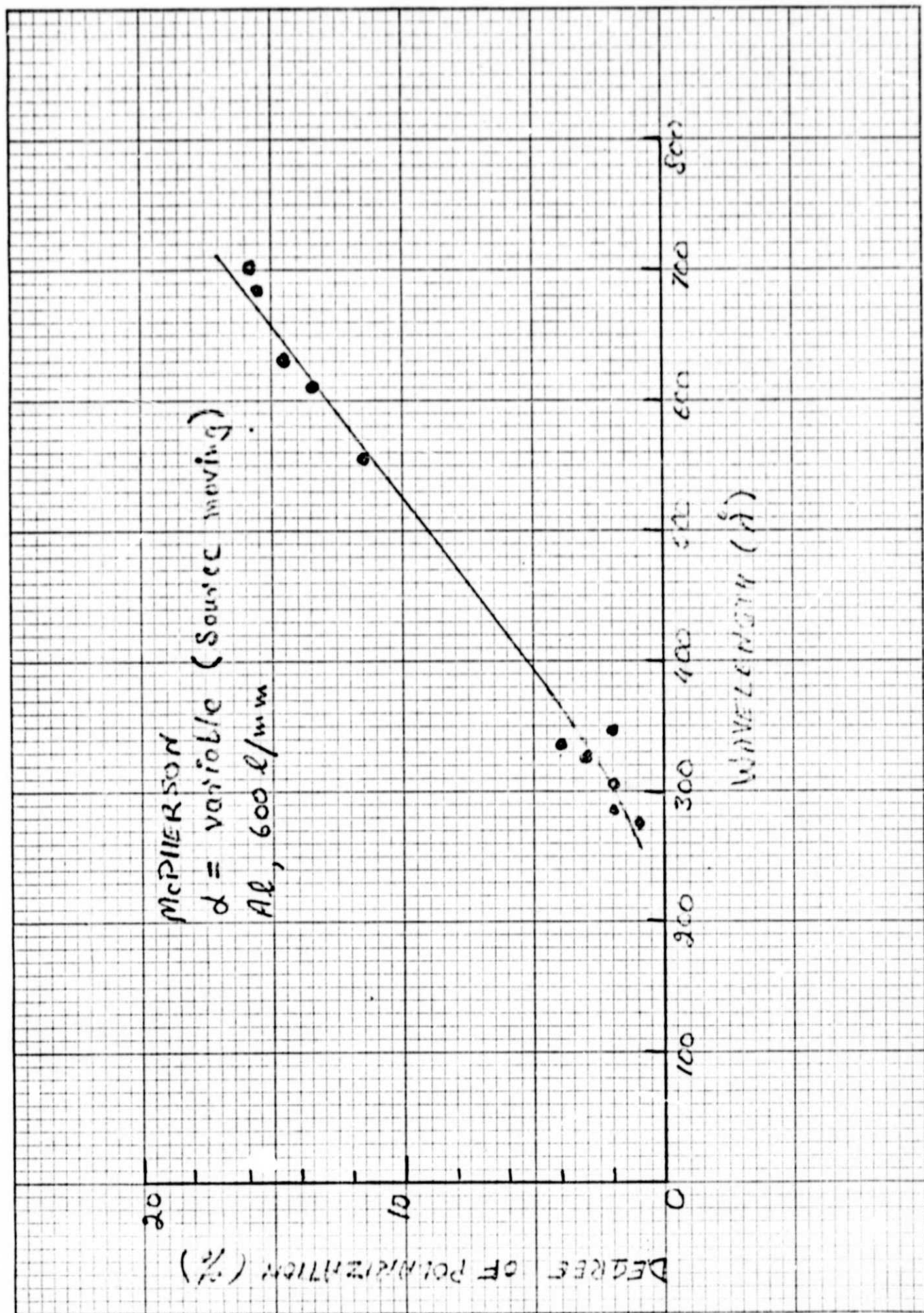


Fig. 19.

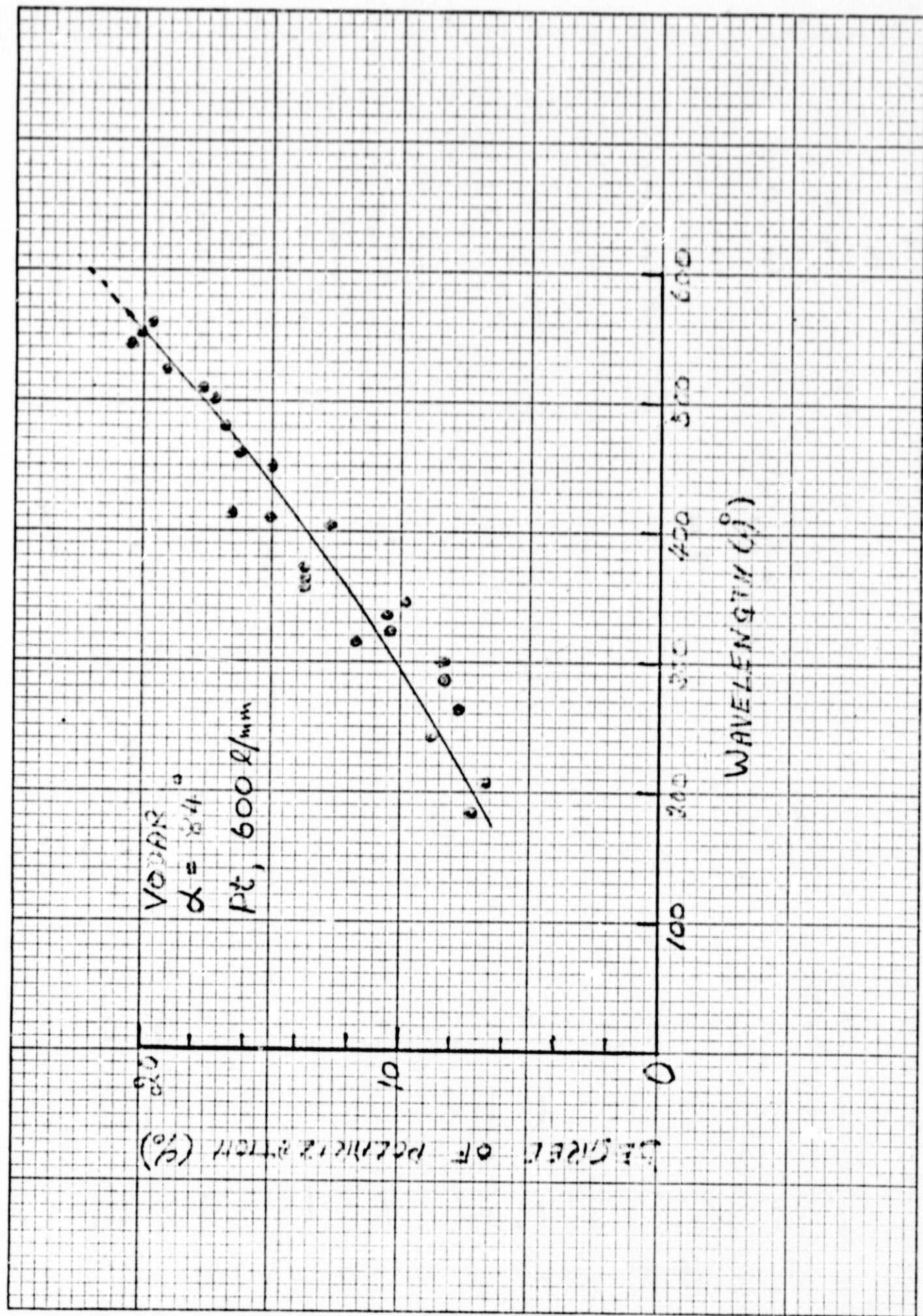


Fig. 20.

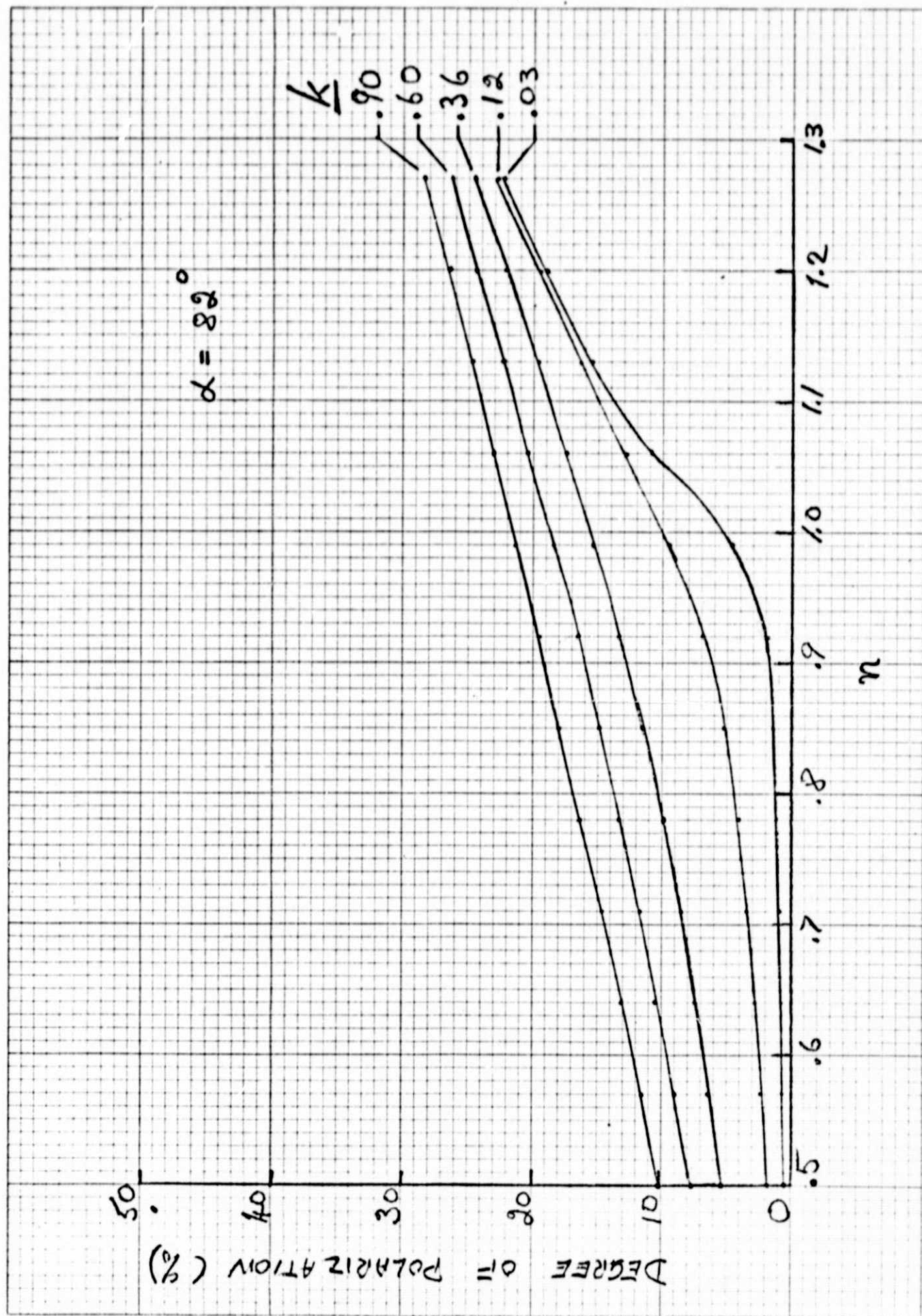


Fig. 21.

TABLE III. Optical Constants of Some Grating Materials

λ Å	Pt ^a	Au ^b	AlO ₃ ^b	Al ^c	Glass ^c	Cer-Vit ^d
584 n	0.85	1.24	0.81	0.84	0.82	0.80
k	0.91	0.88	0.71	0.13	0.40	0.47
304 n	----	0.80	0.85	----	----	0.90
k	----	0.32	0.14	----	----	0.09

^aG. Hass, J. B. Ramsey, and W. R. Hunter, Appl. Optics 8, 2255 (1969).

^bH. J. Hagemann, W. Gudat, and C. Kunz, DESY report SR-74/7, May 1974.

^cE. Uzan, H. Damany, and J. Romand, C. R. Acad. Sci. 250 B, 5735 (1965).

^dJ. F. Osantowski, J. Opt. Soc. Am. 64, 834 (1974).

are in the wavelength range from 300 to 1200 Å. [Ref: T. T. Cole and F. Oppenheimer, Appl. Optics 1, 709 (1962); and G. Stephan, J. C. Lemonnier, and S. Robin, J. Opt. Soc. Am. 57, 486 (1967).] Again, the same decrease with wavelength is observed.

There appears to be no question that the trend reported here is a general one for typical conditions found in grazing incidence spectrometers. Minimum polarization is found around 200 Å. However, absolute values depend on grating coatings and angle of incidence. For wavelengths shorter than 200 Å the DESY reports shows that for most materials n begins to increase and k is usually less than 0.1. Thus, an increase in the degree of polarization is expected for wavelengths shorter than 200 Å. This trend is already visible in Fig. 16.

The actual measurements of the degree of polarization produced by the gratings was performed as follows: The reflectance R_1 of a front surface gold mirror was measured at 45° in the horizontal plane using the radiation diffracted by the grating. The mirror was then rotated 90° and the reflectance R_2 measured again ^{at 45°} (vertical plane). The degree of polarization is then obtained from the relation,

$$P = (R_2 - R_1) / \left\{ 1 + R_1 + R_2 - \left[1 + 4(R_1 + R_2) \right]^{\frac{1}{2}} \right\}.$$

The reflectometer or polarization analyzer was constructed as shown in Fig. 21(a). Three identical gold mirrors were made by evaporation of gold onto flat glass substrates. Each mirror had an electric contact connected. Mirror #1 was used as a photodiode to monitor the intensity of the incident monochromatic light. This detector could then be rotated out of the beam to

allow the radiation to strike mirror #3. This is the mirror we wish to measure the reflectance at 45° . The reflected light then strikes mirror #2 which acts as a photodiode and thus measures the reflected intensity. The sensitivity of the photodiodes (mirrors #1 and 2) were compared and found to be of equal sensitivity. The ratio of the signals from these two detectors gives the reflectance. Mirror #3 is held at a positive potential (about +50V) to prevent photoelectrons from leaving it and also to provide the field extracting electrons from #2. Mirrors #2 and 3 are then rotated on a fixed assembly to allow the reflectance to be measured at 90° .

In the grating reflectometer unit constructed for the GSFC the polarization analyzer mounts onto a detector assembly that is free to move along the Rowland Circle. An electric motor was mounted onto the analyzer so that rotation could be performed by remote control and while the apparatus was under vacuum (the motor is not an integral part of the unit as it was borrowed from equipment belonging to the University of Nebraska).

V. PHOTOELECTRIC YIELD STUDIES OF VARIOUS CATHODES

The photoelectric yield of several compounds of fluorine and iodine were investigated for their stability to humidity. The absolute yields of these cathodes and of Be, BeO , BeCu , and Pt were also measured.

A double ionization chamber was used to provide the absolute calibration of a tungsten photocathode. The test cathodes were then measured relative to this standard cathode. A grazing incidence monochromator was used to provide radiation from 150 to 600 Å. Absolute calibrations were made with a discrete line emission source in the laboratory while the relative yields were measured with the continuum radiation emitted from the Wisconsin synchrotron radiation source. This provided information at the absorption edges of Li and Mg.

1. LiF , NaF , MgF_2 , RbF_2 , SrF_2 , CaF_2 , CsI , KI .

The chemicals used were all reagent grade powders obtained from three sources. All but two of the eight chemicals were ordered from Alfa-Products in Beverly, Massachusetts. These were: NaF , MgF_2 , RbF_2 , SrF_2 and CsI . Each was at least 99.5% pure. The other two, KI and CaF_2 were purchased from Allied Chemical and from Fisher, respectively.

The stainless steel substrates that the chemicals were evaporated onto measured approximately 1" x 1 1/2" x 1/8". One side of the substrate was surface ground flat and polished with a buffing wheel to a mirror like finish. The substrates were then cleaned, first using soap and water, then with acetone, and finally with Isopropyl alcohol. In each stage of the cleaning process it was necessary to physically rub the surface with a soft

lint free towel. At the end of the process the substrate was rinsed with Isopropyl alcohol. The cleanliness of the substrate is of utmost importance in obtaining uniform films.

It was important to be able to measure the thickness of the evaporated film as it was being deposited to insure reproducibility. This was accomplished with the use of a quartz crystal film thickness monitor. The results obtained using this instrument may not be absolute in thickness measurement for each material, but the deposition is quite reproducible.

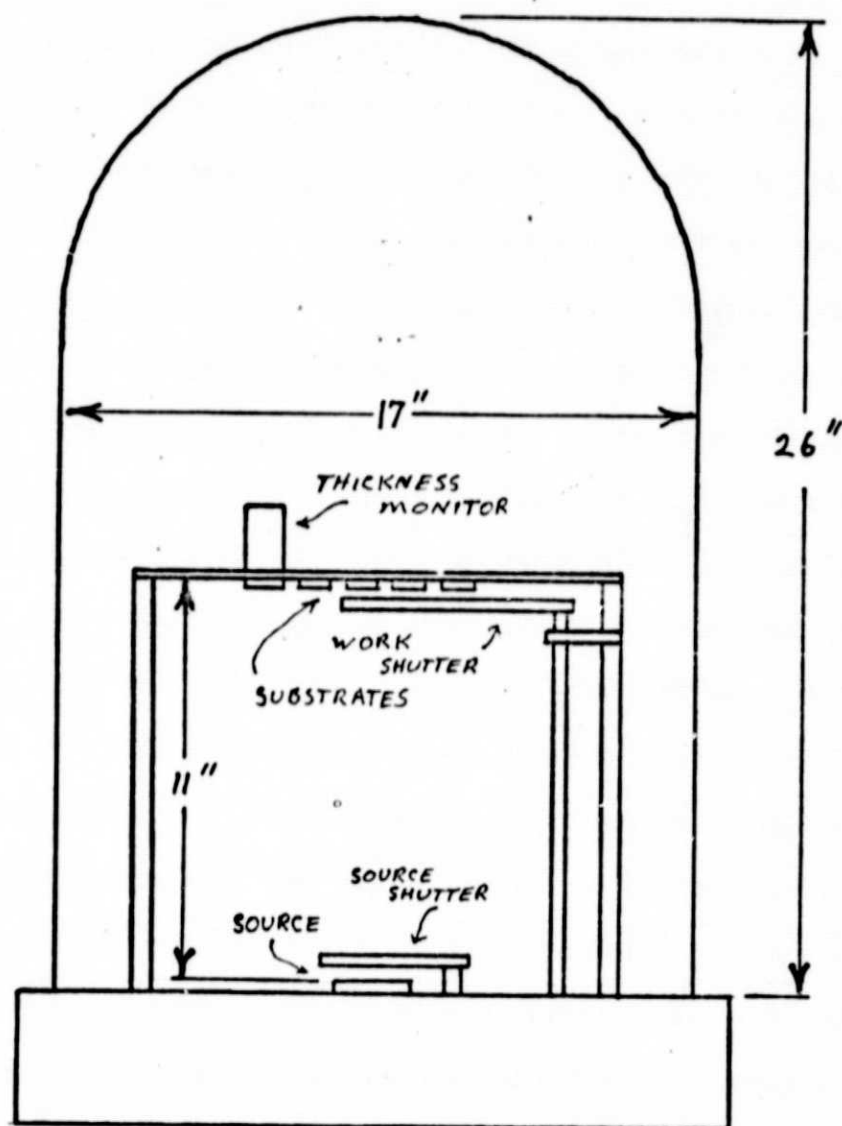
The Evaporation System

The system we used consisted of a glass bell jar measuring 17" in diameter and 26" tall, and related pumping apparatus. The substrates were supported approximately 11" above the evaporation source and situated as close to the center of the bell jar as possible (see Fig. 22).

The system was equipped with two shutters, one just above the source and one just below the substrates (work shutter). The work shutter was designed such that four substrates could be sequentially exposed to the evaporation source and in this way it was possible to make four photo-cathodes of different thickness in one evaporation process. The pressure in the system during most of our evaporation was around 5×10^{-5} Torr and proved to be satisfactory.

Because the chemicals to be evaporated are powders the system should be roughed out slowly, otherwise the powder will outgas violently and may be thrown out of the source boat. This can also occur if the boat is heated too rapidly.

The source boat we used was made from 0.010" molybdenum and had a capacity of about 2 cc. The length of the boat was about 4 cm and the width about 1 cm. For most of the substances evaporated it was necessary



THE EVAPORATION SYSTEM

FIG. 22

to pass about 200 Amperes through the boat to reach the temperature at which the speed of evaporation was sufficient. The rate we normally tried for was around 50 to 100 Å/sec as observed with the thickness monitor.

Procedure:

The boat is loaded with one of the powders (approx. 2 cc) and is positioned under the source shutter. The substrates are cleaned and mounted above the source. Then the work shutter is adjusted to cover all but one cathode. The thickness monitor is positioned level with the substrates and always in view of the source (when source shutter is open).

After the system has been pumped down the boat is slowly heated (with the source shutter closed) in order to drive out the impurities in the powder. As the temperature of the boat increases the powder should melt and wet the boat. At this point the current to the boat is turned down and the pressure in the system allowed to come down to about 5×10^{-5} Torr (initial heating of the boat will cause the pressure to rise). When this pressure has been reached the boat is reheated (again with the source shutter closed) and the frequency of the monitor noted. The source shutter is then opened and the desired thickness of material evaporated. In our case this is done four times (once for each substrate). The thickness of the film on the first cathode is the sum of all the thicknesses evaporated. The thickness of the film on the second cathode is the sum of the last three films put down, etc. This is because the cathodes are exposed to the source sequentially and once exposed are left exposed (EXCEPT for being blocked by the source shutter). It should be noted that the two iodides are very hygroscopic and should be protected from the atmosphere, particularly after the evaporation process. This was done in our case by backfilling the evaporation system with He instead of merely allowing air to enter. The cathodes were then quickly transferred to a desiccator with very low humidity.

Tests were made of the insulating cathodes to check for saturation effects. In particular, cathodes of varying thicknesses of LiF and MgF were evaporated onto a steel substrate. The photoelectric yield of these samples was measured relative to a standard tungsten sample at 584 Å.

Figure 23 shows the raw data for LiF. The photoelectric current from tungsten (W) is shown on the same scale as the LiF cathodes (for constant 584 Å flux). The thickness (in Å units) of each cathode is marked on the Figure. The signal response shown should ideally be rectangular, since it represents "light on" and "light off". Deviation from this indicates charging phenomena caused by the LiF.

When the samples are thick, the LiF charges up quite rapidly thereby preventing further electrons to escape. The onset for this saturation effect appears to be about 1000 Å.

In the case of MgF_2 , (Figure 24), a saturation effect in reverse is noticed for these samples. (This is the case for LiF too, but it is not so noticeable). This increase in signal with time may be caused by the positive charge on the surface accelerating photoelectrons, ejected in the body of the cathode, towards and out of the surface. These photoelectrons are the ones which would not have escaped had the surface been neutral. As the thickness increases, the positive charge cannot be neutralized as fast as the photoelectrons leave and the signal ceases to increase. At present, this occurs at 866 Å. However, as the thickness increases, we expect saturation effects similar to LiF. The results of Figures 23 and 24 are replotted as the response of the cathodes relative to the tungsten standard. The maximum response of the fluoride cathodes have been taken and plotted as a function of thickness. These are shown in Figures 25 and 26. The response of the uncoated stainless steel substrate is also shown relative to tungsten.

Li F (584 Å)

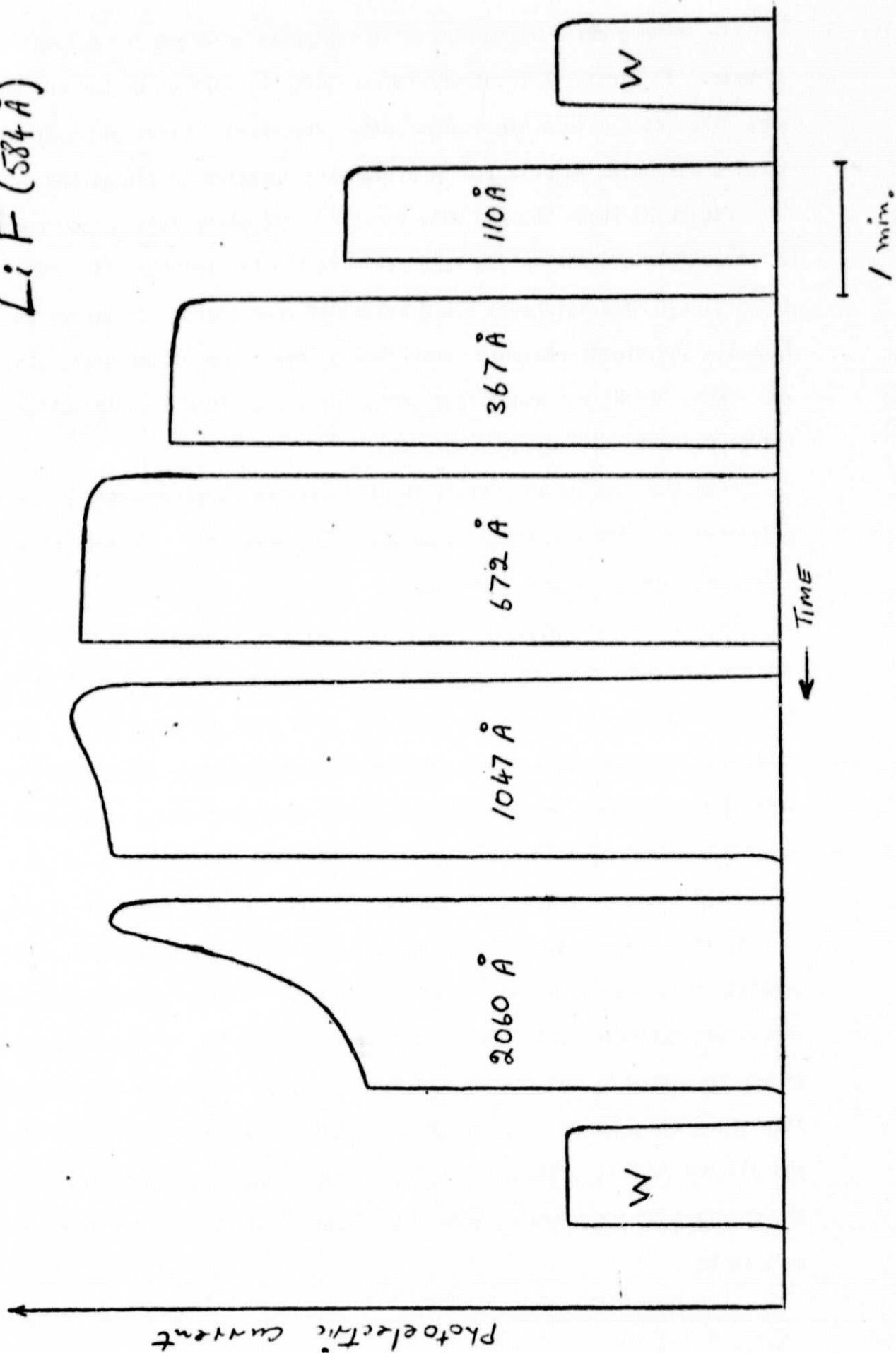


Fig. 23.

$Mg F_2 (\lambda = 584 \text{ \AA})$.

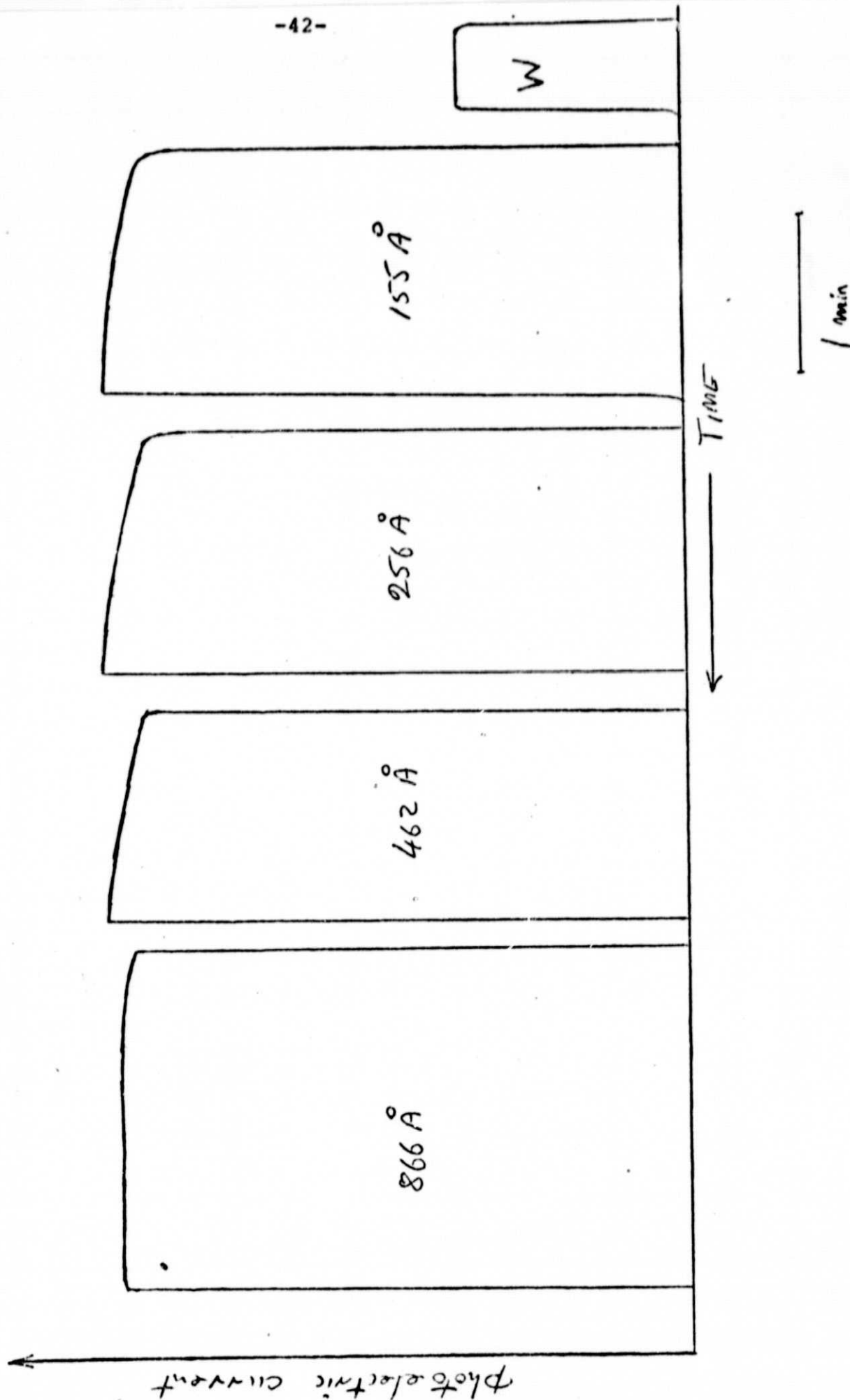
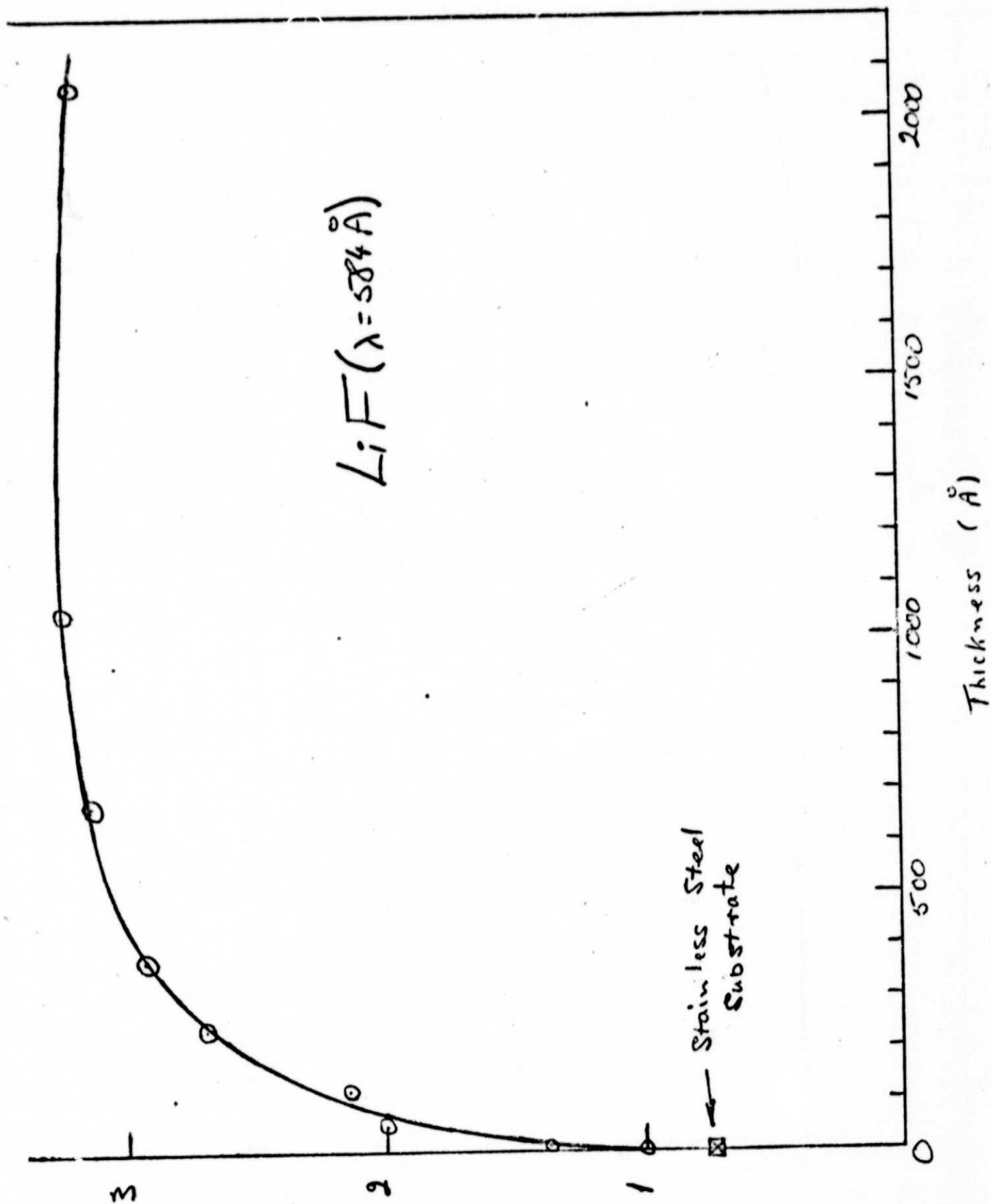


Fig. 24.



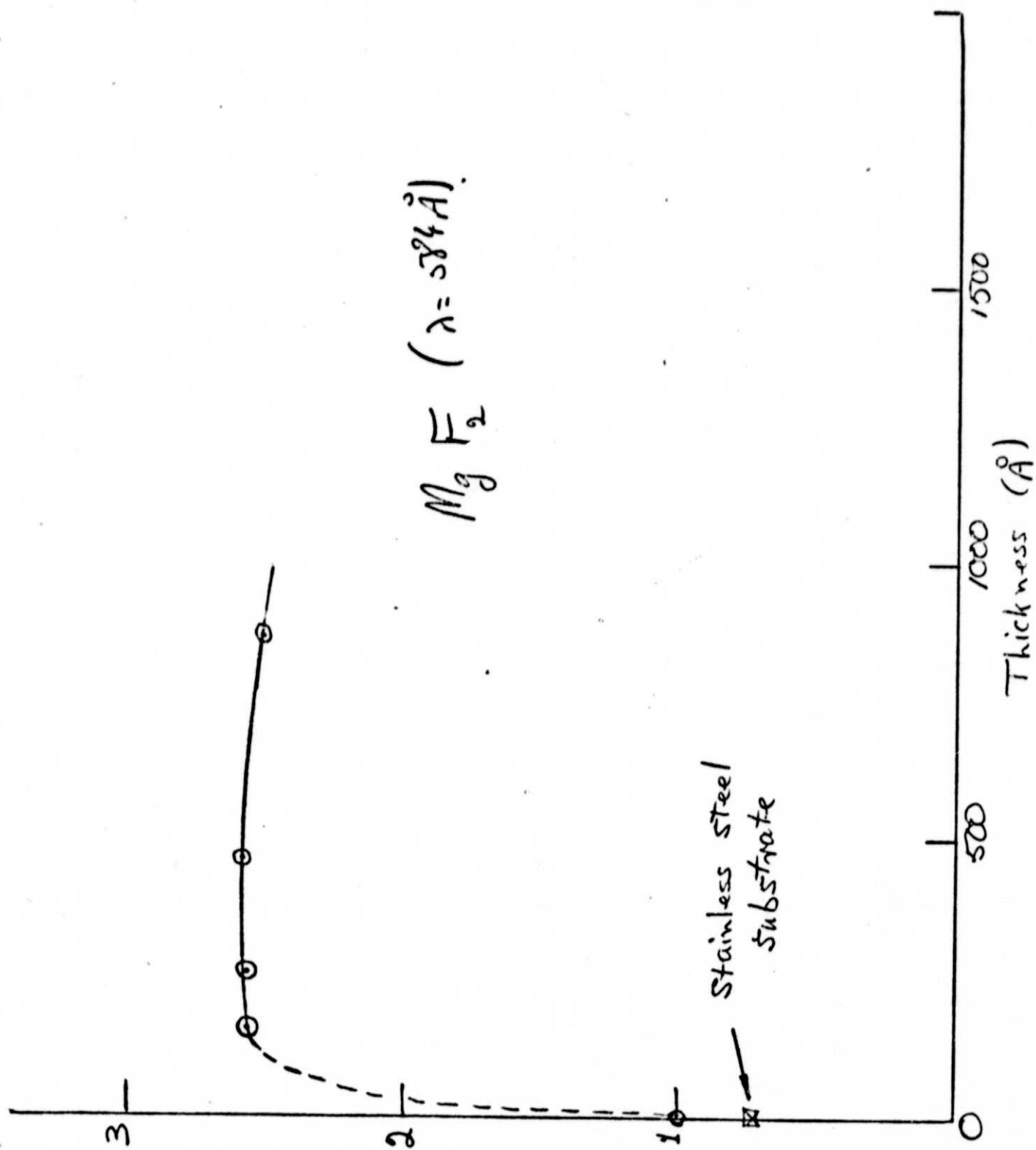


Fig. 26.

The present results recommend a cathode thickness of about 800 to 900 Å for both LiF and MgF₂.

After preparation of the cathodes they were exposed to various percentages of humidity. The first test was of Mg, Li, Sr, and Ca fluorides. The yields were all measured at 584 Å relative to tungsten. The results are shown in Table IV.

The yields of these cathodes were measured from 150 to 350 Å before and after the humidity test. The results are shown in Figures 27-30. After the humidity tests were made the yield measurements were extended to 1000 Å. See Figures 31-34. The yields of fresh samples of RbF, NaF, CsI, and KI were measured at 584 Å as a function of their exposure of a humid atmosphere. The results are shown in Table V. The efficiency of both CsI and KI were ruined with exposure to moisture. In between measurements, the cathodes were stored in dust free boxes, but in a normal laboratory environment, the RbF film discolours rapidly when exposed to air and did not give reproducible results. It sometimes recovered to its original yield.

The yields of these cathodes were measured as a function of wavelength before exposure to the humid atmosphere. The results are shown in Figures 35-38.

The following fresh cathodes were measured using the Synchrotron facility at Wisconsin, namely, Li, Mg, Na, Ca, Sr, and Rb fluorides and CsI. It was hoped that we would get absolute yields to shorter wavelengths. However, the scattered light from the grating monochromator was too great to allow quantitative measurements.

We re-ran humidity tests on these new cathodes. The results are given in Table VI for exposures to different degrees of humidity. In this test, the yield of the MgF₂ cathode dropped on exposure to moisture, whereas, our earlier test in the laboratory indicated it to be stable.

The humidity environment was created by placing the following saturated solutions in a desicator along with the cathodes under test:

$\text{CaCl}_2 \cdot 6\text{H}_2\text{O}$	produces 32.3% humidity
$\text{Na}_2\text{Cr}_2\text{O}_7 \cdot 2\text{H}_2\text{O}$	produces 52% humidity
K_2CrO_4	produces 88% humidity

In between measurements the cathodes were stored in a dust free box in a normal laboratory atmosphere.

Although the humidity of the laboratory environment was not measured, it can be estimated to be less than 20 percent owing to the time of year (January)!

In Tables IV, V, and VI the quoted percent humidity has been rounded off to 30, 50, and 90 percent.

TABLE IV. Photoelectric yields of cathodes relative to tungsten
at 584 Å after various exposures to humidity.

Condition of Cathode	MgF ₂	LiF	SrF ₂	CaF ₂
new coating	2.59	3.14	1.50	2.40
after exposure to lab. atmos.	2.40	2.90	1.52	--
after exposure to lab. atmos.	2.39	2.80	1.47	1.83
after 48 hrs. in 30% humidity	2.37	2.82	1.50	1.86
after 48 hrs. in 58% humidity	2.40	2.69	1.55	1.88
after 72 hrs. in 88% humidity	2.31	2.54	1.53	1.87
after 48 hrs. in 0% humidity	2.29	2.53	1.54	1.88
after exposure to lab. atmos.	2.28	2.51	1.57	1.88

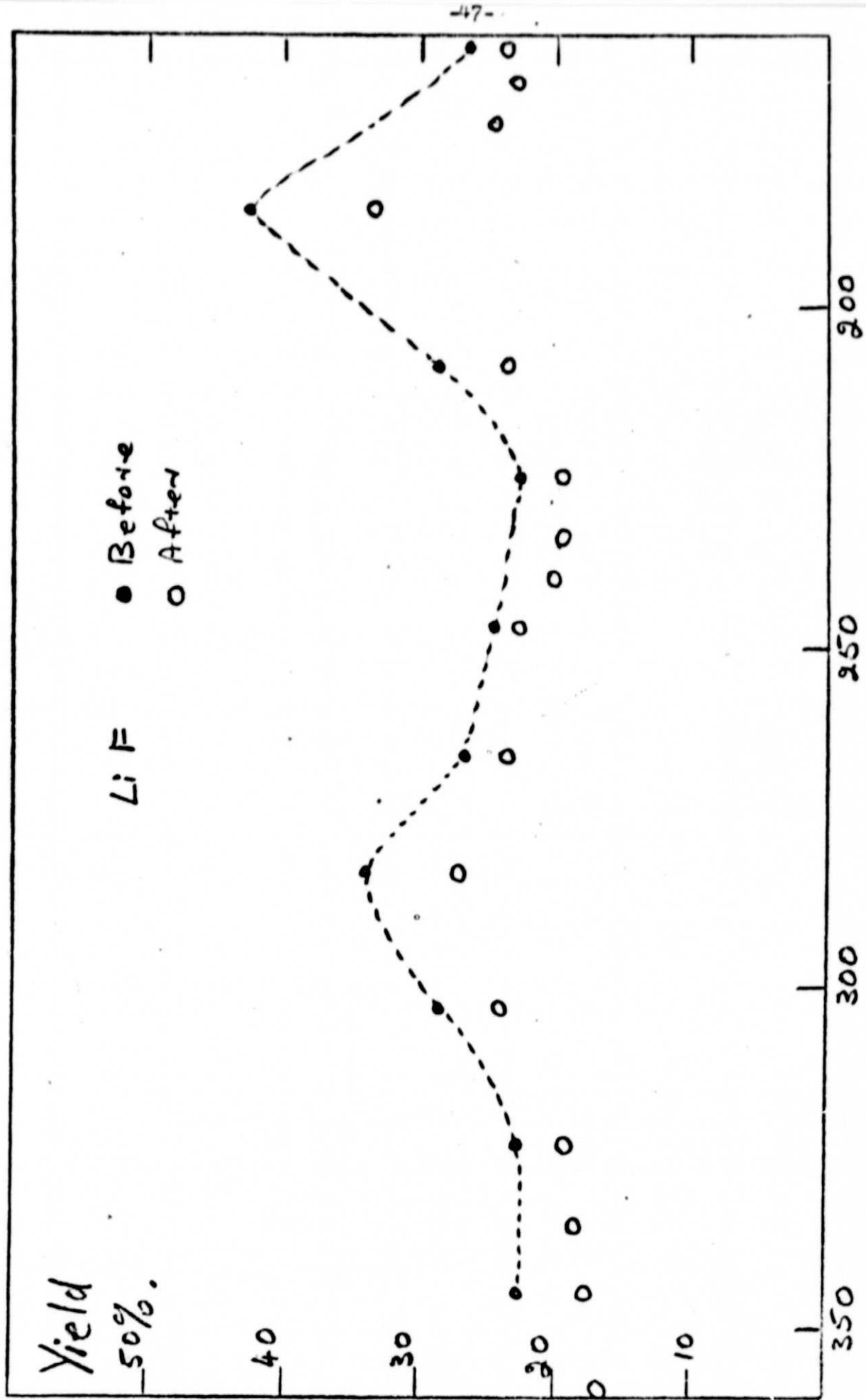
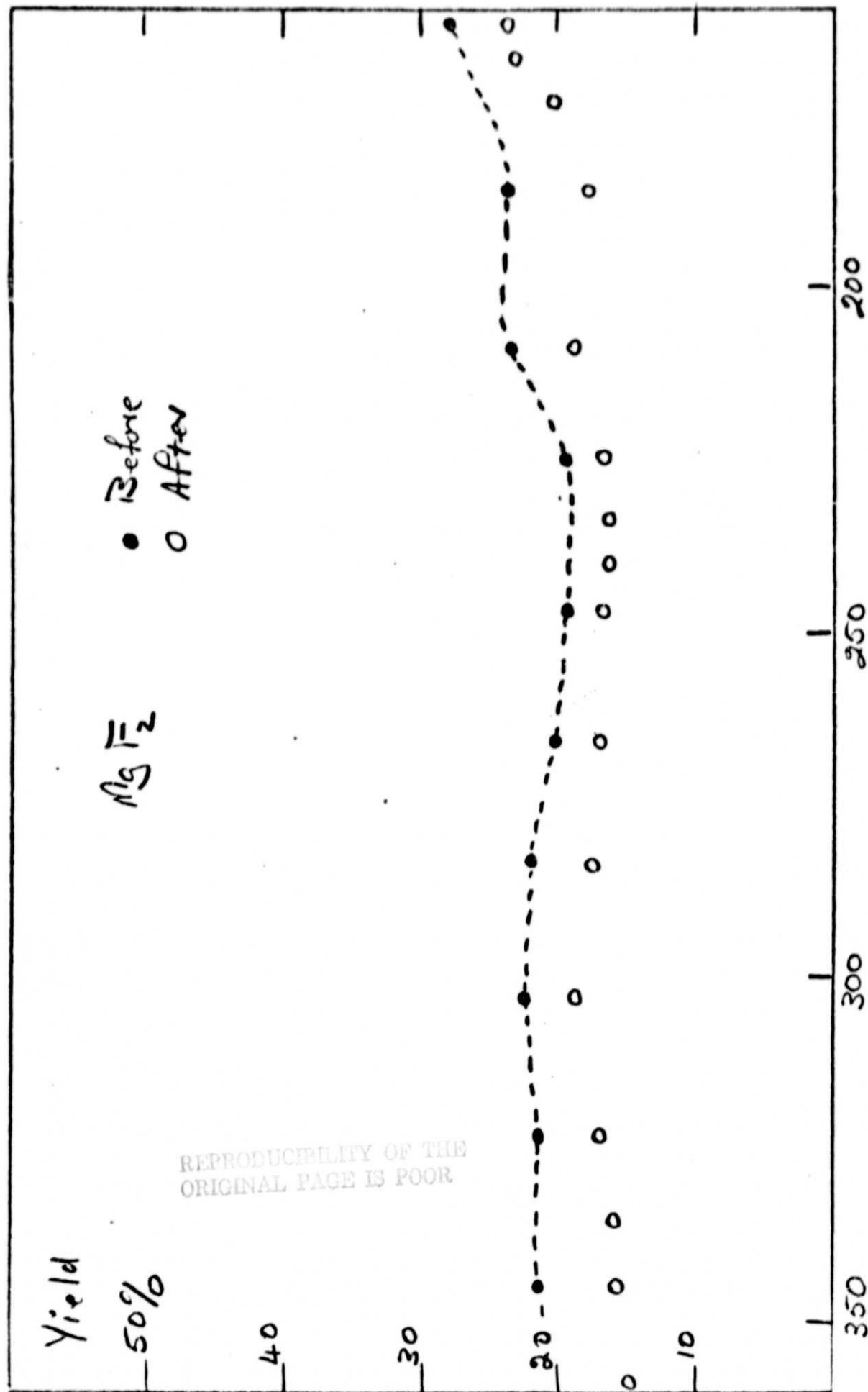


Fig. 27

Wavelength (Å)



Wavelength (Å)

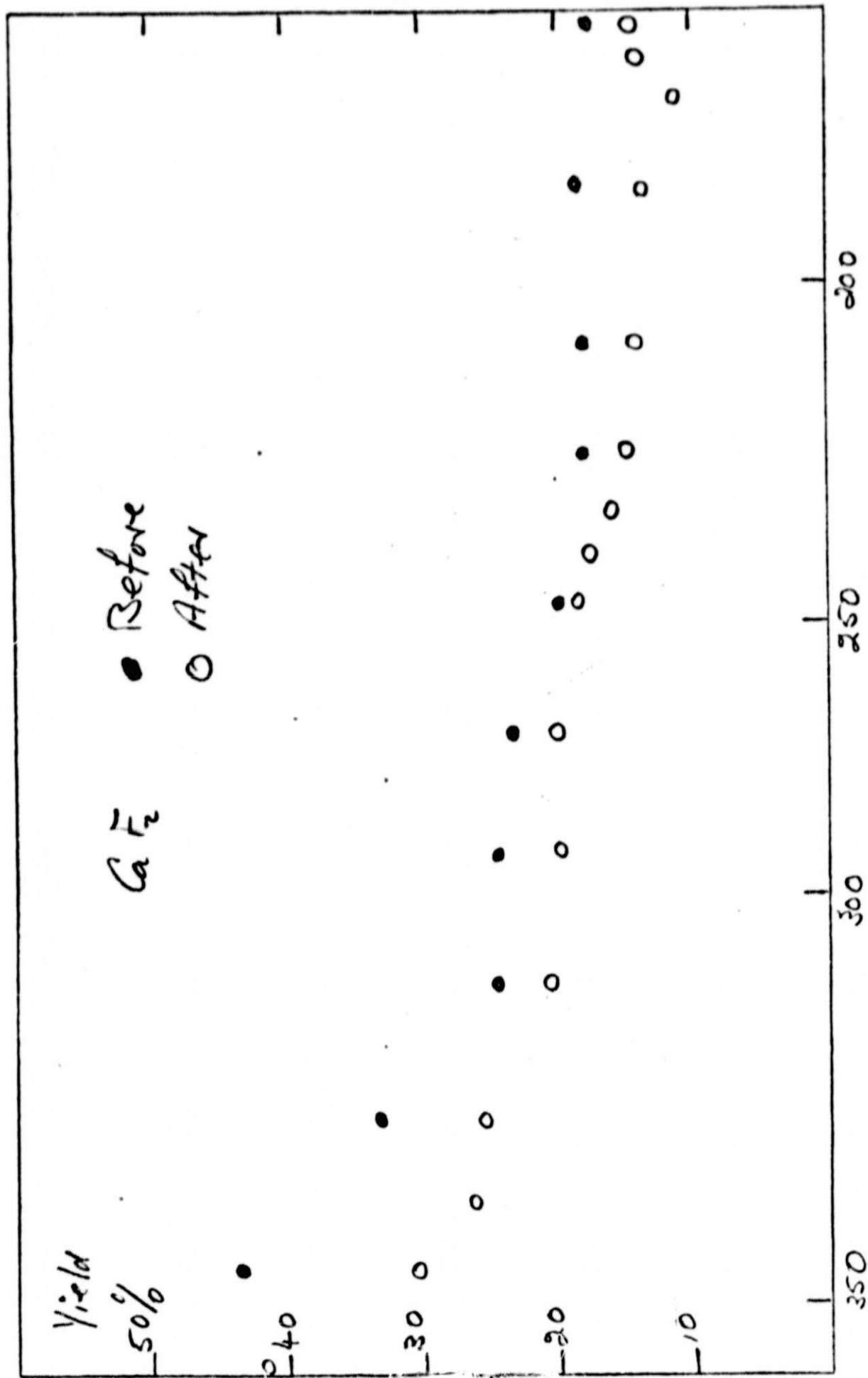


Fig. 29

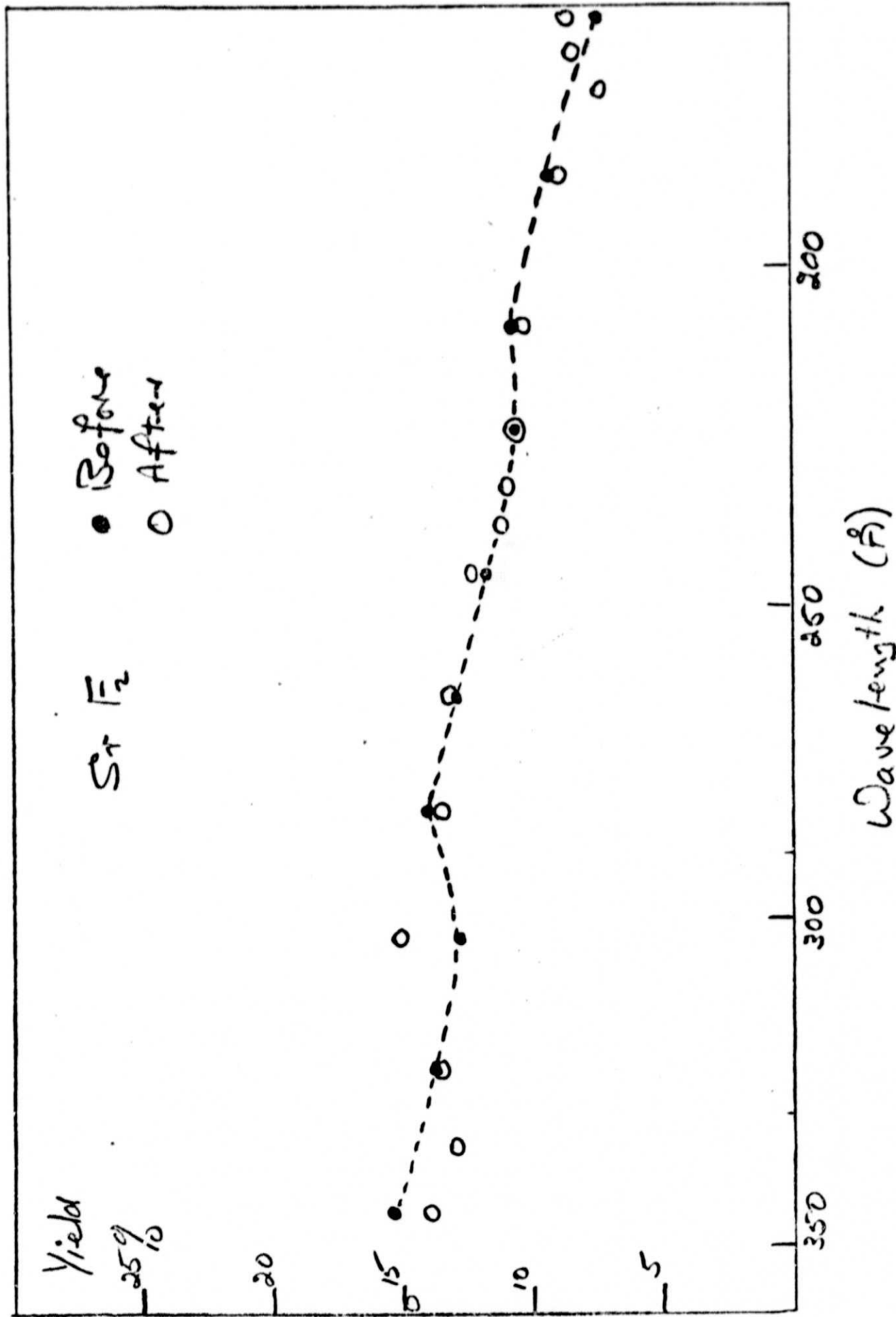


Fig. 30

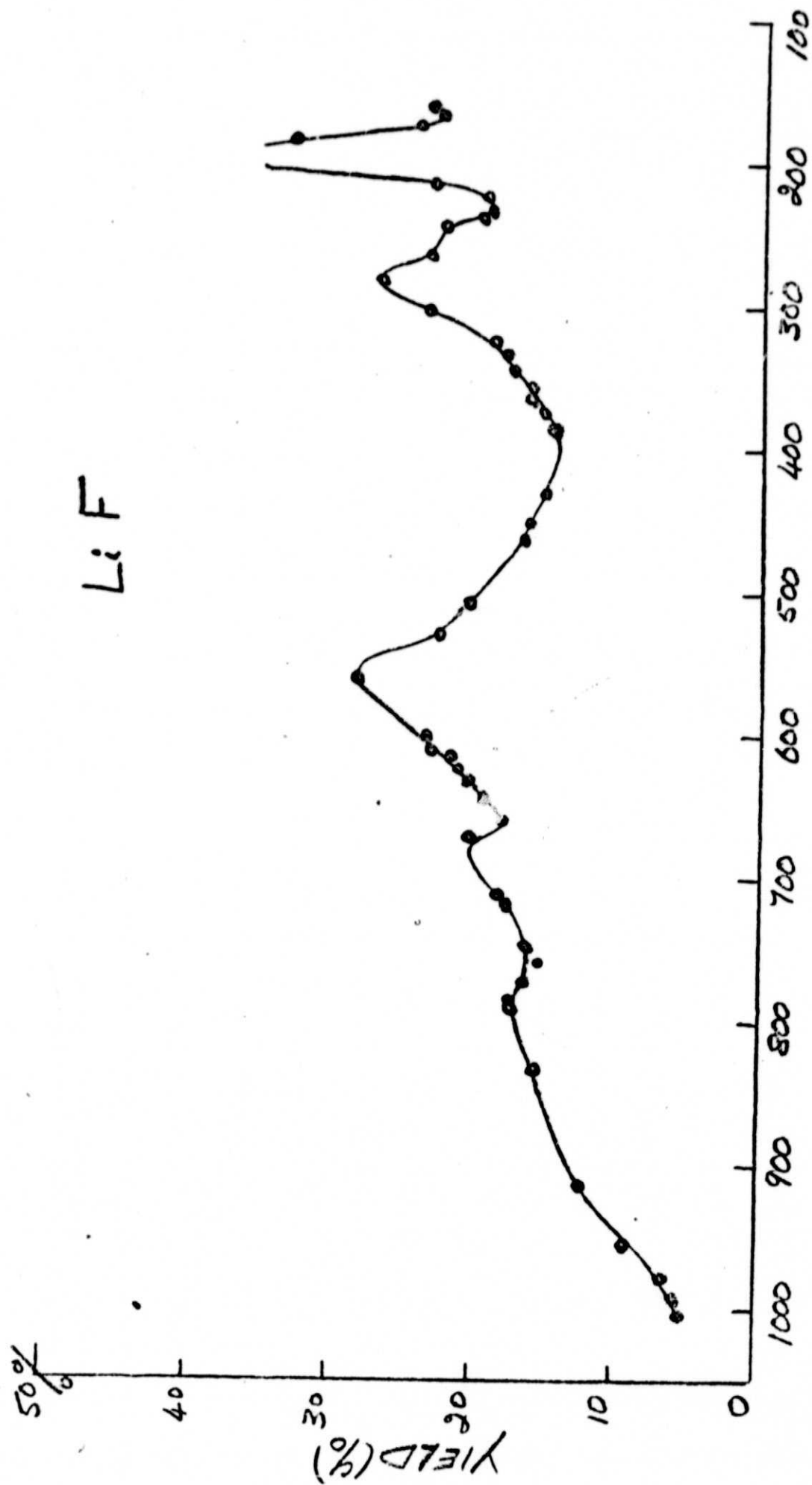


Fig. 31

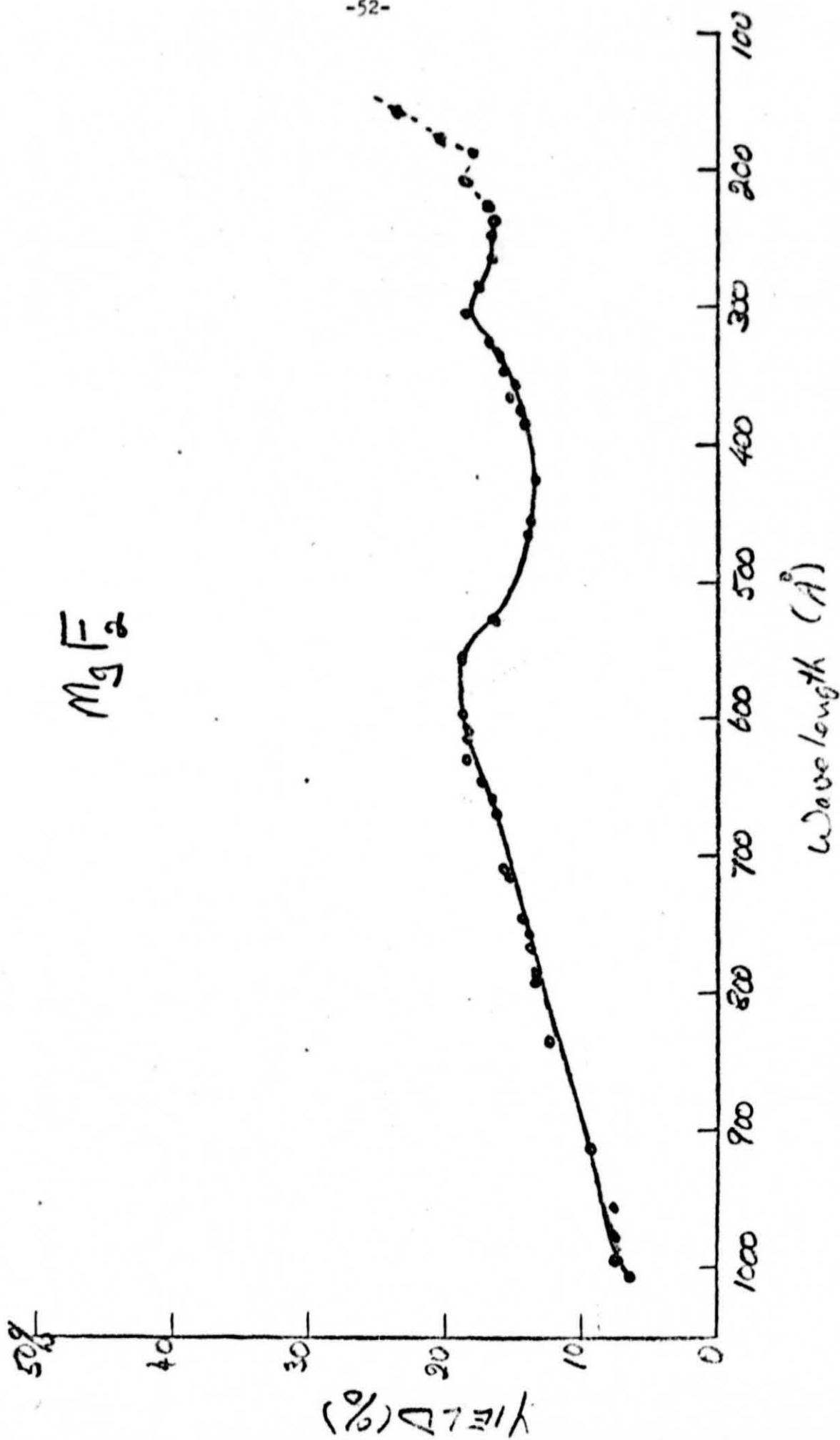


Fig. 32

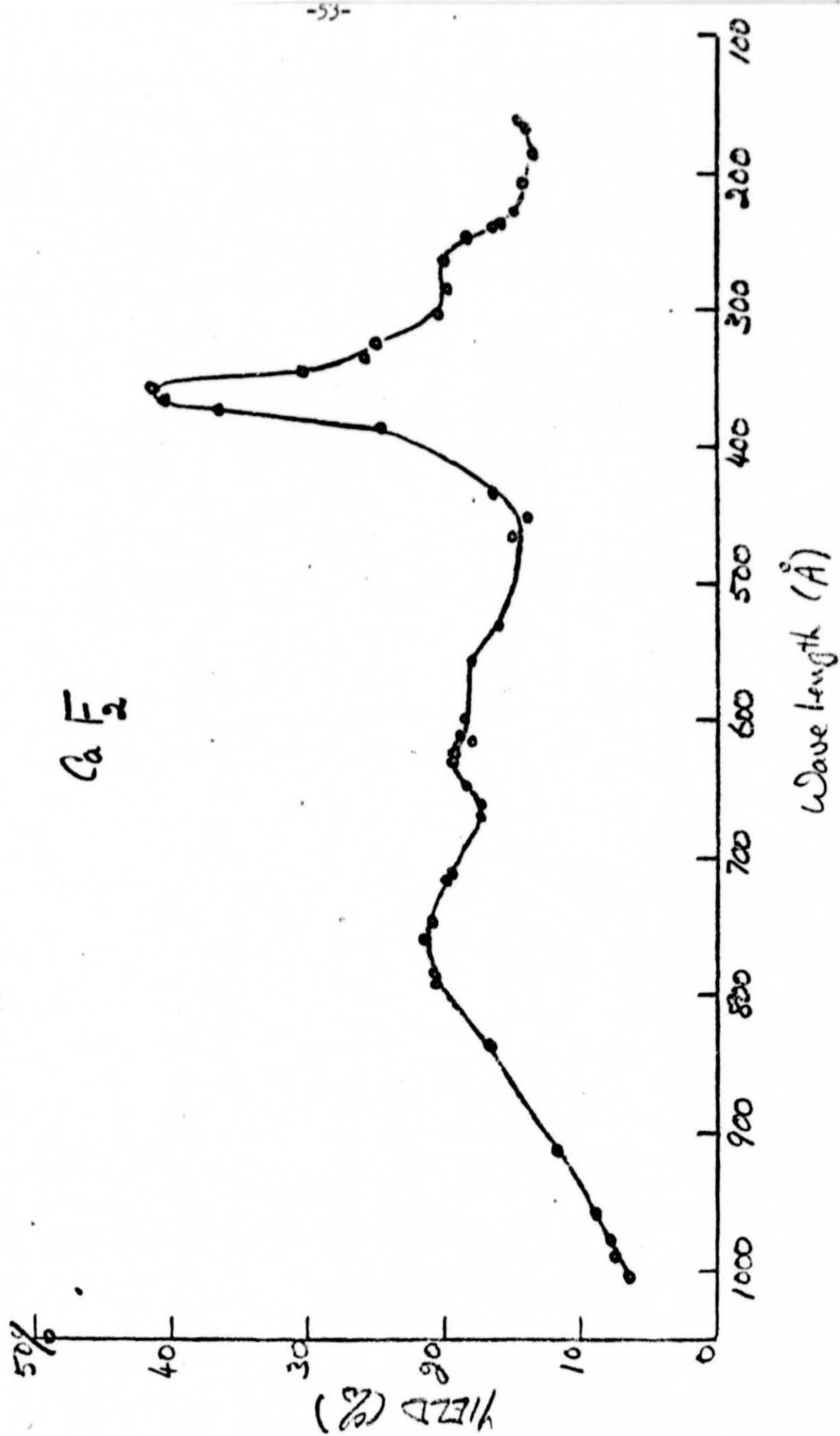
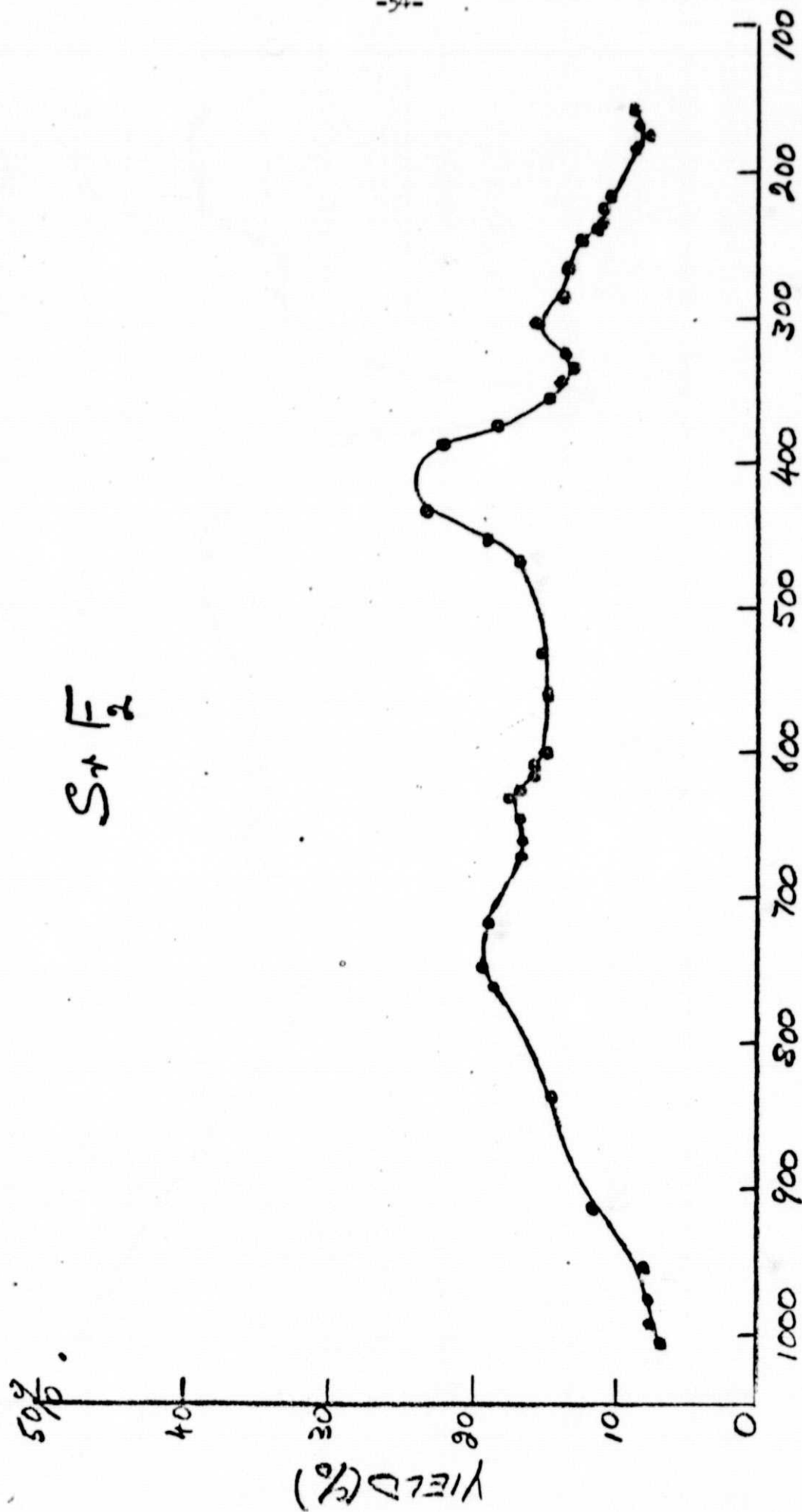


Fig. 33

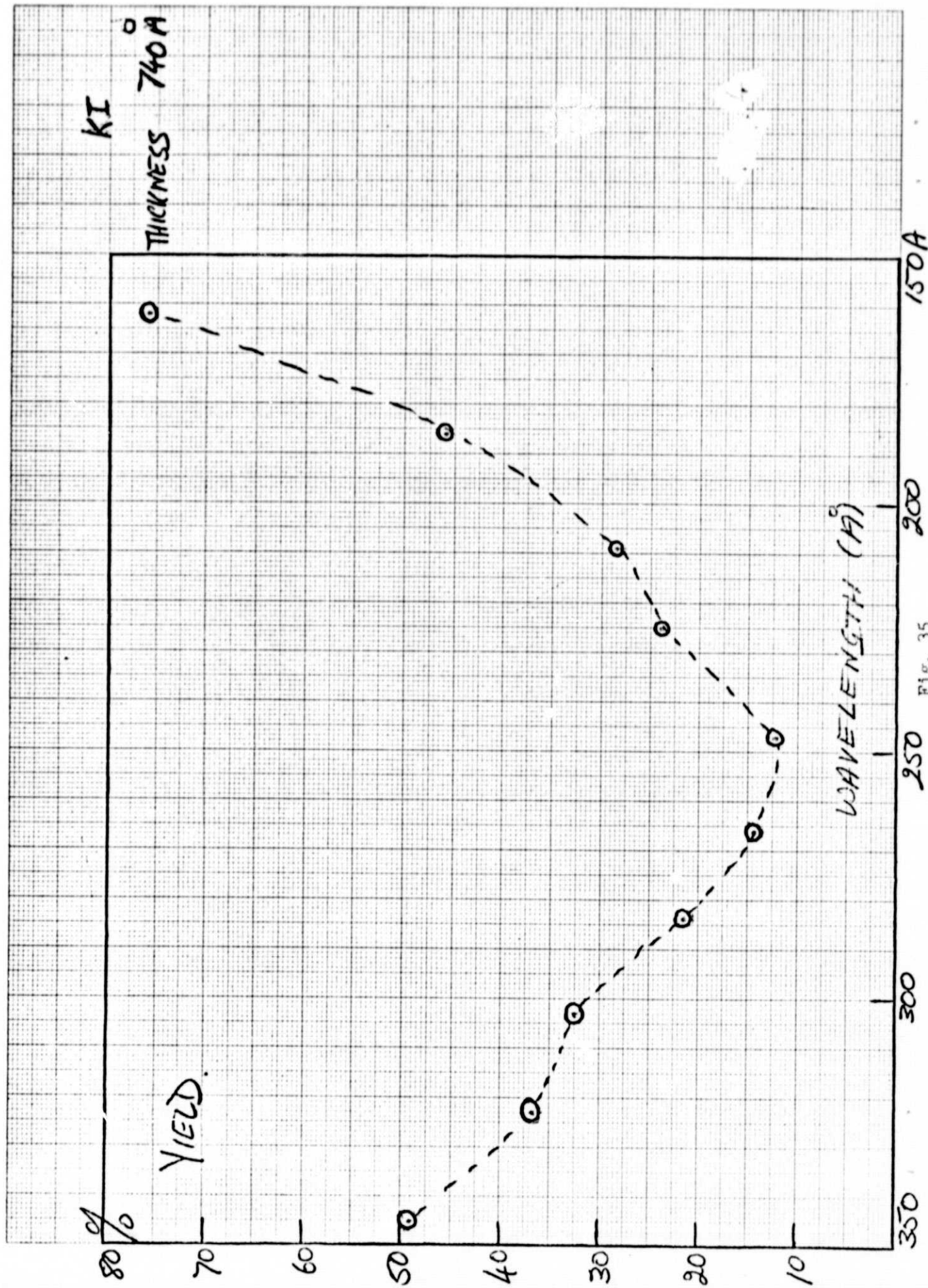


Wavelength (Å)

Fig. 34

TABLE V. Photoelectric yields of cathodes relative to tungsten at 584 Å after various exposures to humidity.

Condition of Cathode	C _s I	KI	RbF	NaF
new coating	4.68	4.80	1.40	3.37
" " 1 week later	4.00	3.93	1.55	2.90
exposure to 30% humidity	3.76	3.60	1.57	2.90
exposure to 50% humidity	3.16	1.00	1.38	2.80
exposure to 90% humidity	1.17	1.02	1.29	2.73
Recovery (exposed to lab atmos.)	1.11	0.99	1.43	2.68



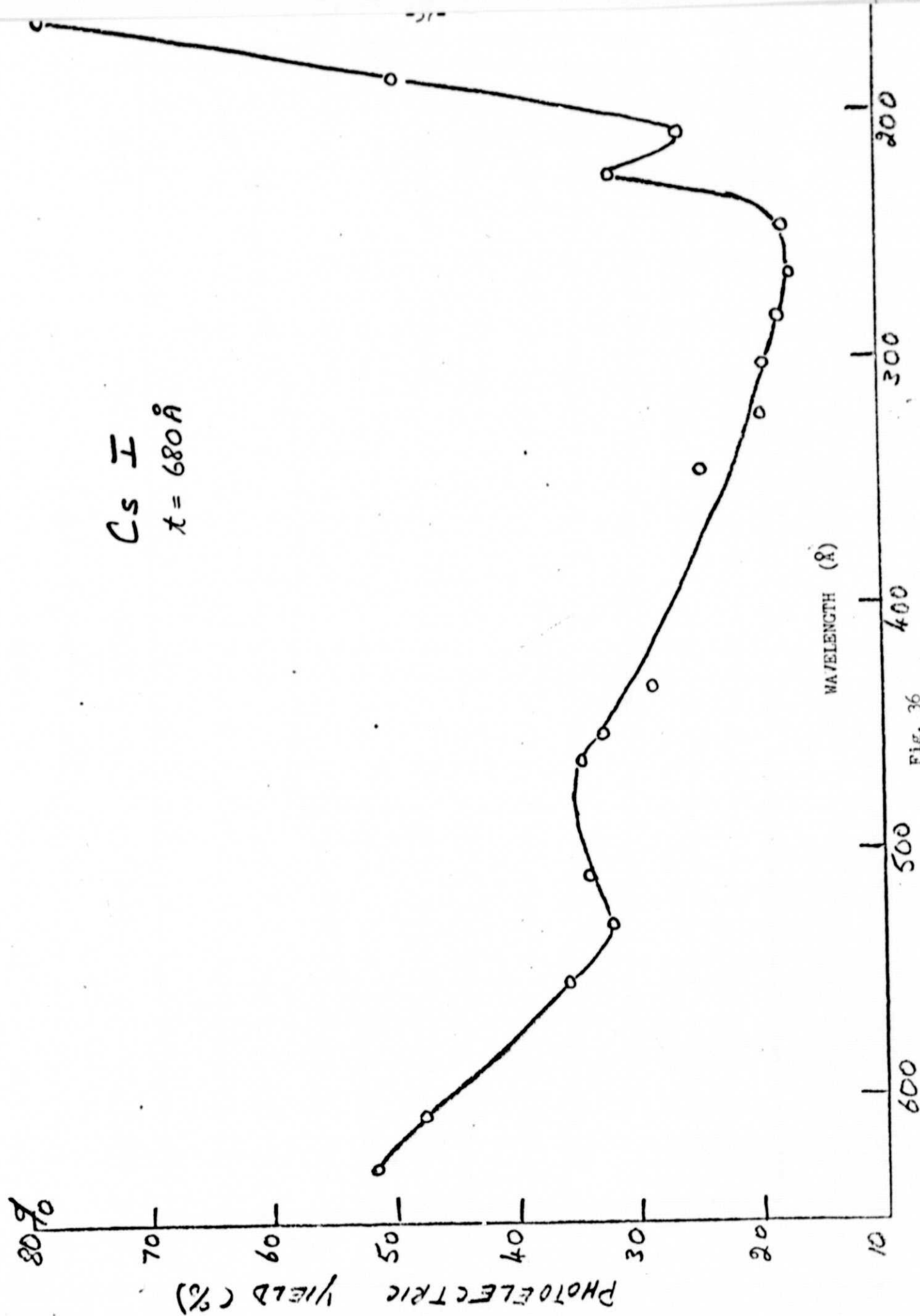


Fig. 36

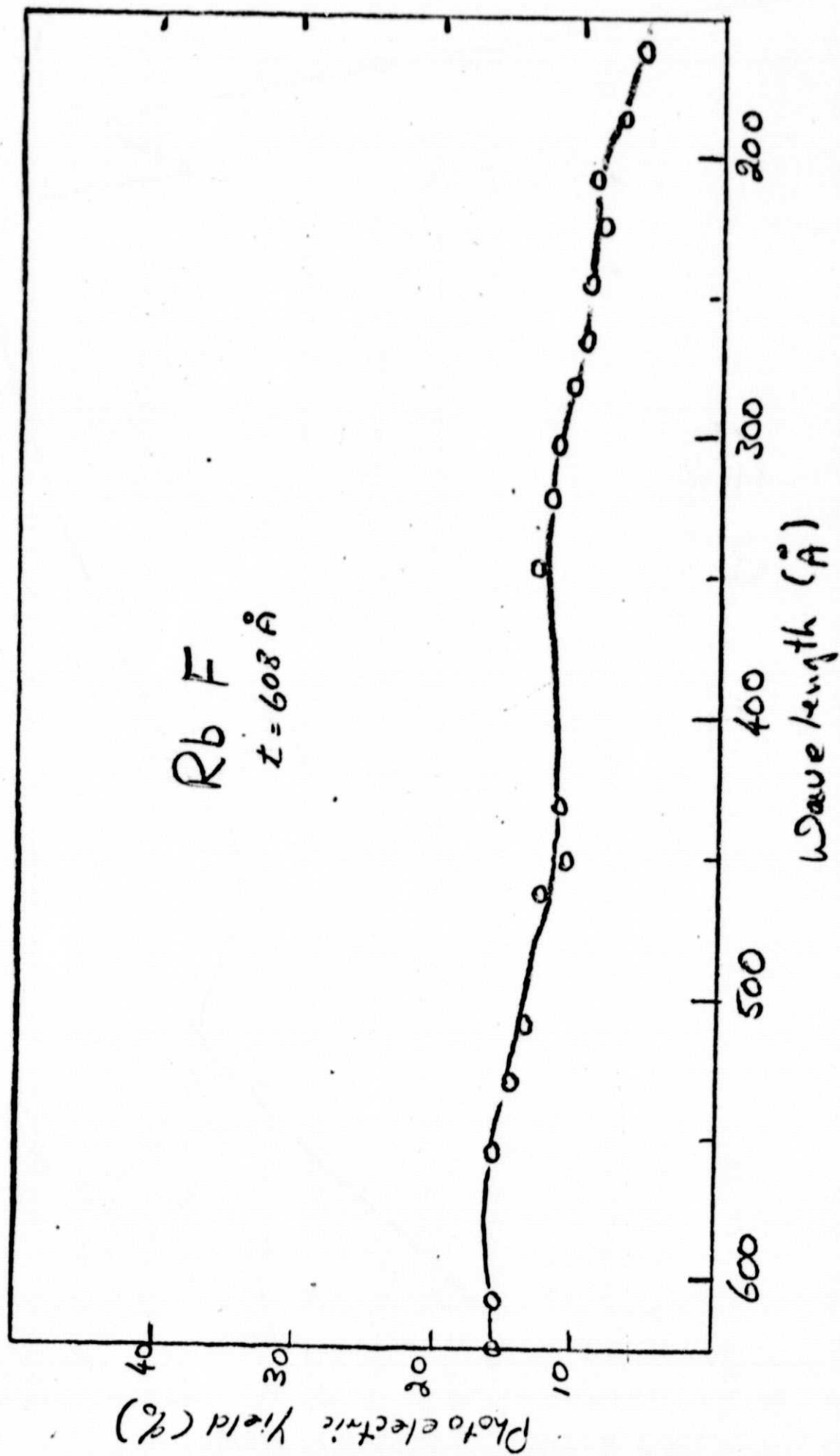


Fig. 37

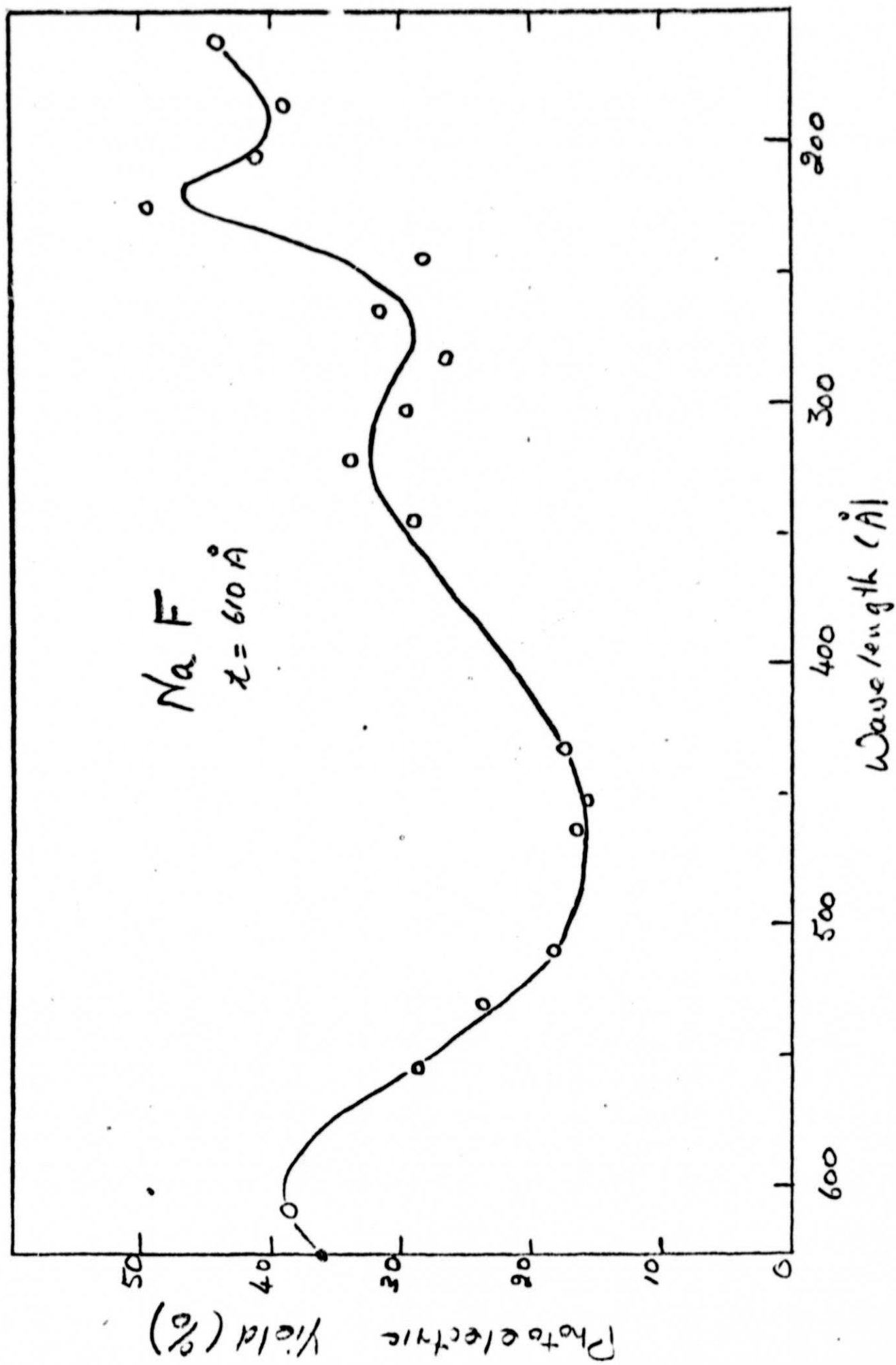


Fig. 38

Table VI. Humidity tests on cathodes with Synchrotron Radiation. The yield of a fresh cathode is normalized to unity at each wavelength and the results of humidity are measured relative to this value.

$\lambda(\text{\AA})$	New	<u>30%</u>	<u>50%</u>	<u>90%</u>
<u>LiF</u>				
179	1	0.94	0.85	0.79
200	1	0.93	0.82	0.78
280	1	0.92	0.81	0.77
420	1	0.94	0.89	0.89
530	1	0.94	0.86	0.81
750	1	0.90	0.80	0.90
<u>MgF₂</u>				
171	1	0.89	0.76	0.61
280	1	0.88	0.79	0.66
420	1	0.87	0.78	0.67
530	1	0.88	0.80	0.69
750	1	0.82	0.77	0.66
<u>NaF</u>				
171	1	0.85	0.74	0.68
280	1	0.85	0.72	0.65
420	1	0.84	0.75	0.70
530	1	0.85	0.71	0.63
750	1	0.88	0.82	0.76
<u>CaF₂</u>				
171	1	0.98	0.95	0.92
280	1	0.96	0.93	0.88
420	1	0.95	0.90	0.86
530	1	0.95	0.92	0.88
750	1	0.95	0.94	0.90

Table VI (continued)

$\lambda(\text{\AA})$	New	<u>30%</u>	<u>50%</u>	<u>90%</u>
		<u>SrF₂</u>		
171	1	0.90	0.76	0.81
280	1	0.88	0.76	0.78
420	1			
530	1	0.90	0.81	0.80
750	1	0.85	0.81	0.80
		<u>CsI</u>		
171	1	1.76	1.56	0.35
280	1	1.56	1.35	0.30
420	1			
530	1	0.93	0.70	0.29
750	1	0.64	0.58	0.18
		<u>RbF</u>		
171	1	1.01	0.72	0.87
280	1	0.93	0.67	0.77
420	1	0.77	0.67	0.60
530	1	0.83	0.63	0.61
750	1	0.84	0.67	0.66

The absolute yield of fresh samples of LiF and MgF_2 were measured at normal and grazing angles (70°) of incidence. The results are shown in Figs. 39 and 40, respectively. The structure in the curves around 200 \AA , shown as the dashed lines, are taken from the data obtained from the synchrotron runs (monthly report #19) and from the data of Lukirskii [E. P. Savinov and A. P. Lukirskii, Optics and Spectroscopy 23, 163 (1967)]. The major peaks can be identified as emission from the Li K-shell and the Mg L-shell.

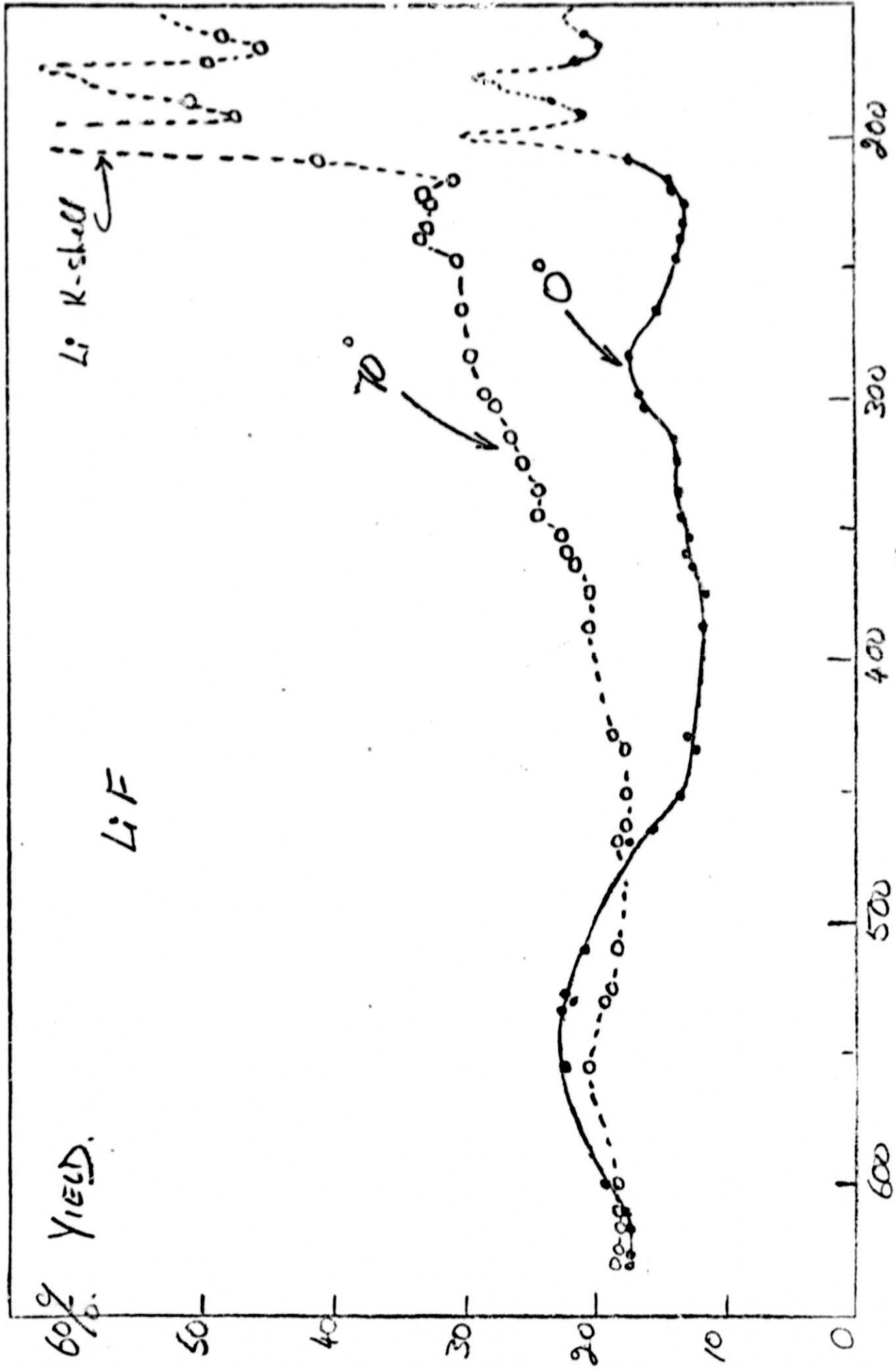
2. Platinum (Pt)

The absolute yield of a GSFC cathode of Pt was measured from 150 to 350 \AA . The results were taken before and after cleaning in isopropyl alcohol. The yields are given in Fig. 41.

3. Beryllium Copper (BeCu)

The photoelectric yield of a commercially prepared BeCu cathode was measured from 400 to 1100 \AA . This material is specially prepared for the dynodes of the Johnston type Focused Mesh Electron Multipliers.* The manufacturer does not supply details of the activation of these dynodes. However, since various claims are often made about the extremely high secondary emission of specially prepared cathodes (for electron bombardment) it was of interest to see what type of yield could be expected from photon bombardment. The cathode was exposed to air but kept in a closed dessicator.

The results of the efficiency measurements are shown in Fig. 42 are those from a solid cathode of BeCu. In the actual multipliers the dynodes are perforated as shown in Fig. 43. The yield of the perforated cathode was only about 10% lower than the solid cathode although the open area of the perforations is about 20 percent. This anomaly can be explained by the fact that on the etched side of the perforated cathode the radiation



WAVELENGTH (Å)

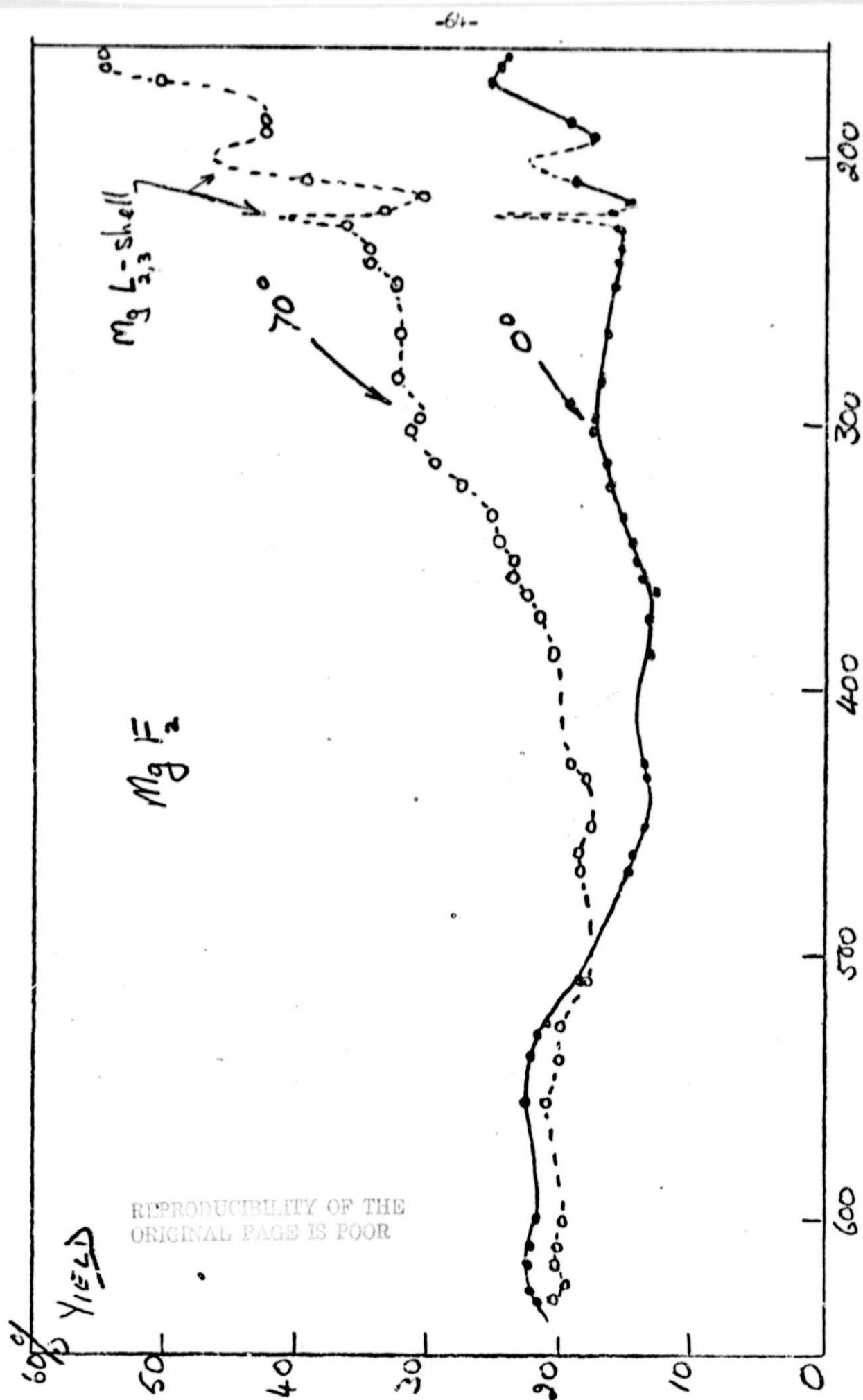


Fig. 40

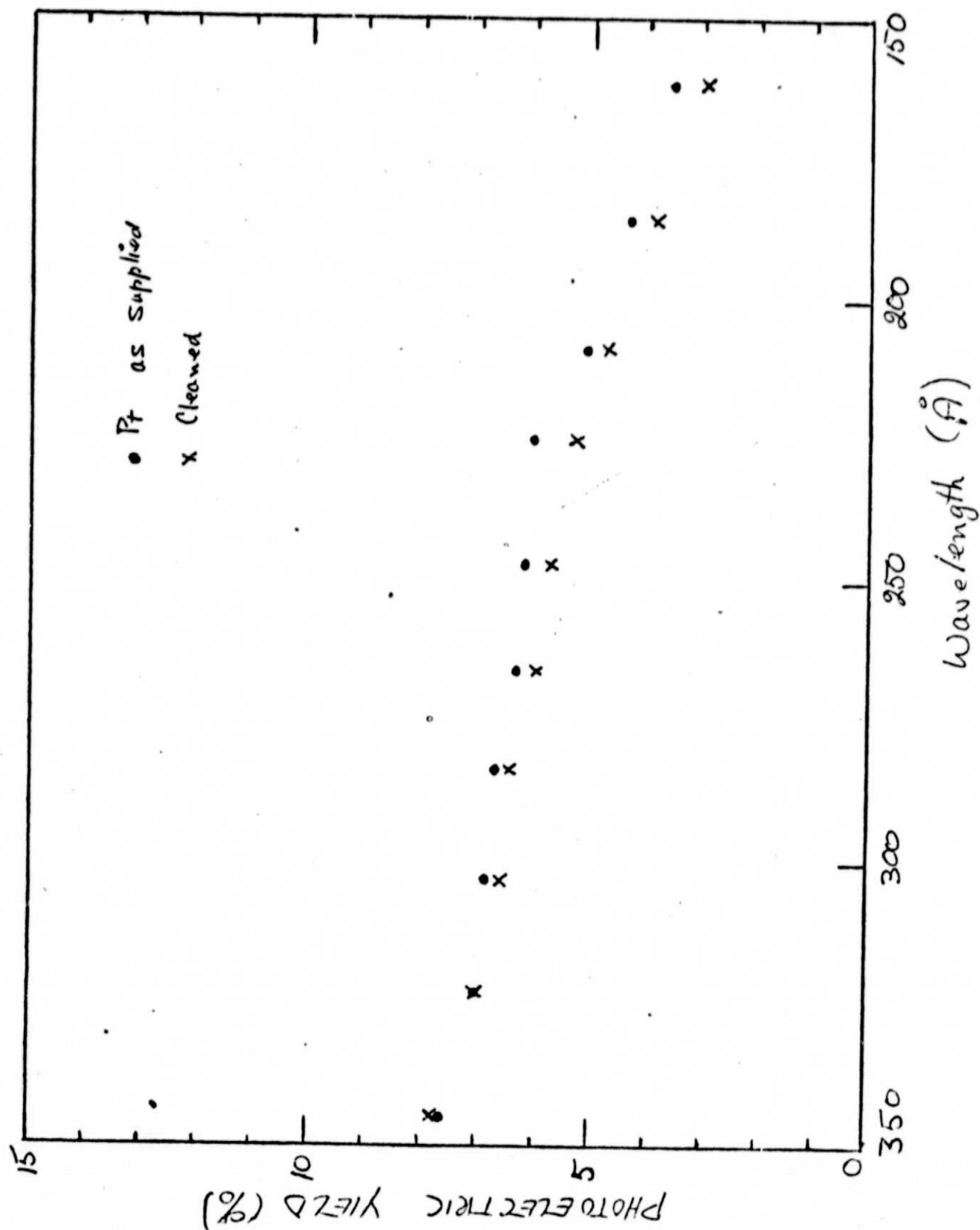


Fig. 41

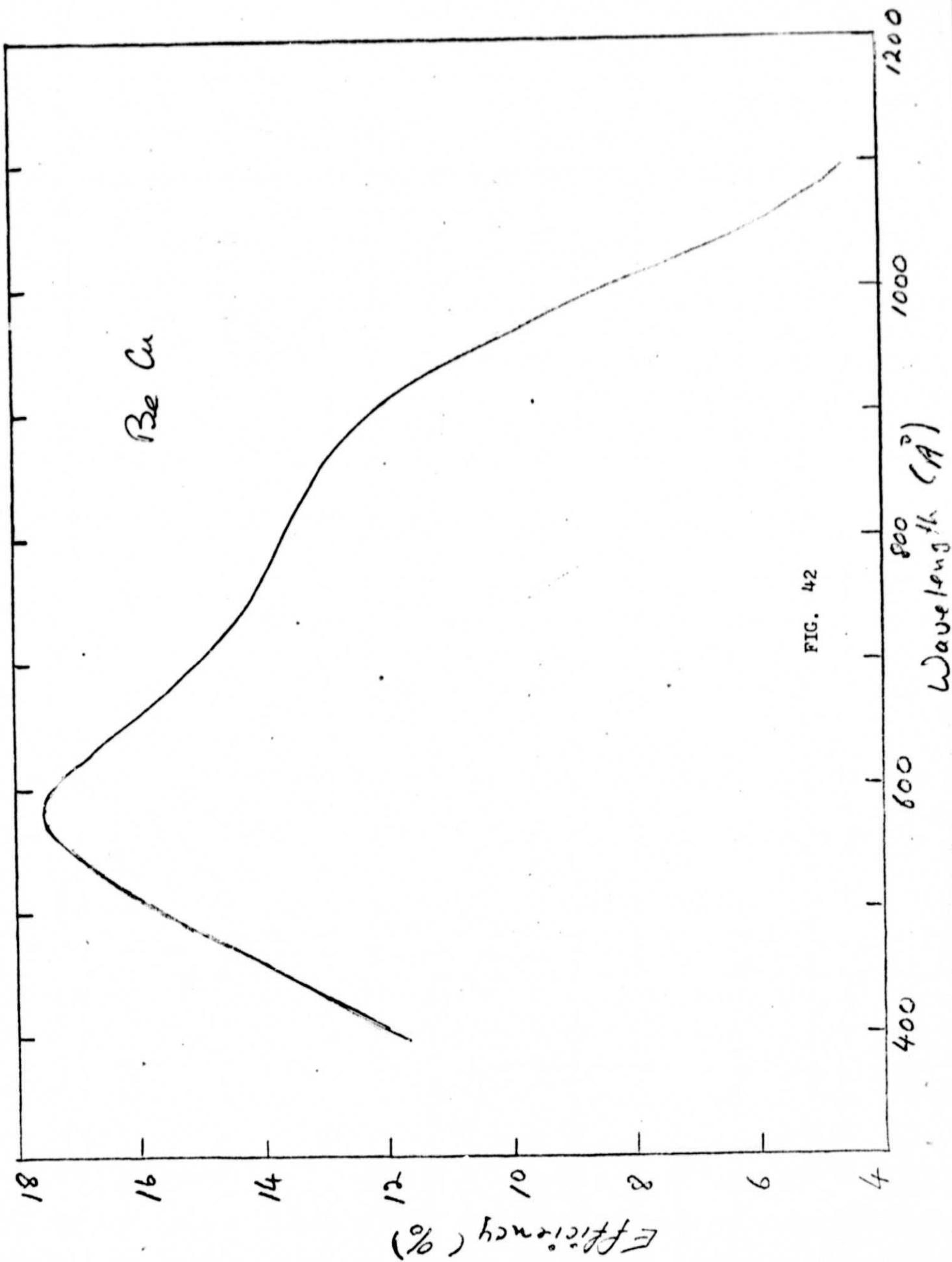


FIG. 42

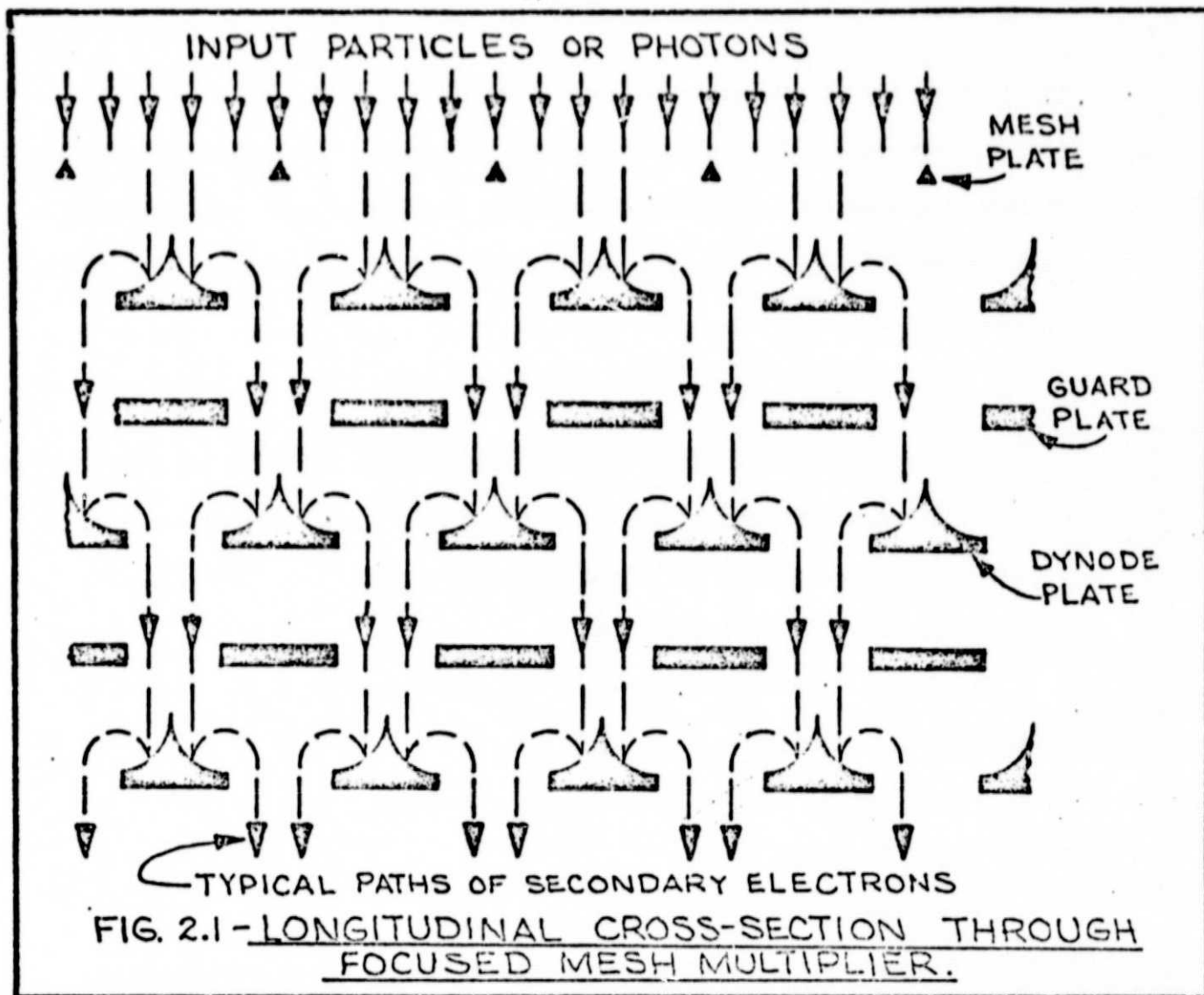


Fig. 43. Johnston type electron multiplier dynode structure.

is striking the BeCu peaks at a high angle of incidence (see Fig. 43) and thereby increasing the yield. Figure 44 illustrates the relative efficiency of both cathodes as a function of angle of incidence. It is interesting that the efficiency of the perforated cathode is almost constant from normal incidence to 70°.

4. Be, BeO

The photoelectric yields of Be and BeO cathodes were investigated at normal incidence (0°) and at angles of incidence of 50° and 70°. The yields were measured from 150 to 625 Å. In addition the stability of the BeO cathodes were investigated.

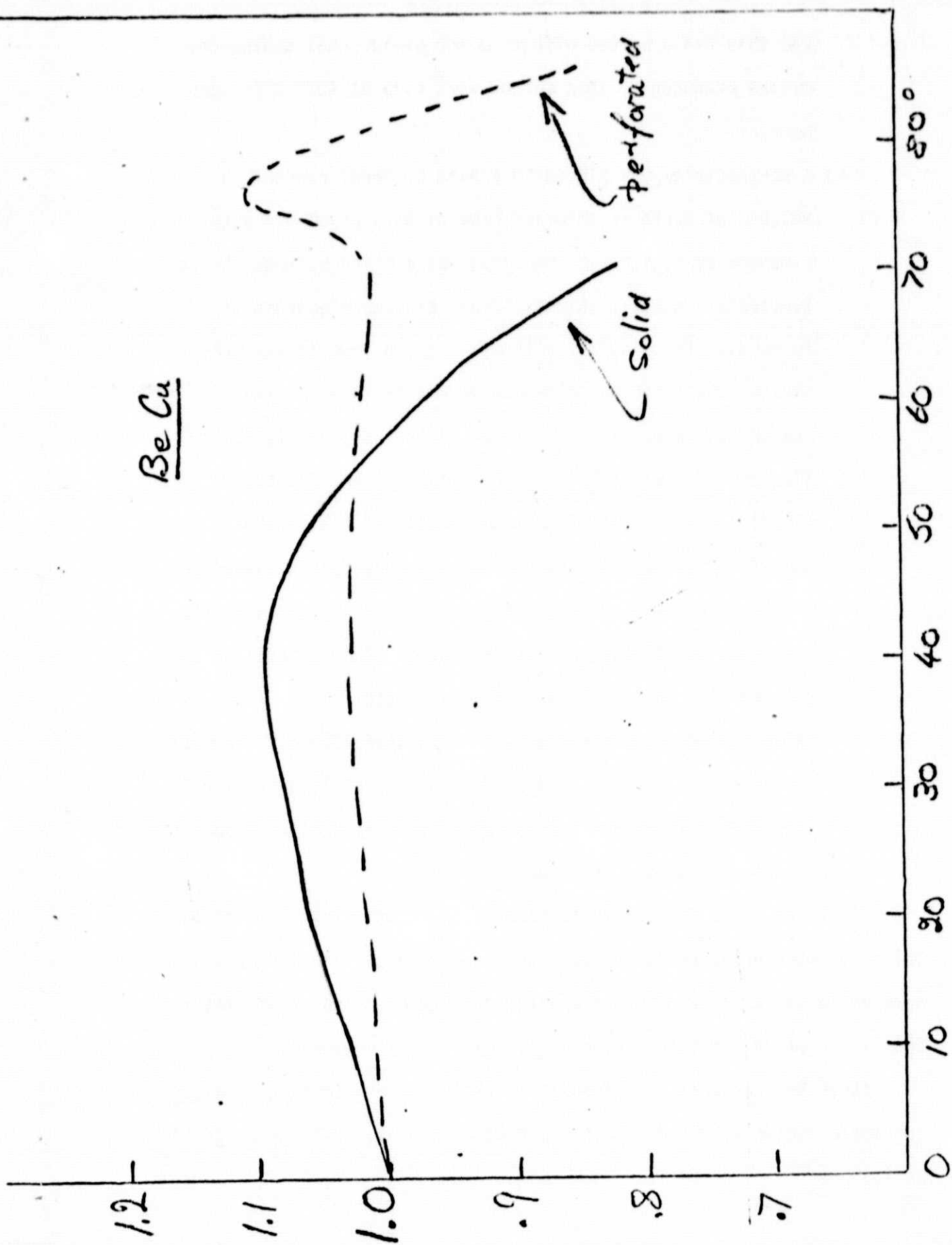
The Be was obtained from Kawecki Berylco Industries, Inc., Reading, Pennsylvania, in sheet form precut 1 x 1.5 x 0.04 inches. It was polished to a 10 RMS finish. The assay quotes the Be to be 99% pure with 1% BeO as the major impurity.

To oxidize Be, several methods were tried.

- a) Exposure to the discharged products of a microwave discharge in O₂ (5 to 10% of the products are atomic oxygen). There was no change in the yield after one half hour exposure to the discharge.
- b) Anodizing in a sulfuric acid bath (12% solution). This did increase the yield slightly, however, there was little control over the degree of oxidation. The Be surface was roughened and very grey in color.
- c) Be sample maintained in a hot O₂ atmosphere. This is a technique used to rejuvenate the yield of CuBe dynodes. Maintaining the sample at 250° C for one hour in O₂ had little effect. The temperature was increased to 400° C for one hour

Be Cu

EFFICIENCY RELATIVE TO NORMAL INCIDENCE



Angle of incidence.

Fig. 44

and this had a marked effect on the yield. All subsequent oxides produced by this method were made at 400° C for one hour.

- d) A Be substrate was placed in a bath of three percent, by weight, of tartaric acid and brought to a pH of 5.5 with ammonium hydroxide. A potential was applied between the Be substrate (positive potential) and another electrode of Be (ground). An oxide layer then starts to form on the substrate, the thickness of which is proportional to the applied voltage. This is the procedure used to anodize aluminum as used by G. Hass, J. Opt. Soc. Am. 39, 532 (1949). A potential of 23 V was applied. After about two mins. the current had dropped to a negligible value and the substrate was removed. Assuming the oxide grows at the same rate as it does on Al (that is, at 13 Å per volt) then the BeO film should be 300 Å thick. Whatever the actual value this procedure was subject to a high degree of control. The oxidation process is dependent on the applied voltage only. When the current drops close to zero a film of specific thickness has been produced.

It proved to be impossible to measure the film thickness with the Tolansky interferometer as the Be substrates were supplied as machined from solid stock and did not have the necessary high degree of flatness that is required for interferometric thickness measurements.

Three BeO cathodes of different thickness were made by method (d) and their yields measured within a period of one hour. The results were as follows.

Thickness (Å)	Yield (%)	
	304 Å	584 Å
150	10.4	18.4
300	10.8	18.6
600	10.4	17.5

The yield for a 600 Å thick BeO film appears to drop; but more significantly saturation effects are apparent. A thickness of 300 Å was chosen as a standard thickness for the life-time studies.

Three identical photo-cathodes were prepared by this anodizing method with an assumed BeO film of 300 Å. These cathodes are labeled #1A, 2A, and 3A.

Two photo-cathodes were prepared by the process of heating in oxygen. One Be substrate had been prepared earlier (see monthly report #20-21) and is labeled #1. This cathode had been stored for many months in a laboratory atmosphere (in a plastic box). The second substrate was identified as #2.

The photoelectric yield of Be was taken in the condition the cathodes were received. The results are shown in Fig. 45 along with the yields of BeO sample #1 measured at 0° and at 70° angle of incidence. In Fig. 46 the yield of BeO was repeated at 50° angle of incidence. The reason for this was that from the data reported in Fig. 45 it was apparent that at some angle between 0° and 70° the yield as a function of wavelength should be relatively flat. We found 50° to be about the best. The data points all lie within 15 to 20% for wavelengths between 150 and 600 Å.

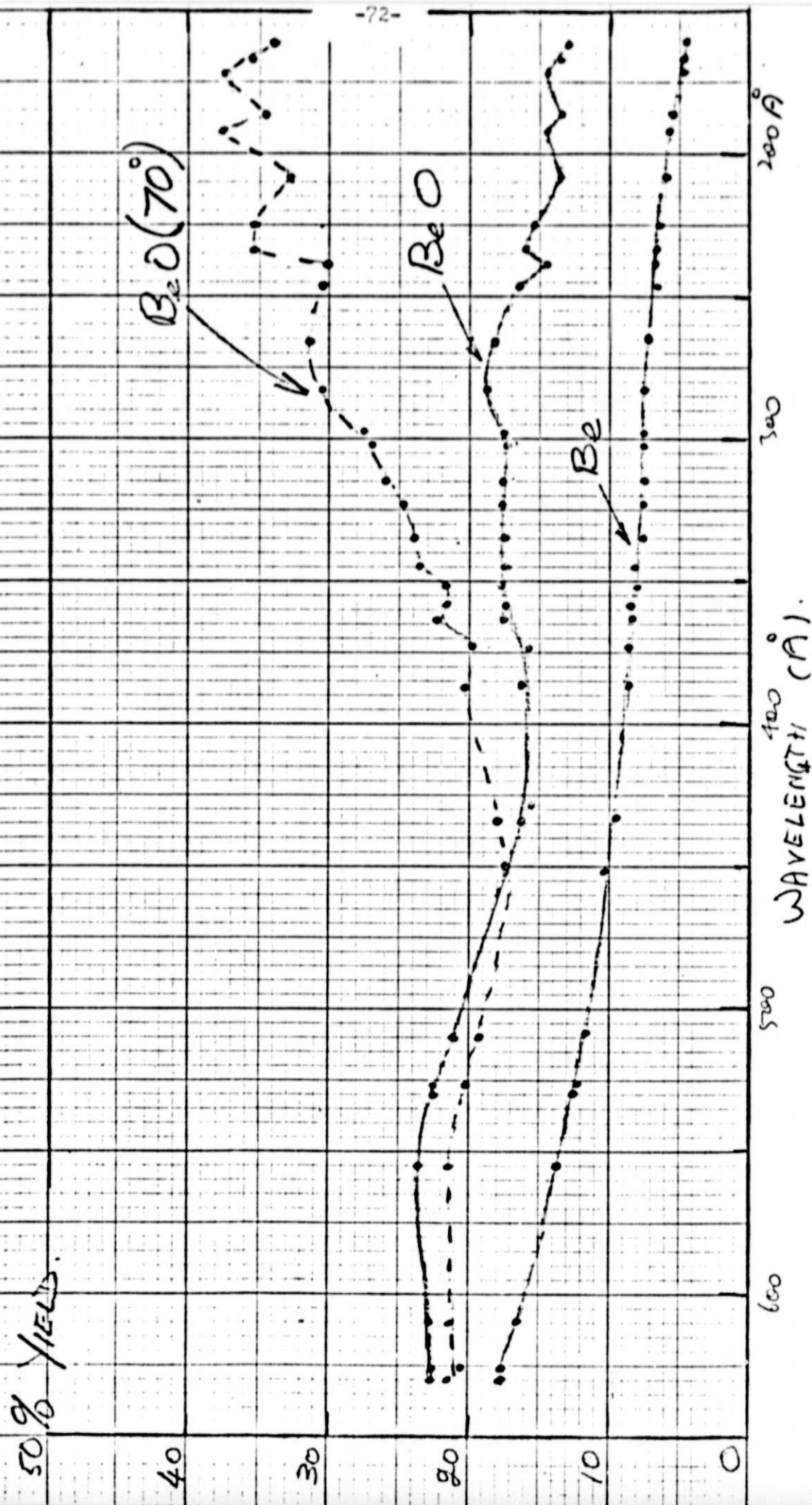
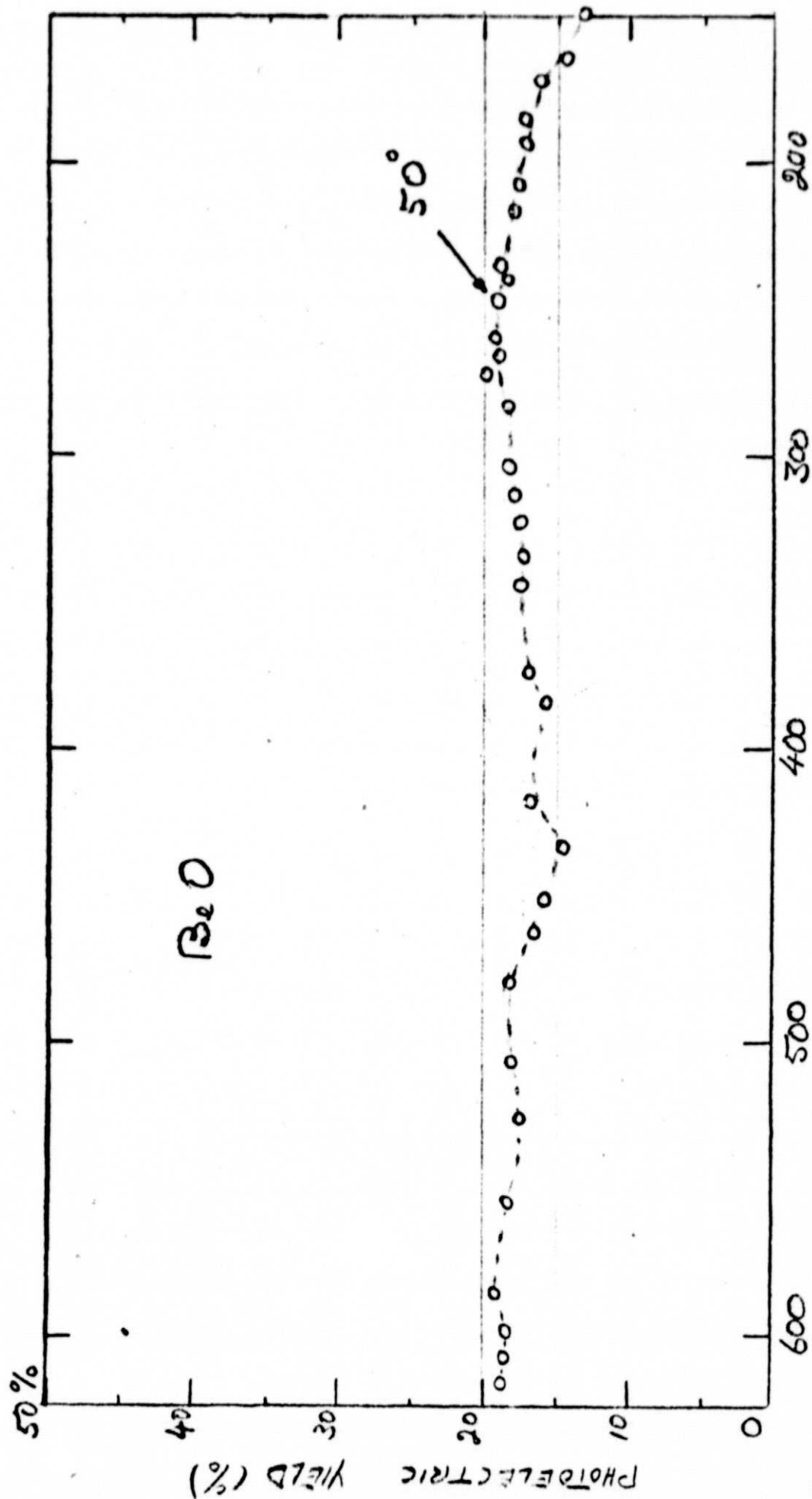


FIG. 45



Wave/length (Å)

FIG. 46

Stability Tests

The photoelectric yield of BeO was measured at 584 and 304 Å and monitored for a period of seven months at intervals of a few days to about one week. Five samples were attached onto a rotating mount along with a standard tungsten cathode. The yield of the tungsten could be periodically checked and determined to remain constant. The yields of the BeO samples were measured relative to this tungsten standard.

At various times some of the BeO cathodes were removed and cleaned by different methods. These were:

- a. Methanol (rubbing with laboratory tissue, e.g., Kim Wipe)
- b. Isopropyl alcohol (rubbing with laboratory tissue, e.g., Kim Wipe)
- c. Freon TF (rubbing with laboratory tissue, e.g., Kim Wipe)
- d. Freon TF (rubbing with laboratory tissue, e.g., Kim Wipe)
- e. Freon TF (ultrasonic cleaner)

The results of this investigation are shown in Figs. 47 and 48. The time scale relates to the date as follows:

day 1 = 24 March, 1975

day 2 = 16 Oct., 1975

In Fig. 47 the yields of three BeO cathodes are shown. These were the oxides produced by the chemical anodizing procedure (d). Each is characterized by a high initial yield between 19 and 20% (at 584 Å). There is an immediate drop in the yield during the following month or two at both wavelengths. Cathode #1A was cleaned first with methanol (a). An immediate drop in yield was observed. After a few days subsequent cleaning in isopropyl alcohol (b) and with freon (c) restored the yield partially. It is unknown what causes this erratic behavior. The yield of cathode #1A decreased by eight percent during the next 100 days. Cleaning with freon

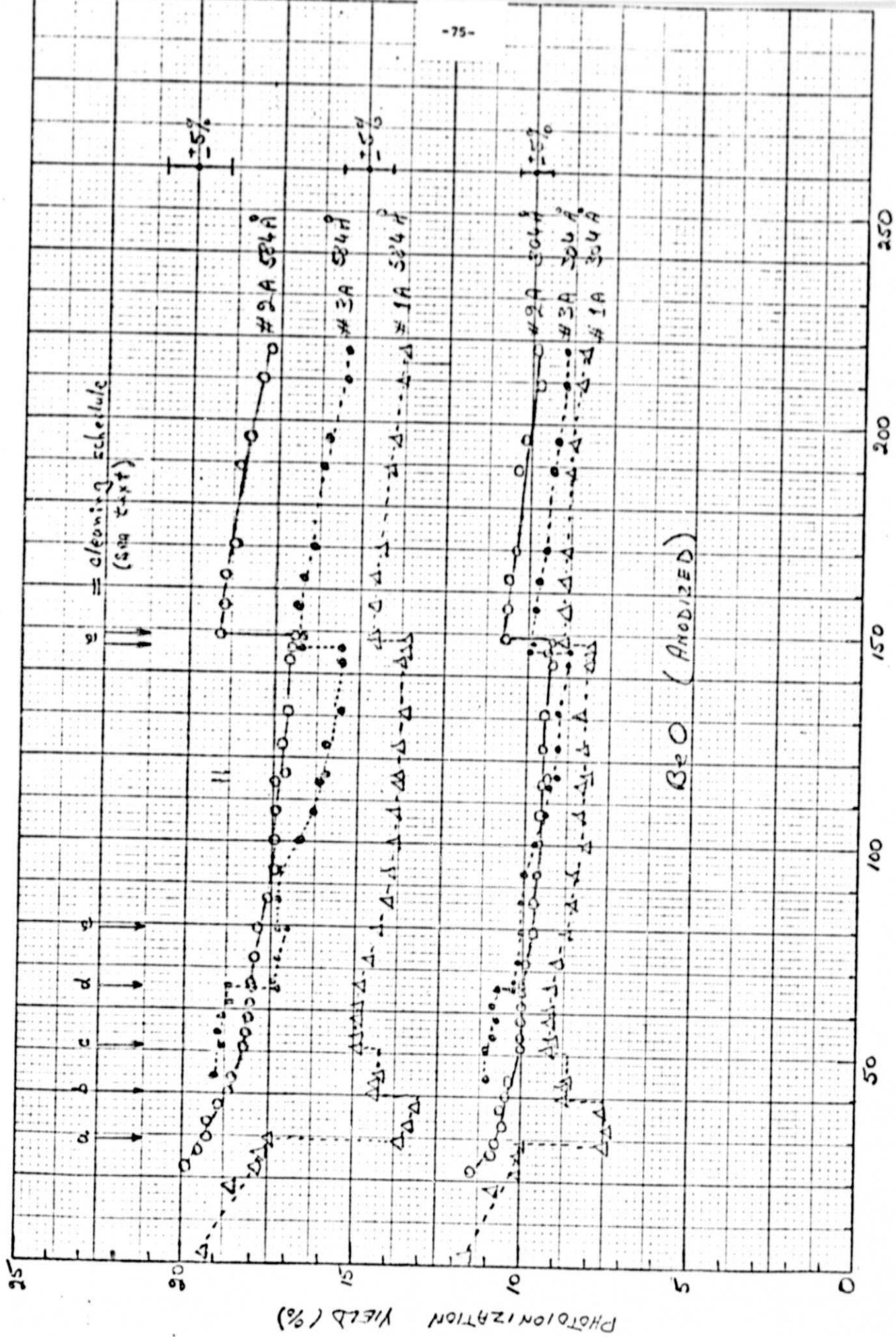
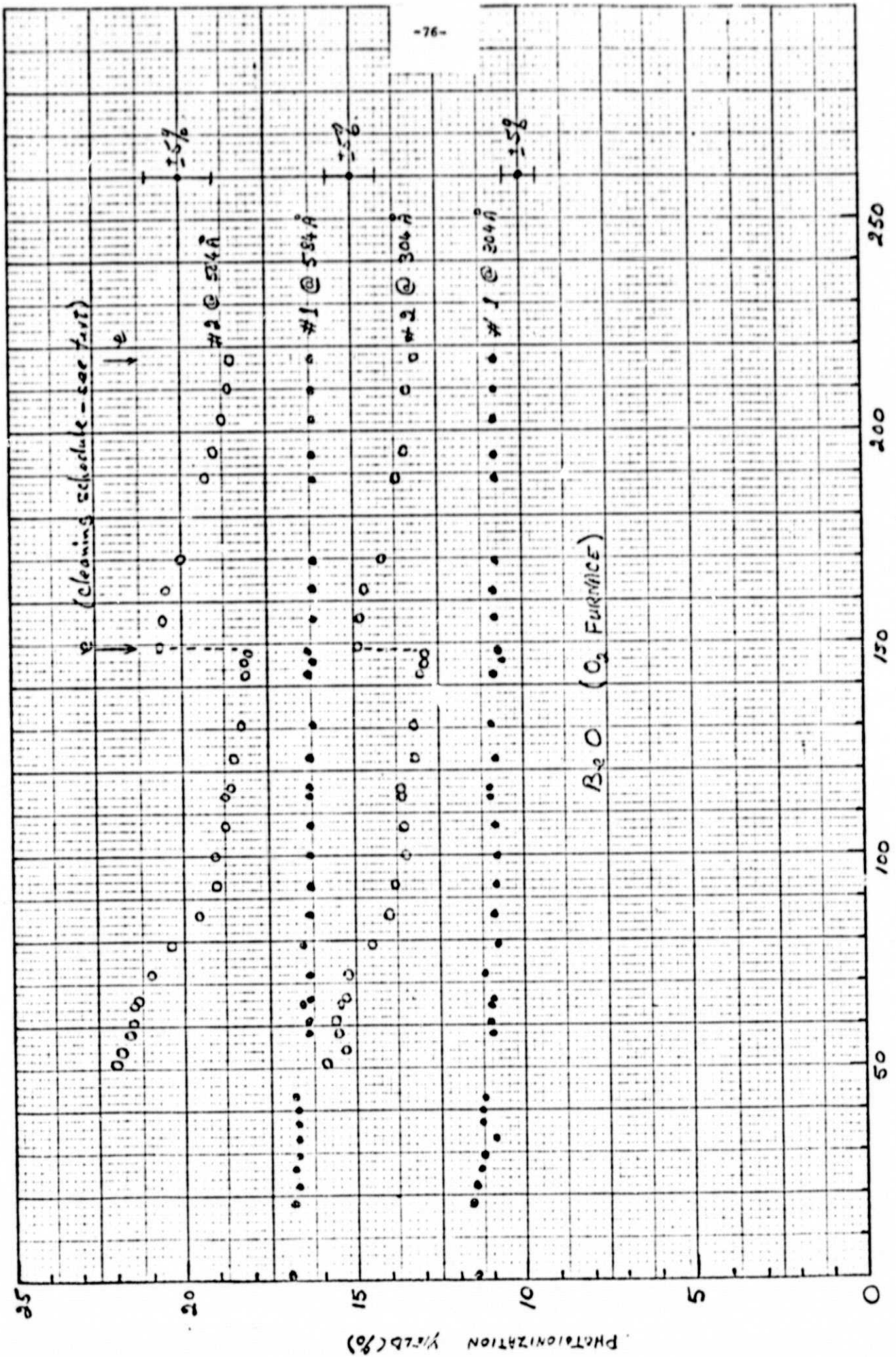


FIG. 47



TIME (DAYS)

FIG. 48

in the ultrasonic cleaner restored its yield (e). Once again a slow decay in yield took place during the next 70 days. But there is an indication that the yield is approaching a constant value. Similar behavior is seen with the other two cathodes. If we consider the yields after the poorer cleaning techniques of a-d and of the uncleaned cathode #2A then we see that a constant yield can be quoted for each cathode which will vary less than $\pm 6\%$ over a period of about 160 to 200 days. This includes the treatment in the ultrasonic bath with freon (e). This latter cleaning process appears to bring the yield back to near its original value (i.e., the value after the a-d treatment).

For the first 114 days all cathodes remained in their mount and attached to the vacuum monochromator. Although stored in the vacuum environment the cathode chamber was always closed from the monochromator and pumping system after measurements were taken. For the next two days all cathodes were exposed to the laboratory air and then remeasured. There was essentially no change in yield. Thereafter, the cathodes were stored as before, in a closed-off vacuum environment.

In Fig. 48 the yields of Be treated in the molecular oxygen furnace, procedure (c), are recorded as a function of time. Cathode #1 was actually prepared many months before the tests were started. It was stored in the laboratory. This cathode was not cleaned during the testing period and shows a total decrease of about six percent over the 217 day testing period. Cathode #2 was prepared during this testing period and shows an immediate decrease in its high yield of 22% (584 \AA). The decrease is most rapid during the first 40 days and then starts to level off. Presumably, cathode #1 had already reached this stage when measurements were started. (Referring back to monthly report #20-21 we note that the yield at 584 \AA for cathode

#1 was 23%). About half of the lost yield of cathode #2 was restored by ultrasonic cleaning, but again, the characteristic drop-off occurs in the following days.

CONCLUSION

The chemical treatment gave reproducible yields of about 11 and 19%, respectively, for 304 and 584 Å for freshly prepared cathodes.

The O₂ treatment at 400° C was also relatively reproducible giving on the average, for freshly prepared cathodes, yields of 16.7 and 22.5%, respectively, for 304 and 584 Å. The O₂ treatment appears to produce cathodes with the highest yields. No saturation effects occurred so it is assumed the BeO film was less than 300 Å thick. Cathode #2 at the start had a yield 1.9 times greater than tungsten for 584 Å and 2.7 times greater at 304 Å.

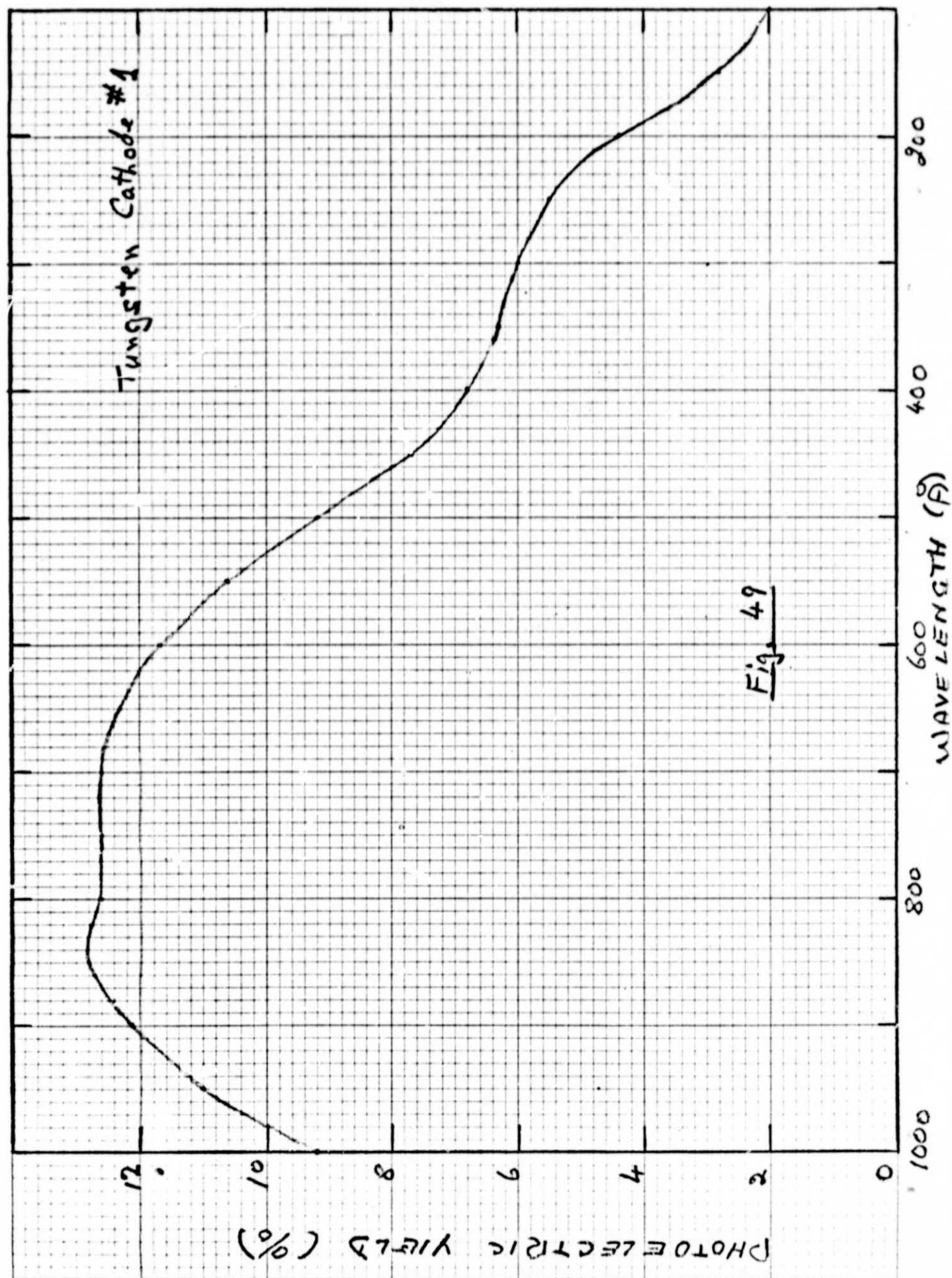
Regardless of the procedure for preparing the BeO film there was always a steady decay in yield vs time. The yield could be restored (at least, partially) by cleaning with Freon TF in an ultrasonic cleaner for two minutes. Contamination in the vacuum environment is the most likely source of this steady drop in yield. But, surprisingly, the environment had little effect on the tungsten standard. When it was cleaned by the same procedure essentially no change was observed. It is assumed that the high efficiency brought about by oxidization is more sensitive to contamination. However, even in its aged and stable condition (and perhaps contaminated?) #1 BeO had a yield of 1.8 times greater than tungsten at 304 Å and 1.4 times greater at 584 Å.

The next logical step would be to clean cathode #1 to see if its initial high yield is returned. Then to store it continually in the laboratory

atmosphere and expose it for as short a period of time to the vacuum environment. Ideally, of course ultra high vacuum technology should be used. This would require the vacuum monochromator also to be compatible with ultra high vacuum techniques.

5. Tungsten (W)

A tungsten photocathode, which was calibrated with a double ion chamber over the range 100 to 1000 Å, was used as a secondary standard. The results are shown in Fig. 49. This is an extension of the data given in monthly report #13.



VI. APPENDIX

The major piece of apparatus constructed under this contract was the grating reflectometer system. Part of the existing vacuum chamber remains the same. However, the entire inside fixtures, eg, Rowland Circle, etc, were rebuilt.

The grating holder was constructed with a kinematic mount. The mating base was designed to lock in at a variety of angles of incidence. The single Rowland Circle was located to give a reasonable focus regardless of the angle of incidence within the range 80 to 85°.

A detector base was mounted on the drive screw and constrained to move along the Rowland Circle. A directional arm constrains the detector base in such a manner that it is always facing the center of the grating. Some of these features can be seen in the following plates.

Plate 1 shows the lead screw and nut assembly with the Rowland Circle plate mounted above. The ball-bearings can be seen that allow the detector base to move smoothly. The directional arm rod can be seen protruding from the end of the detector base.

Plates 2 and 3 show a top view of the Rowland Circle with its ball-bearings. The polarization analyzer is shown mounted on the detector base complete with the remote control motors to rotate the analyzer.

Plate 4 shows the grating mount inside part of the vacuum chamber. Underneath the grating mount is the pivot for the directional arm rod.

A complete set of drawings for the Reflectometer is being sent under separate cover to M. Kalet of GSFC.

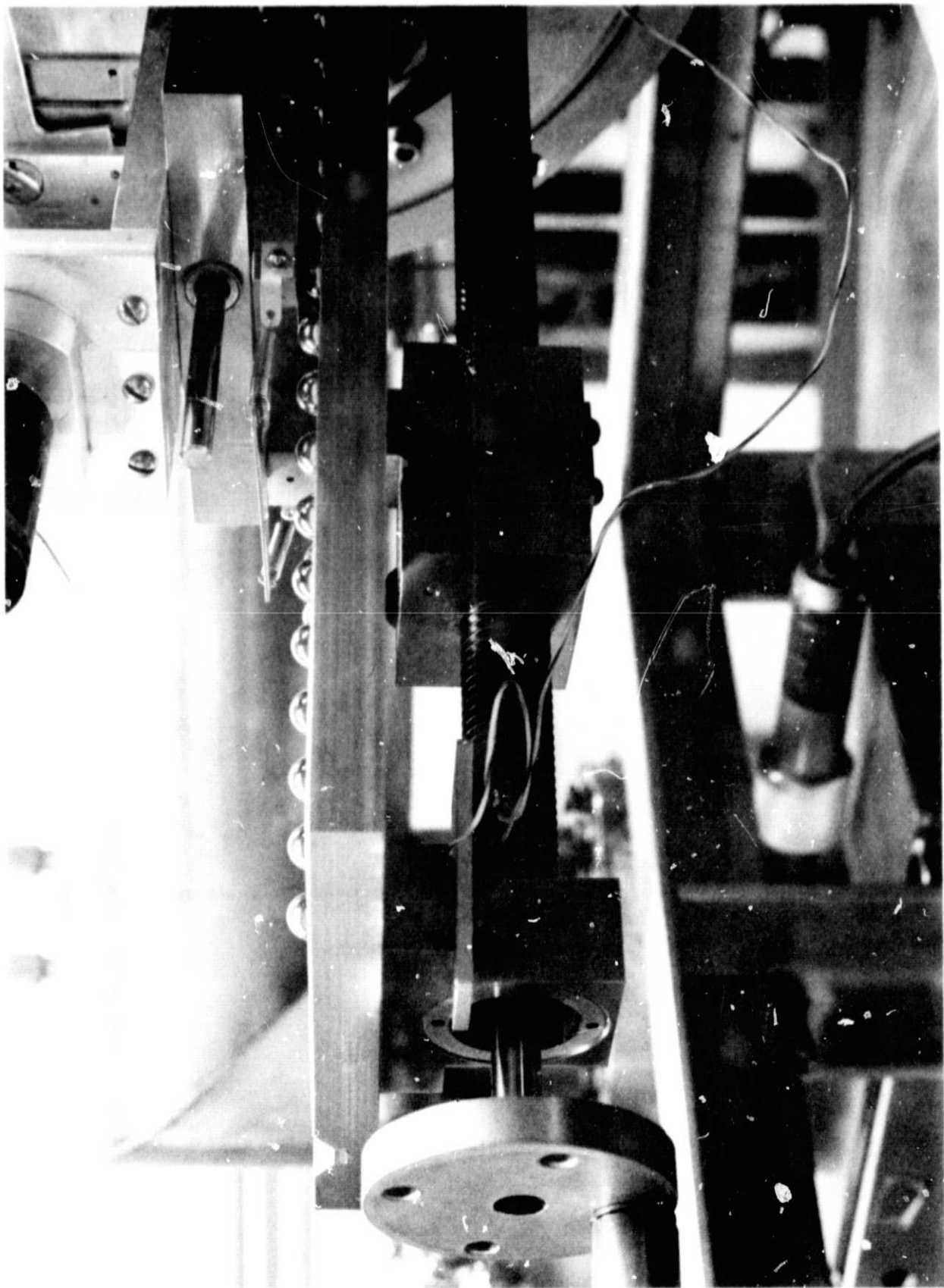


Plate 1

REPRODUCIBILITY OF THE
ORIGINAL PAGE IS POOR

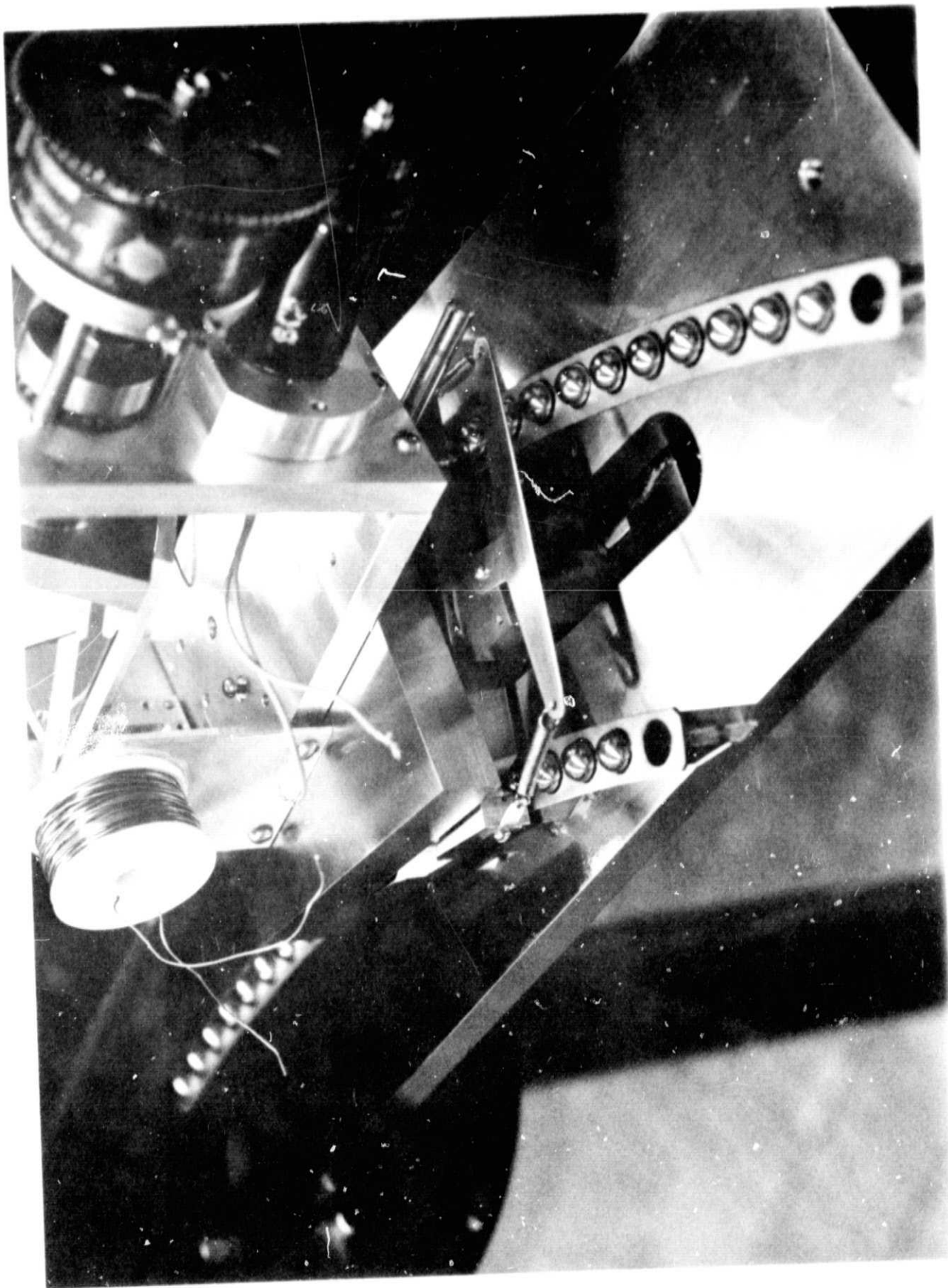


Plate 2

REPRODUCIBILITY OF THE
ORIGINAL PAGE IS POOR

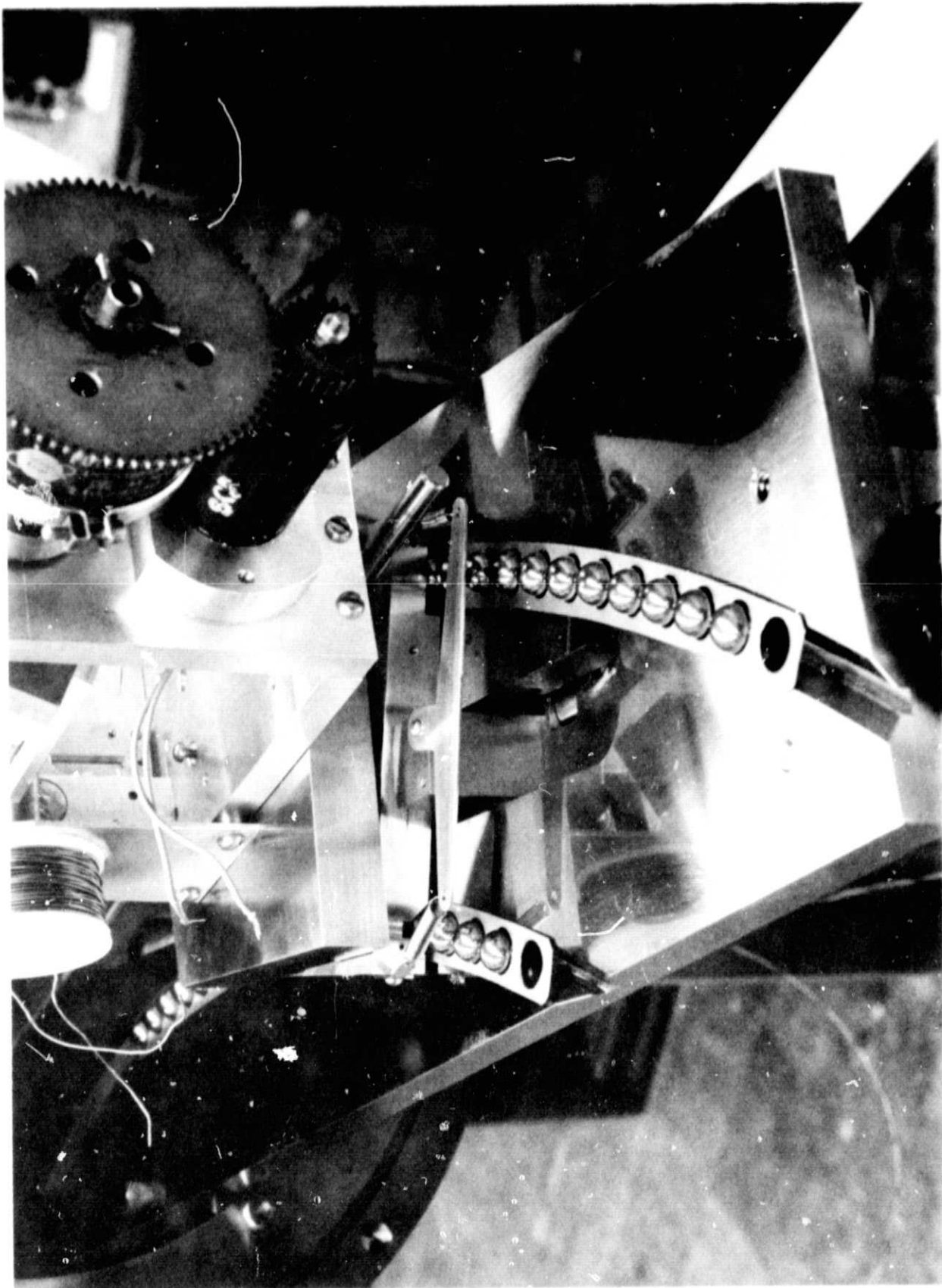


Plate 3

REPRODUCTION OF THE
ORIGINAL FOR 2-13-1947

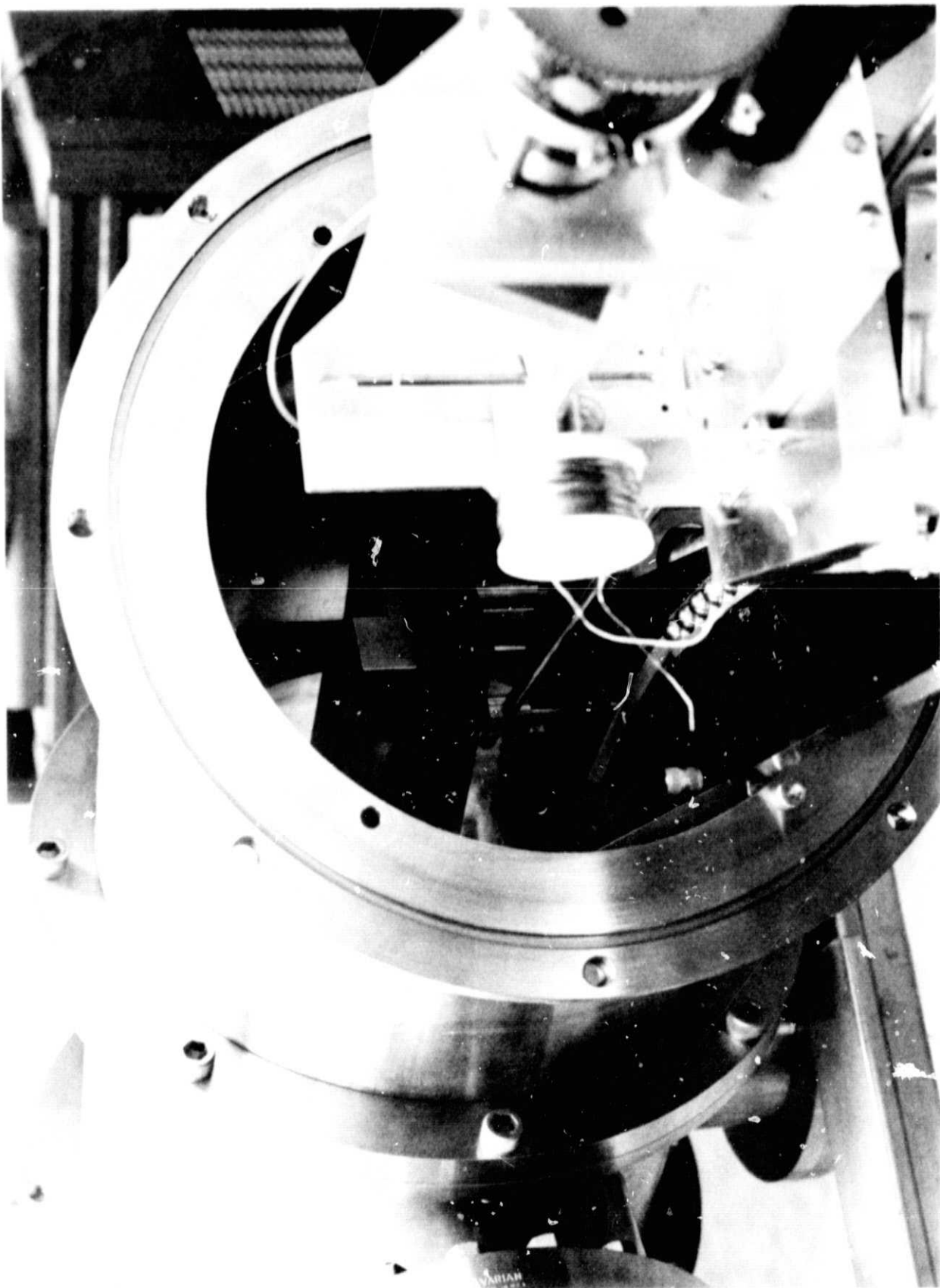


Plate 4